2011

The characterisation of Pax3 expressant cells in adult peripheral nerve

Judith A. Blake
Edith Cowan University

Edith Cowan University

Copyright Warning

Doctor of Philosophy

(Human Biology)

Thesis

The Characterisation of Pax3 Expressant Cells in Adult Peripheral Nerve

PhD Candidate:

Judith A Blake (MSc)

Supervisor:

Dr Melanie Ziman

Edith Cowan University

Faculty of Computing, Health and Science

School of Medical Sciences

2011

ABSTRACT

Pax3 has numerous integral functions in embryonic tissue morphogenesis while knowledge of its complex function in cells of adult tissue continues to unfold. Across a variety of adult tissue lineages, the role of Pax3 is principally linked to maintenance of the tissue's resident stem and progenitor cell population. In adult peripheral nerves, Pax3 is reported to be expressed in nonmyelinating Schwann cells, however, little is known about the purpose of this expression. Based on the evidence of its role in other adult tissue stem and progenitor cell maintenance, it was hypothesised that the cells in adult peripheral nerve that express Pax3 may be Schwann glioblasts. Here, methods have been developed for visualisation of Pax3 expressant cells in normal 60 day old mouse peripheral nerve. Visualisation allowed morphological, anatomical and phenotypic distinctions to be made between these Pax3 expressing cells and Remak bundle nonmyelinating Schwann cells. The distinctions described herein, together with the finding that Pax3 expressing cells co-express stem cell marker Sox2, provides compelling support for the suggestion that a progenitor Schwann cell population may be present in adult mouse peripheral nerve.

I certify that this thesis does not, to the best of my knowledge and belief:

i. incorporate without acknowledgement any material previously submitted for a degree or diploma in any institution of higher education;

ii. contain any material previously published or written by another person except where due reference is made in the text of this thesis; or

iii. contain any defamatory material.

Judith A. Blake

ACKNOWLEDGEMENTS

The author would like to gratefully acknowledge research supervisor Dr Mel Ziman, Dr Paul Rigby for expert guidance and instruction using the scanning laser confocal microscope and Dr Michael Fontés for the generous donation of the C22 transgenic tissues. The author would also like to acknowledge Tammy Esmaili and Andrew Wilson for assistance with animal work, Dr Mark Brown and Rebecca Slattery for assistance with RT-PCR investigations, the late Dr John W Griffin, Drs Wei-Ming Yu, Rhona Mirsky and Jenny Thompson for insightful immunohistochemical advice and Dr Angus Stewart for instruments necessary for quality nerve fibre preparations. The Pax3 monoclonal antibody, developed by C.P. Ordahl, was obtained from the Developmental Studies Hybridoma Bank developed under the auspices of the NICHD and maintained by the University of Iowa, Department of Biological Sciences, Iowa City, IA, USA. BioRad microscopy was carried out using facilities at the Centre for Microscopy, Characterisation and Analysis, The University of Western Australia, which is supported by University, State and Federal Government funding.

CONTENTS

	PAGE
ABSTRACT	**ii**
DECLARATION BY CANDIDATE	**iii**
ACKNOWLEDGEMENTS	**iv**
CONTENTS	**v**
LIST OF TABLES	**viii**
LIST OF FIGURES	**ix**
ABBREVIATIONS	**xi**
CHAPTER ONE	
LITERATURE REVIEW: *The Expression and Function of Pax3 from the Embryo to the Adult.*	1
1.1 Introduction	2
1.2 The *PAX3*/*Pax3* gene	2
1.3 *Pax3* governs the development of embryonic skeletal myoblasts	7
1.4 *Pax3* inhibits differentiation of regenerative myoblasts of adult skeletal muscle	8
1.5 Aberrant *PAX3*/*Pax3* expression in myoblasts	9
1.6 *Pax3* regulates the specification and survival of embryonic melanoblasts	12
1.7 *Pax3* orchestrates the regenerative proliferation of adult melanocytic stem cells and inhibits the differentiation of their progeny	14
1.8 Aberrant *PAX3*/*Pax3* expression in melanoblasts	19

1.9 How does *Pax3* govern the development of embryonic peripheral glioblasts? 22

1.10 Why do nonmyelinating Schwann cells of adult peripheral nerve continue to express *Pax3?* 26

1.11 What is the role of *Pax3* in regenerative glioblasts of adult peripheral nerve? 29

1.12 Conclusion 32

HYPOTHESES/AIMS 33

CHAPTER TWO

METHODS **36**

2.1 Animals 37

2.2 Isolation of RNA from whole sciatic nerve specimens 37

2.3 RT-PCR amplification of *Pax3* from whole nerve specimens 38

2.4 Preparation of frozen nerve sections 40

2.5 Preparation of teased nerve specimens 41

2.6 Preparation of whole-mount nerve fascicle specimens 42

2.7 Antibodies used for immunohistochemistry and immunofluorescence. 42

2.8 Procedure for immunofluorescent staining of frozen sections 43

2.9 Procedure for enzyme-linked immunohistochemical staining of frozen sections 43

2.10 Procedure for immunofluorescent staining of teased nerve fibres 44

2.11 Procedure for double immunofluorescent staining of whole mount nerve 44

2.12 Microscopy 45

CHAPTER THREE

RESULTS **46**

3.1 *Pax3c* and *Pax3d* transcripts are expressed in 60 day old mouse sciatic nerve 47

3.2 The morphology of mouse NMSCs of sciatic nerve 50

3.3 p75Ngfr unveils the structural complexity of adult NMSCs *in vivo* 54

3.4 The use of Pax3 as a marker of NMSCs in adult mouse sciatic nerve 57

3.5 The expression pattern of Pax3 protein in normal adult mouse sciatic nerve 65

3.6 Characterisation of cells that express Pax3 in normal adult mouse sciatic nerve 66

3.7 Summary of the results 71

CHAPTER FOUR

DISCUSSION **73**

4.1 A distinct population of Pax3 expressing cells in adult mouse peripheral nerve 74

4.2 The characterisation of Pax3 expressing cells and Remak NMSCs 75

4.3 Pax3 expression in C22 adult mouse peripheral nerve 78

4.4 Immunohistochemical hurdles 79

4.5 The significance of the research findings 81

4.6 Research conclusion 84

REFERENCES **85**

LIST OF TABLES

Table 1. **PCR Reaction Composition.** 39

Table 2. **Thermal Cycler Conditions.** 40

Table 3. **Assessment of fixation and permeabilisation procedures.** 98

Table 4. **Assessment criteria used to assess immunohistochemical methods.** 99

LIST OF FIGURES

Figure 1. ***Pax3*** **transcripts.** 4

Figure 2. **Modification of** ***Pax3*** **transcripts with inclusion of a glutamine residue.** 5

Figure 3. **Pax3 protein structure.** 6

Figure 4. **Photomicrograph of a** ***Splotch*** **embryo.** 10

Figure 5. **Vitiligous repigmentation.** 18

Figure 6. **Children affected by Waardenburg Syndrome I with piebaldism.** 20

Figure 7. **Schwann cell development.** 26

Figure 8. **Remak Schwann cells.** 27

Figure 9. **The organisation of Remak Schwann cells in peripheral nerve trunk.** 28

Figure 10. **Generation of the** ***Pax3c*** **and** ***Pax3d*** **transcripts.** 49

Figure 11. **RT-PCR results.** 50

Figure 12. **Whole mount nerve morphology.** 51

Figure 13. **Mouse nonmyelinating Schwann cell morphology.** 52

Figure 14. **Morphological characteristics of the nonmyelinating Schwann cell nucleus.** 53

Figure 15. **Immunohistochemical methods affect tissue autofluorescence.** 55

Figure 16. **p75Ngfr is a reliable cell surface marker for Remak bundles.** 56

Figure 17. **The complex structure and distribution of Remak bundles in normal adult mouse peripheral nerve.** 57

Figure 18. **Pax3 is undetectable in frozen cross sections.** 59

Figure 19. **The Pax3 immunolabel in frozen longitudinal sections.** 60

Figure 20. **Pax3 expression in transgenic C22 sciatic nerve**. 62

Figure 21. **Endoneurial collagen.** 63

Figure 22. **Optimisation of the Pax3 immunofluorescent histochemistry.** 64

Figure 23. **Verification of nuclear immunofluorescent histochemistry.** 65

Figure 24. **The distribution of Pax3 protein in adult mouse sciatic nerve.** 67

Figure 25. **A Pax3 expressant cell *in situ*.** 68

Figure 26. **p75Ngfr and Pax3 co-localisation in adult nerve** 69

Figure 27. **Pax3 is expressed in a subset of nonmyelinating Schwann cells of adult nerve.** 70

Figure 28. **Transcription factors Pax3 and Sox2 co-localise in cells of adult Nerve.** 71

Figure 29. **The proposed retention of peripheral nerve progenitor cells from embryogenesis.** 77

ABBREVIATIONS

BCL2L1	human BCL2-like1 antiapoptotic factor
C22	mutant mouse strain with phenotypic traits in common with humans affected with CMT1A
cKit	stem cell factor receptor
CMT1A	Charcot-Marie-Tooth disease, demyelinating type 1A
cMet	gene that encodes murine hepatocyte growth factor receptor
Dct	gene that encodes murine dopachrome tautomerase
FKHR	gene that encodes human forkhead transcription factor
Gapdh	gene that encodes mouse 'housekeeping' enzyme glyceraldehyde-3-phosphate dehydrogenase
GFAP	gene that encodes human glial fibrillary acidic protein
Gfap	murine glial fibrillary acidic protein
iPSCs	adult somatic cells artificially induced into pluripotent stem cells
L1Cam	gene that encodes murine L1 cell adhesion molecule
µm	micrometer
Mitf	gene that encodes murine micropthalmia transcription factor
Myf5	murine myogenic factor 5
MyoD	murine myogenic differentiation antigen

NCBI	National Center of Biotechnology Information database
NGS	normal goat serum
NMSCs	nonmyelinating Schwann cells
p75NGFR	Human low-affinity nerve growth factor receptor
p75Ngfr	Murine low-affinity nerve growth factor receptor
PAX3	gene that encodes human transcription factor PAX3
Pax3	gene that encodes murine transcription factor Pax3
PAX3/FKHR	PAX3/FKHR fusion protein
PBS	phosphate buffered saline
PFA	4% paraformaldehyde in 0.1M phosphate buffer
Sox2	gene that encodes murine Sry-box 10 transcription factor
Sox9	gene that encodes murine Sry-box 9 transcription factor
Sox10	gene that encodes murine Sry-box 10 transcription factor
TBS	Tris buffered saline
Tw20	Tween20 polysorbate surfactant
TX100	Triton-X100 nonionic surfactant

1

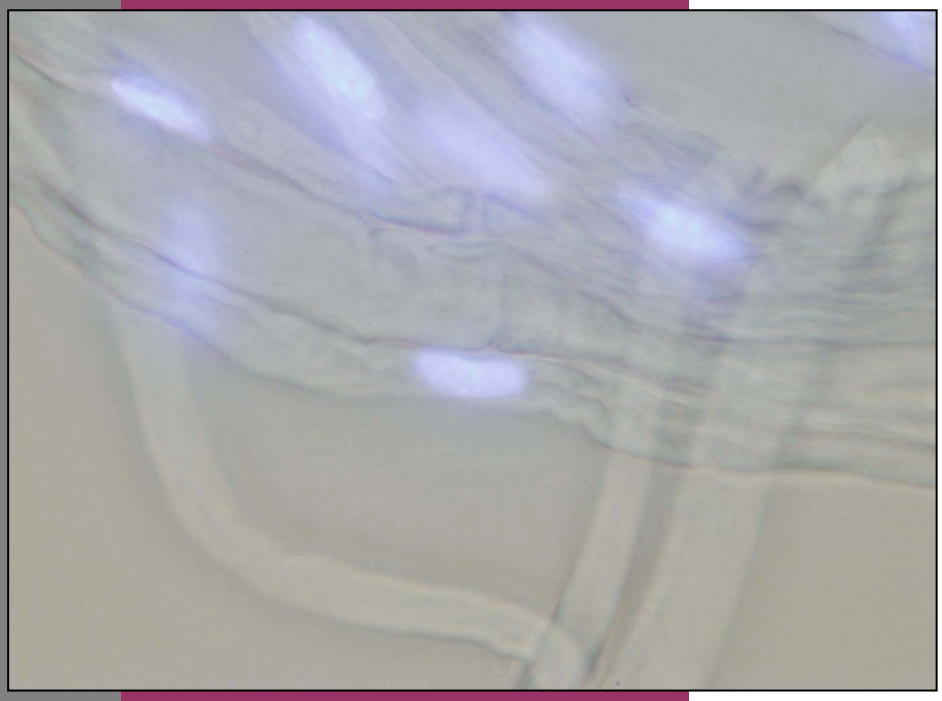

LITERATURE REVIEW:

The Expression and Function of Pax3

from the Embryo to the Adult.

1.1 Introduction

The master regulatory gene, *PAX3*, is known to orchestrate cellular phenotypes across several tissue lineages during embryonic development. The multiple protein isoforms encoded by *PAX3* are transcription factors that direct downstream target genes involved in cellular proliferation, migration, apoptosis and differentiation. The specific function of the many transcribed PAX3 isoforms is contingent upon the stage of development of the cell and the age of the tissue in which the cell is incorporated. *PAX3* continues to function past embryogenesis and has several regulatory roles in the ontogeny of stem cells throughout the postnatal lifespan of the organism. This literature review summarises the known functions of *PAX3/Pax3* in skeletal muscle, melanocyte and Schwann cell development, in adult cells of these tissues and in the diseased state. The objective of the review is to highlight the principle role of *PAX3/Pax3*, namely, regulation of the progenitor cell state, across a diverse and complex spectrum of cell types through stages of development and maturation.

1.2 The *PAX3/Pax3* gene

The *paired-box homeotic gene 3* (*PAX3*) encodes the PAX3 transcription factor which derives its name from the 384 base pairs of DNA that encode a highly conserved DNA binding motif of 128 amino acids known as the paired domain (Burri et al., 1989; Krauss et al., 1991). Throughout the review, the conventional use of italics for gene and RNA transcript names (e.g., *PAX3*) and regular case for protein isoforms (e.g., PAX3) is observed; similarly, it is convention that the human gene or protein is indicated with uppercase letters (*PAX3*/PAX3) while the mouse gene or protein is denoted using lowercase letters (e.g., *Pax3*/Pax3).

PAX3 is located on chromosome two at 2q35 of the human genome (Ishikiriyama, 1993)

while *Pax3* is located on chromosome one of the mouse genome. The coding region of human *PAX3* consists of 10 exons (Barber et al., 1999) from which seven transcripts are produced via alternate post-transcriptional splicing (Tsukamoto et al, 1994; Barber et al, 1999; Parker et al, 2004) (Fig. 1). Each transcript produced may also encode a glutamine residue in the linker region between the subdomains of the paired-domain of the protein (Vogan & Gros, 1996) (Fig. 2). A search of the mouse genome in the National Center of Biotechnology Information database (NCBI) of the U.S. National Library of Medicine and National Institutes of Health reveals that four transcripts of *Pax3* are produced in mouse. Three of these transcripts have been sequenced, with *Pax3c* and *Pax3d* expressed in cells of the melanogenic lineage (Barber et al, 1999), while *Pax3^8* is expressed in myoblasts (Pritchard et al, 2003). The mouse sequences of *Pax3c*, *Pax3d* and *Pax^8* are homologous to human sequences *PAX3c*, *PAX3d* and *PAX3g*, respectively. Barber et al (1999) have isolated an embryonic mouse cDNA where exon 9 is spliced onto exon 5; they designated it *Pax3f*, however, sequence data is unavailable (personal communication). Like human *PAX3*, each mouse *Pax3* transcript is able to encode an additional transcript that contains a glutamine residue in the paired-domain of the protein (Vogan, Underhill & Gros, 1996; Barber et al., 1999).

Functional diversity of *PAX3* is linked to its ability to produce alternatively spliced transcripts which alter the structure and, consequently, the DNA binding activity of the encoded transcription factors (Tsukamoto et al., 1994; Underhill & Gros, 1997; Seo et al., 1998). PAX3/Pax3 transcription factors contain two DNA-binding domains, a paired and a homeodomain, and a highly variant transactivation domain that regulates transcription of bound target genes. The DNA binding domains recognise and bind

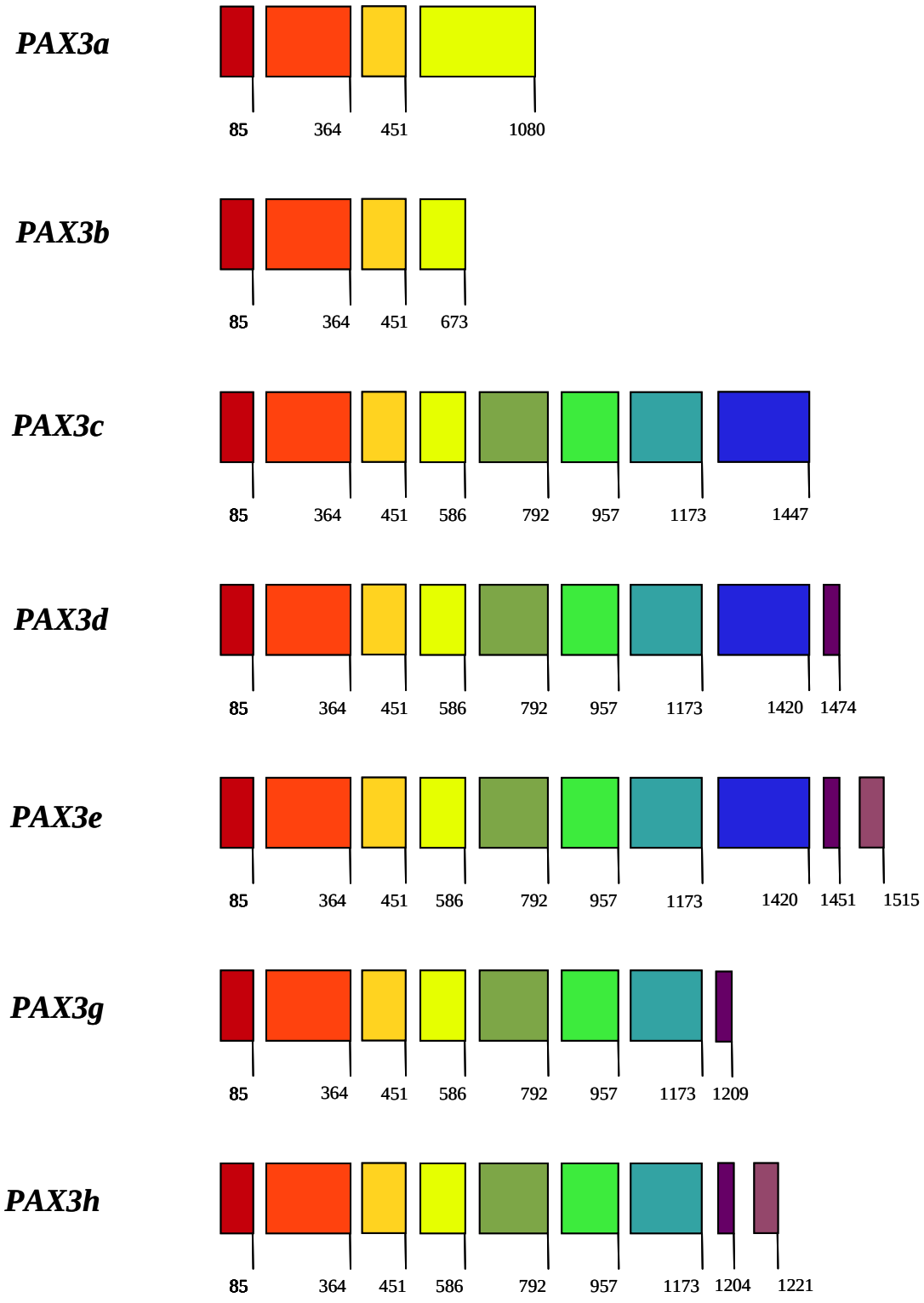

***Figure 1. Pax3* transcripts.** Schematic representation of human *PAX3* mRNA splice variants shows the exons and their respective sizes (coloured boxes). The vertical black lines and respective numbers indicate the nucleotide number of the acceptor splice sites of each exon. The representation is based upon current information for human *PAX3* mRNA available on NCBI.

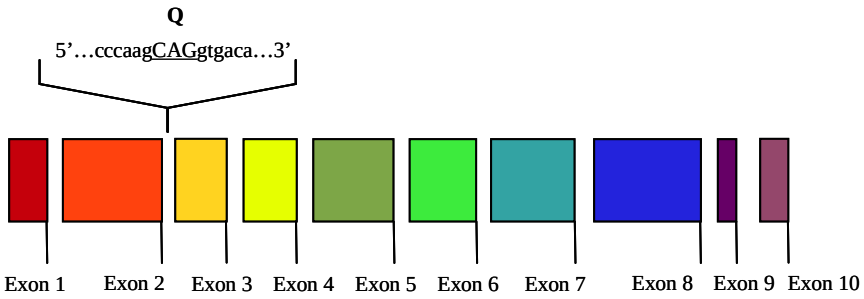

Figure 2. **Modification of *Pax3* transcripts with inclusion of a glutamine residue.** Location of the alternative nucleic acid sequence encoding a glutamine (Q) residue that occurs at the intron 2/exon 3 junction. The codon encoding the Q residue is underlined.

specific regulatory sequences within promotor, enhancer and silencer regions of target DNA while the transactivation domain recruits components of the pre-initiation complex and other transcription factors to the area of the gene promotor. This facilitates the signals to RNA polymerase to begin initiation and transcription of the downstream gene (Ptashe, 1988). Alternate PAX3 transcription factors activate a variety of downstream cellular pathways by variant use of the paired domain, the homeodomain or the combined use of both to bind to target gene promoter sequences (Underhill & Gross, 1997; Vogan & Gross, 1997) (Fig. 3).

The paired domain, which is the definitive structural and functional motif of all Pax proteins, is divided into N-terminal and C-terminal subdomains, each of which bind independently to DNA recognition sequences (Jun & Desplan, 1996). Both of the subdomains contain three alpha-helices and the DNA-binding motif for both subdomains is a helix-turn-helix motif (Xu et al., 1995; Xu et al., 1999). *Pax3* also encodes a homeo- DNA binding domain (homeodomain) and a conserved octapeptide region that participates in protein binding interactions. The helix-turn-helix homeodomain is capable of binding DNA via interaction with other homeodomain-containing proteins (heterodimerisation) or by homodimerisation (Bennecelli et al., 1995).

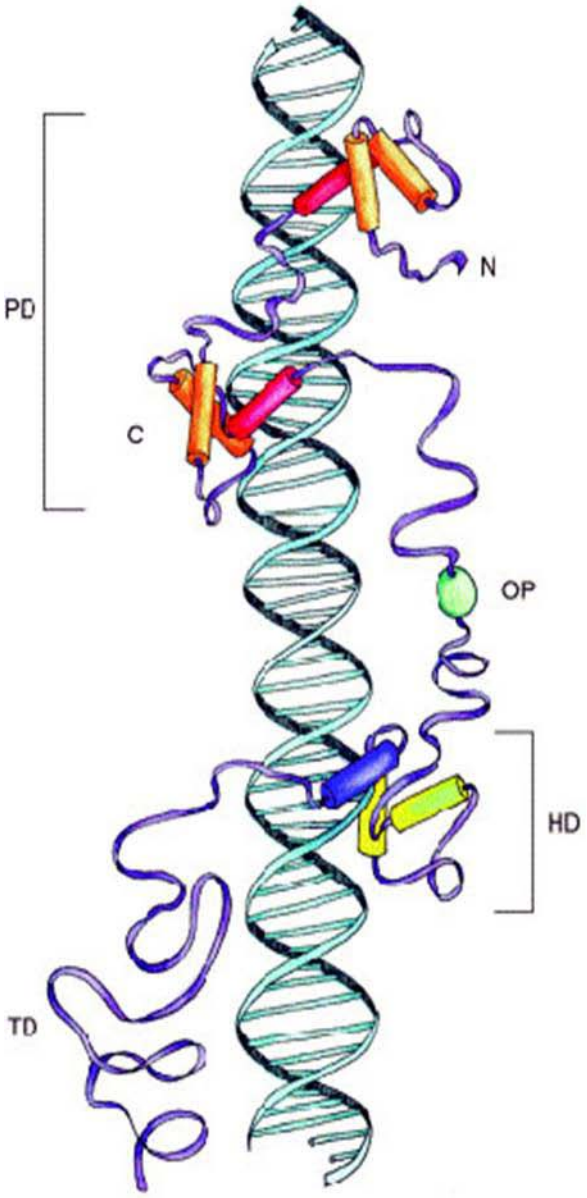

***Figure 3*. Pax3 protein structure.** A depictation of the Pax3 protein is shown juxtaposed to a DNA helix. The paired-box domain is indicated by PD, with the amino and carboxyl termini indicated by N and C, respectively. The octopeptide, homeodomain and transactivation domains are indicated by OD, HD and TD, respectively. *(Figure courtesy of Xu et al., 1999).*

In addition to the numerous DNA sequences bound individually by the paired domain or the homeodomain, cooperative interaction between the DNA binding motifs permits binding to additional nucleotide combinations (Treisman, Harris & Desplan, 1991; Underhill, Vogan & Gros, 1996; Jun & Desplan, 1996). Conversely, one of the functions of the paired domain is inhibition of homeodomain dimerisation which further affects

PAX3/Pax3 function (Jun & Desplan, 1996; Underhill & Gros, 1997). A mutation in either DNA binding domain affects DNA binding by the other and suggests that the two domains function dependently (Fortin et al., 1997). The Pax3 transactivation domain also plays a role in regulation of homeodomain binding (Cao & Wang, 2000). Overall, the protein structure of PAX3/Pax3 permits specific control of binding to a large array of DNA sequences that regulate transcriptional activation or repression of a broad spectrum of downstream genes in a variety of developmental pathways.

1.3 *Pax3* governs the development of embryonic skeletal myoblasts

Specification of the skeletal muscle lineage begins when *Pax3* is initially expressed in cells of the caudal segmental plate, the early mesoderm compartment that contains the precursors of skeletal muscle (Schubert et al., 2001). As compartmentalisation of the somites forms along an anterior-posterior axis, polarity is generated in the anterior mesoderm via Pax3 synergy with the T-box protein 18 (Farin et al., 2008). As somites mature, *Pax3* expression becomes repressed in the anterior half of the somite and becomes restricted to the dermomyotome (Cairns et al., 2008). Sonic Hedgehog signals pattern the somite into dermomyotomal, myotomal and sclerotomal cell fates where different levels of signalling elicit loss of myotomal markers and activation of sclerotomal gene expression. Using explants of presomitic mesoderm, it was demonstrated that forced expression of *Pax3* in developing somites blocks Sonic Hedgehog mediated induction of sclerotomal gene expression and chondrocyte differentiation; thus, *Pax3* regulates somite formation (Cairns et al., 2008).

At embryonic day 9.5, *Pax3* expression is concentrated in the dorsomedial and ventrolateral regions of the dermomyotome where modulation of expression levels delineates the medial and lateral halves of the dermomyotome (Williams & Ordahl,

1994). At the onset of myogenesis (embryonic day 10.5), myogenic precursors that express Pax3 proliferate and delaminate from the edge of the dermomyotome to form the myotome. Subsequent to loss of the epithelial structure of the dermomyotome, cells of the myotome become highly proliferative (Relaix et al., 2005) and survival of the cells is dependent upon *Pax3* expression (Franz et al., 1993; Bober et al., 1994; Goulding et al., 1994; Tremblay et al., 1998; Borycki et al., 1999; Buckingham et al., 2006). At the same time, *Pax3* expressant myoblasts migrate from the lips of the dermomyotome into the limb buds (Bober et al., 1994; Williams & Ordahl, 1994; Relaix et al., 2005).

Between embryonic day 11.5 and 17.5, myogenic determination genes, myogenic factor 5 (*Myf5)* and myogenic differentiation antigen (*MyoD),* are increasingly upregulated in migrant limb myoblasts (Bajard et al., 2006; Hu et al., 2008), as the cells reach their target destination in the limb. Pax3 is required for regulation of this myogenic-specific transcriptional program (Tajbakhsh et al., 1997; Kassar-Duchossoy et al., 2004; Buckingham et al., 2006). Subsequently, *MyoD* and *myogenin* activate formation of differentiated muscle in pre- and neonatal myoblasts as downregulation of *Pax3* occurs during myocyte fusion and elongation (Venters et al., 2004). A second population of Pax3 (and Pax7) expressant cells is formed between embryonic days 11.5 - 17.5 that is distinguishable from myoblasts that express myogenic genes. Between embryonic day 16.5 and 18.5, this cell population is enclosed within the forming basal lamina of nascent muscle fibres where it remains as the resident progenitor cells, or satellite cells, of adult skeletal muscle (Gros et al., 2005; Relaix et al., 2005).

1.4 Pax3 inhibits differentiation of myoblasts in adult skeletal muscle

Satellite cells are the skeletal muscle progenitor cells responsible for postnatal and adult

muscle growth and repair (Charge & Rudnicki, 2004). In response to skeletal muscle growth and injury, quiescent satellite cells are activated to proliferate, self-renew and form a pool of myoblasts which fuse and differentiate in order to produce mature myofibres. Upon satellite cell activation, increased *Pax3* expression does coincide with *MyoD* upregulation (Hyatt et al., 2008); however, in this context, *MyoD* is upregulated independently of *Pax3* via Notch signalling (Relaix et al., 2006; Crist et al., 2009). That conditional *Pax3* inactivation in mutant satellite cells does not compromise muscle regeneration and that *Pax3* is not required for injury-induced myogenesis in adulthood suggests that it functions in satellite cell progenitors solely to decrease the propensity of the myoblast to differentiate by transient repression of *MyoD* (Relaix et al., 2005; Lepper et al., 2009). *Pax3* expression is decreased as satellite cell-derived myoblasts begin to differentiate (Olguin & Olwin, 2004; Zammit et al., 2004) and exemplifies that, in adult skeletal muscle, Pax3 functions to temporally maintain myoblasts in a progenitor cell state.

1.5 Aberrant *PAX3*/*Pax3* expression in myoblasts

The importance of *PAX3*/*Pax3* expression in the development of skeletal muscle cells is highlighted by mutant phenotypes that have altered PAX3/Pax3. For example, the mutant *Splotch* mouse has a five nucleotide sequence variation in intron three of *Pax3*, including a nucleotide deletion and transversion at the invariant 3' splice acceptor site. This genomic mutation prevents the normal splicing of intron three, resulting in four incorrectly coded mRNA transcripts, three of which result in a stop codon at the splice site (Epstein et al., 1991). Homozygous *Splotch* mice die in utero around embryonic day 13.5 due to severe neural tube defects (spina bifida and exencephaly), a lack of limb skeletal musculature and deficiencies in neural crest-derived lineages including Schwann cells, dorsal root and cranial ganglia and melanocytes (Franz, 1990; Epstein et

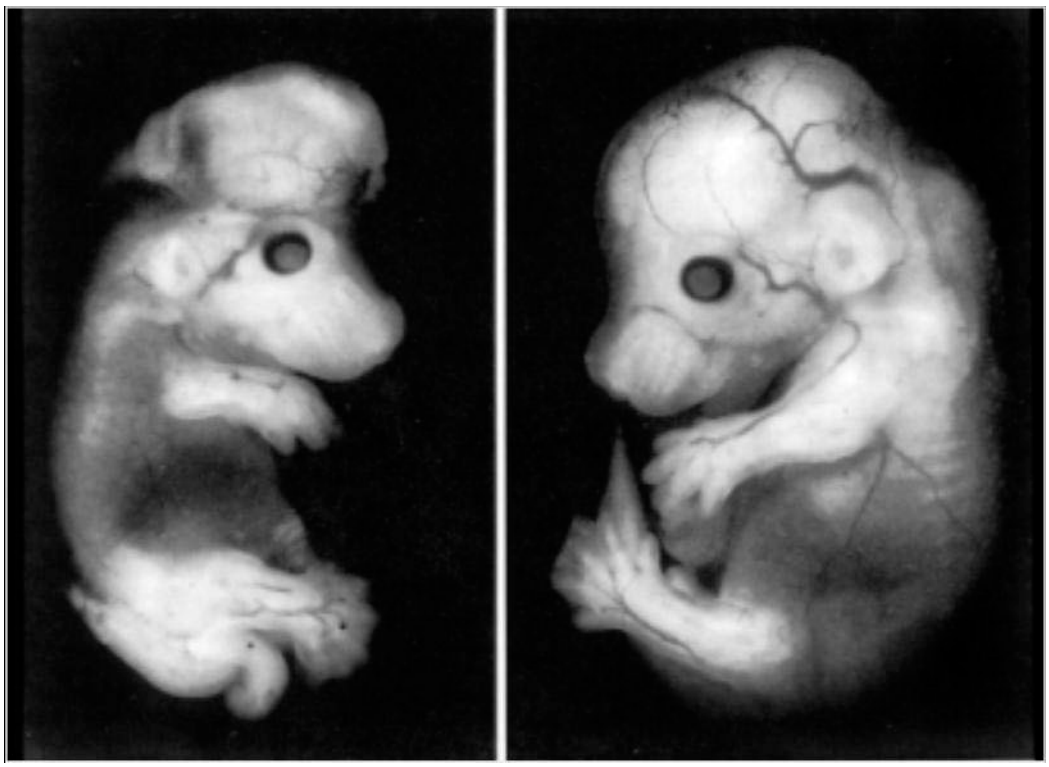

Figure 4. **Photomicrograph of E13.5 *Splotch* embryos.** The mouse embryo on the left is a *Pax3* mutant "*Splotch*" mouse. Note the defects in the area of the neural tube, neural crest derived cranial facial structures and forming limb buds as compared to the wild type mouse on the right. *Photo courtesy of Conway et al., 1997.*

al., 1991; Bober, 1994) (Fig. 4). Homozygous *Splotch* mice fail to develop limb musculature as cells derived from the somites either do not migrate into the limbs due to the absence of *Pax3* in premigratory cells or the cells that do migrate are few in number due to the loss of *Pax3* (Daston et al., 1996; Epstein et al., 1996). The *Splotch* phenotype indicates that *Pax3* has an early, key role in normal skeletal muscle development.

In humans, aberrant *PAX3* gene dosage causes the soft tissue tumour alveolar rhabdomyosarcoma (Sorensen et al., 2002). This paediatric cancer is linked to a somatic translocation t(2;13)(q35;q14) in which the *PAX3* paired and homeodomain encoding regions are juxtaposed with the region that encodes the DNA-binding motif of the homeotic gene '*forkhead* ' (*FKHR)*; the fusion protein is referred to as PAX3/FKHR (Galili et al., 1993). Heterozygotes display a phenotype linked to both a gain-of-

function effect on downstream PAX3 target genes (due to a more transcriptionally active PAX3/FKHR fusion protein) (Xia & Barr, 2004) and the dominant negative effects of the fusion protein on wild type *PAX3* expression (Keller et al., 2004a). Experimental models of *Cre*-mediated conditional knock-ins of *Pax3/Fkhr* into the *Pax3* locus at distinct times throughout embryonic and postnatal myogenesis illustrate how *Pax3* regulates the development of myoblast progenitors across the lifespan. For example, mice heterozygous for a germ-line *Pax3/Fkhr* knock-in partially phenocopy the *Splotch* phenotype as animals have pathogenic limb and diaphragm muscles (Keller et al., 2004a). The mutant animal has a complete absence of wild-type *Pax3* linked to *Pax3/Fhkr* repression; paradoxically, mice display aberrant myoblast migration that results from Pax3/Fkhr mediated overexpression of downstream Pax3 target genes, hepatocyte growth factor receptor (*cMet)* and *MyoD* (Keller et al., 2004a). The model demonstrates the importance of *Pax3/*Pax3 regulation of delamination and migration of somitic muscle progenitor cells in early embryonic development.

To study the consequences of Pax3/Fkhr in satellite cells, a conditional *Pax3/Fkhr* knock-in allele was combined with a *Pax7*-driven *Cre* allele. *Pax7* expression was found to be increased in the mutant mice and was linked to *Pax3/Fkhr* inhibition of *Pax3* which, in turn, normally represses *Pax7* (Borycki et al., 1999). Despite increased *Pax7* expression, viable animals had postnatal growth defects and a decreased number of satellite cells (phenocopying a *Pax7* deficiency) which was correlated to the dominant-negative effects of Pax3/Fkhr on downstream Pax7 targets (Oustanina et al., 2004). Results of the study demonstrated that *Pax3/Fkhr* expression in satellite cells does not directly lead to alveolar rhabdomyosarcoma (Keller et al., 2004a). In fact, the progeny cells of an activated satellite cell that harbours the *PAX3/FKHR* allele best demonstrate the effects of the PAX3 mutation. In transformed myoblasts, the gain of

function of PAX3/FKHR on PAX3 targets is thought to cause oncogenesis at the stage of terminal differentiation, where *PAX3* expression is normally down-regulated (Qualman et al., 1998). At this stage, continued *PAX3/FKHR* expression leads to enhanced transcription of PAX3 downstream target genes that regulate the inhibition of cell cycle withdrawal (Keller at al., 2004b). Thus, the failure of myoblasts to differentiate into myocytes is thought a principle cause of neoplasia (Roeb et al., 2007; Charytonowicz, 2009, 2011).

To summarise, *Pax3* has an early role in cell fate and tissue mapping of the embryonic mesoderm and somites. As the proliferation and migration of specified myogenic precursors occurs within the developing muscle masses of the embryo, *Pax3* has a key role in the survival of the cells. In order for developmental myoblasts to advance into the myogenic program, *Pax3* is required for upregulation of regulatory factors *Myf5*, *MyoD* and *myogenin* and subsequent terminal differentiation. In embryonic development, the surrounding mesenchyme, together with Pax3, has a principle role in prevention of precocious differentiation of myoblasts. A population of *Pax3* expressant progenitor cells remains in adult skeletal muscle as satellite cells. When activated by injury, satellite cells transiently upregulate *Pax3* where expression does not have a direct role in cell survival but rather functions to inhibit precocious differentiation of myoblasts via repression of *MyoD*. *Myogenin* expression, indicative of differentiation, coincides with downregulation of *Pax3*. At this stage of myoblast development in adult tissue, if downregulation of *PAX3* does not occur, it is thought that oncogenesis ensues linked to the inability of the myoblasts to properly differentiate.

1.6 *Pax3* regulates the specification and survival of embryonic melanoblasts

Pax3 functions similarly in neural crest cells as they develop along the melanocytic

lineage where cellular specification, survival, migration and differentiation are regulated by its expression. Development of melanocytes, the pigment producing cells of the skin and hair, begins as the neural crest cells on the mediodorsal edge of the closing neural folds undergo an epithelial to mesenchymal transition (Le Douarin, 1980). At the axial trunk level, following an accumulation near the dorsal neural tube in a 'migration staging area' neural crest cells migrate in two waves to populate target embryonic tissues. One wave proceeds ventrally, adjacent to the neural tube and within the anterior portion of the somite where formation of the peripheral ganglia and nerves occurs. A further wave proceeds along a dorsolateral path between the ectoderm and the dermomyotome.

Pax3 is, in fact, an early marker of the neural crest lineage in mice where expression is detected at embryonic day 8.5 (Goulding et al., 1991). As neural crest cells segregate from the neural epithelium to the transient migratory staging area, *Pax3* is implicated in regulation of the neural and ectodermal interactions required for neural crest induction (Dottori et al., 2001). Around embryonic day 10.5, neural crest cells delaminate and migrate from the neural crest staging area where *Pax3* expression is linked to their specification and proliferation (Hornyak et al., 2001). By E11.5, in cells that undergo dorsolateral migration, the melanogenic determination gene *dopachrome tautomerase* (*Dct)* is expressed and indicates the commitment of the cells to future melanin synthesis (Wehrle-Haller & Weston, 1995). At this stage, micropthalmia transcription factor (*Mitf*), a downstream target of Pax3, is required for survival of the melanoblasts as they migrate through the embryonic mesenchyme (Corry & Underhill, 2005; Watanabe et al., 1998). *Mitf* activation occurs when Sry-box 10 transcription factor *(*Sox10) and Pax3 synergistically bind regulatory consensus sites of its promotor region (Bondurand et al., 2000; Potterf et al., 2000). As *Pax3* has an associative role in the upregulation of the

melanocytic survival factor *Mitf*, it has an indirect role in the survival of migratory melanoblasts.

Following regionalisation of melanoblasts in the mouse dermis (embryonic day 12.5-13.5), Pax3 remains expressed upon entry into the epidermis (Blake & Ziman, 2005). From embryonic day 14.5, melanoblasts that express stem cell receptor (c-Kit) are incorporated into the developing hair follicle. Around embryonic day 15, melanocyte differentiation occurs and pigmentation of the first hairs is induced two days later (Hirobe, 1984; Jordan & Jackson, 2000; Peters et al., 2002). At this stage, a subpopulation of c-Kit negative and Pax3 positive melanoblasts colonise the hair follicle stem cell niche where they persist into adulthood as resident melanocytic stem cells (Peters et al., 2002; Blake & Ziman, 2005; Mak et al., 2006; Medic and Ziman, 2010). While most mouse epidermal melanoblasts undergo apoptosis after birth (Hirobe, 1984), human epidermal melanoblasts terminally differentiate in postnatal skin and are active in pigment production throughout life; in these cells, *PAX3* is not constitutively expressed (Scholl et al., 2001).

1.7 *Pax3* orchestrates the proliferation of adult melanocytic stem cells and inhibits the differentiation of their progeny

Melanocytic stem cells of the adult hair follicle display an exquisite example of the regulatory function of *PAX3/Pax3* in stem and progenitor cell survival. Both the epidermis and the hair follicle are highly regenerative structures which contain a broad range of epithelial stem cell populations and most have the capacity to differentiate into all epidermal cell lineages (Wilson et al., 1994; Taylor et al., 2000; Oshima et al., 2001; Ghazizadeh & Tacichman 2001; Nishimura et al., 2002; Owens & Watt, 2003; Osawa et al., 2005; Levy et al., 2005, 2007; Li et al., 2010). In both the human and mouse hair

follicle, stem cells reside in a distinct anatomical compartment called the bulge, which extends from the sebaceous gland duct to the insertion of the arector pili muscle (Nishimura et al., 2002). There are an estimated five million hair follicles per person (Tobin, 2008), and therefore an abundance of this pluripotent stem cell niche. During postnatal life, the hair follicle continuously undergoes regeneration through cycles of resting, or telogen, (about 3 months in human scalp), followed by active growth, or anagen, (about 3 years in human scalp) and then regression, or catagen (about 2 weeks in human scalp) (Tobin et al., 1999). In response to postnatal hair growth or loss, the hair follicle stem cell niche generates the cell types required for epidermal, hair follicle and sebaceous gland regrowth where the niche is characterised as a specialised microenvironment that supports production and segregation of progeny cells from resident stem cells (Taylor et al., 2000; Oshima et al., 2001; Nishimura et al. 2002; Nishimura et al., 2005; Ohyama et al., 2006). Using the model of hair regeneration, the complex functions of *Pax3*/Pax3 have been elucidated and are definitively linked to the survival and maintenance of melanocytic stem and progenitor cells.

Melanocytic stem cells comprise a subset of cells of the hair follicle stem cell niche that express *Dct* and are responsible for postnatal hair pigmentation (Nishimura et al., 2002; Nishimura et al., 2005). The pigmented hair shaft is produced solely during anagen by programmed changes in the microanatomy and gene expression in the hair follicle. Once activated in anagen, melanocytic stem cells proliferate to give rise to melanoblast progenitors that differentiate to produce pigment for the hair before undergoing apoptosis during catagen (Tobin et al., 1999). The extended anagen growth phase of the hair follicle produces melanocytic cells across a spectrum of differentiation both temporally and spatially. For example, in the transition from telogen to early anagen, the mitotically quiescent melanocytic stem cell is located in the bulge (niche) region.

Following hair growth activation and germitive proliferation, progeny melanoblasts that are amelanotic (or exhibit little melanogenesis) become located in the outer root sheath and proximal hair bulb. In the late stages of anagen the differentiated, melanin producing cells are located in the distal hair bulb, basal layer of the sebaceous gland and infundibulum (Botchkareva et al., 2001). Over the stages of anagen hair growth, melanocytic cells express phenotypic variations linked to anatomical and functional status. Despite species specific differences between human and mouse hair follicle stem cells, it is possible to relate the PAX3/Pax3 functions of each subpopulation of melanocytic stem cells and progeny melanoblasts during hair follicle growth (Lang et al. 2005; Osawa et al., 2005, Medic & Ziman, 2010).

Firstly, quiescence of stem cells requires that they be accompanied by lower metabolic and transcription rates, remain in the G0/G1 phase of the cell cycle, yet have the capacity for intense proliferation once activated. In melanocytic stem cells, the quiescent state is established via direct Pax3 repression of *Dct* (Lang et al, 2005), and a lack of *Sox10* expression which abrogates *Mitf* upregulation and ensures 'stemness' of the cells (Watanabe et al., 1998; Bondurand et al., 2000; Lang et al., 2005; Osawa et al, 2005). Once activated by anagen, progeny of melanocytic stem cells are activated for rapid proliferation and melanocyte differentiation by a complex orchestration of the co-factors Sox10, Pax3, beta-catenin and Mitf. In progenitor melanoblasts, *de novo* Sox10 acts synergistically with Pax3 to activate transcription of *Mitf* which in turn, acts as regulator of proliferation and survival of melanoblasts (Lang et al., 2005). Upregulated Mitf also competes with Pax3 for the *Dct* enhancer region such that when Pax3 is displaced from the enhancer by beta-catenin signalling, melanoblasts are directed into the melanogenic program via Mitf upregulation of *Dct*. When Mitf is initially competitively inhibited from binding *Dct* by Pax3, intracellular Mitf levels increase;

however, once Pax3 mediated repression of *Dct* is removed by beta-catenin/Mitf binding, the melanoblast undergoes rapid terminal differentiation and *Pax3* is downregulated (Lang et al., 2005). In this way, the role of Pax3 in regenerative postnatal melanoblasts of the hair follicle is analogous to the role of Pax3 in skeletal muscle satellite cells; in particular, precocious differentiation of cells is prevented via Pax3 repression of downstream target genes and lifted via cell-mediated signalling.

While much is known about the regeneration of hair follicle melanocytes, the origin of melanocyte replacement cells for the adult human epidermis is poorly understood. The turnover of interfollicular melanocytes is minimal as they rarely undergo mitosis (Jimbow et al., 1975; Pawelek, 1976) and it is acknowledged that normal human epidermal melanocytes have increased longevity with resistance to apoptosis (Plettenberg et al., 1995). The decades of longevity of the melanocyte in the epidermis predisposes it to DNA mutations that can lead to malignant transformation despite cellular processes that focus on cell cycle arrest for DNA excision repair and anti-apoptotic mechanisms (Abdel-Malek et al., 2010). Severely damaged melanocytes, however, do apoptose and are discharged from the epidermis after acute sun exposure before naevi or melanoma formation (Pharis & Zitelli, 2003; Petronic-Rosic et al., 2004). The role of PAX3 in the apoptosis of sun-damaged melanocytes is unfolding; however, the mechanisms of replacement of lost human epidermal melanocytes following trauma or disease remain largely unknown.

The little that is known about epidermal melanocyte replacement has been gleaned through the study of the skin disorder vitiligo, where the loss of epidermal melanocytes results in localised, depigmented patches of skin. Following skin therapy, repigmentation begins perifollicularly and spreads circumferentially outwards in such a

way that the origin of the replacement melanocytes appears to be the hair follicle stem cell niche which is spared in the disease (Grichnik, 2008). Intriguingly, the therapeutic response of hairless skin to vitiligous treatment has a similar concentric repigmentation pattern (Davids et al., 2009) (Fig. 5) where a stem cell population in the interfollicular epidermis is theorised to be responsible for melanocyte replacement (Toma et al., 2001; Yu, 2002; Fernandes et al., 2004; Li et al., 2010).

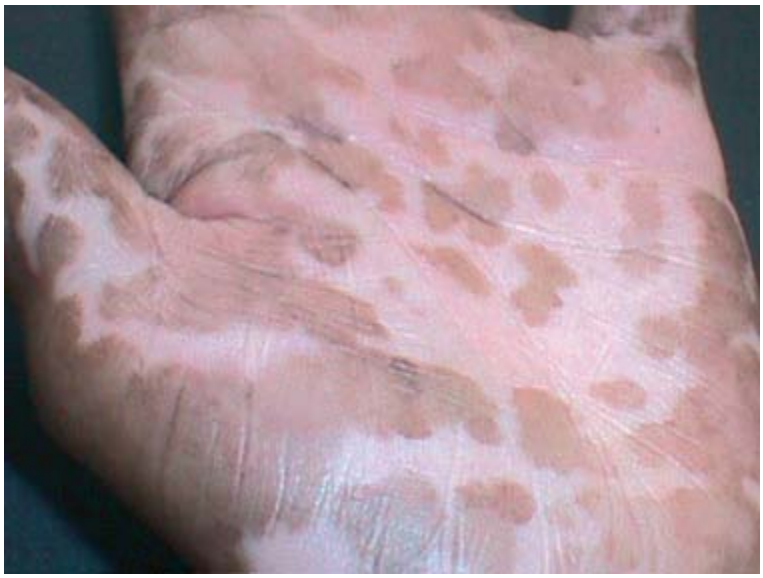

Figure 5. **Vitiligous repigmentation.** The photo shows the therapeutic repigmentation of hairless vitiligous skin where the repigmentation pattern spreads circumferentially. *Photo courtesy of Davids et al., 2009.*

It has been found that a population of stem cells in the interfollicular dermis, called multipotent skin precursor cells, express Pax3 (Fernandes et al., 2004). These particular neural crest-derived cells are said to persist into adulthood as an antigenically distinct subset of stem cells located in the dermis and analysis of their phenotype reveals that they co-express early embryonic genes such as *slug*, *snail* and *twist* (Fernandes et al., 2004). Whether these stem cells contribute to melanocyte replacement, however is undetermined. A final, alternative theory for the origin of replacement melanocytes in human adult skin is that "stem cells persist after birth in the superficial nerve sheath and give rise to ... dermal migratory melanocytes when replacements for epidermal

melanocytes are needed in postnatal skin" (Cramer, 2009). As embryonic melanoblasts are seen in the ventral, neurogenic migratory pathway, this theory may be valid; however, to date, no conclusive evidence exists. The theory is particularly noteworthy, however, in light of the hypotheses proposed in this thesis.

1.8 Aberrant *PAX3*/*Pax3* expression in melanoblasts

As with developmental skeletal myogenesis, *PAX3/Pax3* is expressed in a spatially and temporally restricted manner during developmental melanogenesis. The importance of its regulation of melanocyte development is highlighted by the findings that mutations in PAX3 cause Waardenburg syndrome in humans (Foy, 1990; Hoth et al., 1993; Tassabehji et al., 1993) and the *Splotch* phenotype in mice (Franz, 1990; Epstein, 1991). As detailed above, homozygous *Pax3* mutant *Splotch* mice die in utero around embryonic day 13.5 with deficiencies in neural crest-derived structures such as absence (or severely reduced numbers) of melanocytes. While it has been demonstrated that elimination of *Pax3* in *Splotch* embryos alters the ability of neural crest cells to migrate, it has been determined that *Pax3* is not required for neural crest cell proliferation (Epstein et al., 2000). *Splotch-delayed* is the least severely affected of the known *Splotch* alleles that results from a transversion at nucleotide 421 of the *Pax3* transcript which produces a glycine to arginine substitution in the paired domain of Pax3 such that DNA binding is largely inhibited (Vogan et al., 1993). Full-length transcripts of *Pax3* mRNA are also produced in *Splotch-delayed* mutants, although the amount is 5-fold less than that found in wild-type mice (Goulding et al., 1993). *Splotch-delayed* homozygous embryos survive until embryonic day 18.5 (Moase & Trasler, 1990) at which stage, significant neural crest cell death is observed within the neuroepithelium both prior to emigration and after the migratory cells reach target tissues. These findings are interpreted to suggest that cell death, linked to pertubation of *Pax3*, plays a role in the

Splotch neural crest deficits (O'Shea & Liu, 1987).

In humans, aberrant *PAX3* gene dosage is seen in Waardenburg Syndrome Types I and III. The autosomal dominant conditions are caused by point mutations in *PAX3* which lead to abnormal neural crest development and pathogenesis of melanocytes of the skin, hair and stria vascularis of the cochlea (Epstein et al., 1991; Tassabehji et al., 1992). Heterogenous *PAX3* mutations cause a spectrum of pigmentary symptoms amongst affected individuals, ranging from interruption of melanocyte metabolism to piebaldism (a congenital white forelock, scattered hyperpigmented epidermal macules and a triangular shaped depigmented epidermal patch on the forehead) (Fig. 6). Congenital

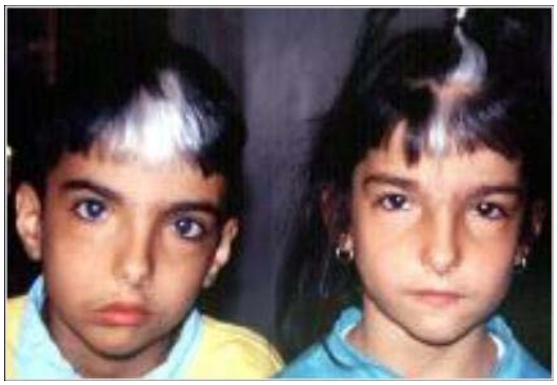

Figure 6. **Children affected by Waardenburg Syndrome I with piebaldism.** The white forelock is a pigmentation defect in the hair follicles due to the absence of functional melanocytes.
Photo courtesy of http://emedicine.medscape.com/article/950277-overview

piebaldism results from either a defect in the migration of melanoblasts from the neural crest or a failure of melanoblasts to survive or differentiate into melanocytes once localised to the ventral aspect of the skin (Bolognia & Pawelek, 1988). Only one example of a patient with Waardenburg Syndrome containing a homozygous defect in *PAX3* has been reported to survive into postnatal life and this individual had a complete absence of pigmentation of the skin, hair and eyes (Zlotogora et al., 1995).

While the pathology of Waardenburg Syndromes I and III is clearly indicative of the

critical role of *PAX3*/PAX3 in embryonic melanocyte development, aberrant *PAX3* gene dosage also has a detrimental effect on maintenance of the adult hair follicle stem cell niche and is evidenced by the fact that 44% of persons with Waardenburg Syndrome I have premature hair greying (Da Silva, 1991). Normally, the stem cell niche of the hair follicle produces fifteen melanocyte generations over an average forty year grey-free lifespan (Tobin, 2008). In Waardenburg Syndrome I, the melanocyte stem cell reservoir is depleted after fewer hair cycles. Either damaged melanocytes or defective melanosomes cause hair bulb melanocytes to continuously undergo apoptosis until replacement by stem cells is exhausted (Sato et al., 1973). This indicates a principle role for *PAX3* in the survival of adult follicular melanocytic stem cells.

In many ways analogous to the transformation of the adult skeletal myoblast by perturbed *PAX3* expression, overexpression of *PAX3* in adult melanocytes is linked to cutaneous malignant melanoma. It is theorised that *PAX3* expression in terminally differentiated melanocytes is linked to oncogenesis and metastasis (Scholl et al., 2001; Muratovska et al., 2003; Parker et al., 2004; He et al., 2005; Plummer et al., 2008; Medic and Ziman, 2011). Moreover, the *PAX3d* transcript is seen overexpressed in transformed melanocytes (Barr et al., 1999, Barber et al., 1999; Blake & Ziman, 2005) where production of the alternate transactivation domain (compared to the constitutive *PAX3c* encoded protein) (Fig. 1) is thought to have significance in the transformation of the melanocyte. Specifically, *in vitro* analyses have demonstrated that *PAX3d* transfected melanocytes grow significantly faster with a higher proportion of cells in S phase compared to control cells (Wang et al., 2006). Normally, melanocytes undergo mitosis infrequently, however recent findings report that a small proportion of melanocytes of extremely sun-exposed skin re-express PAX3 and are proliferative (Medic & Ziman, 2010). Additionally, *PAX3d* transfected melanocytes show a significant inhibition of

apoptosis (Wang et al., 2006). *In vitro* results also report that a high proportion of PAX3 expressant melanocytes of extremely sun-exposed adult skin co-express the PAX3 target anti-apoptotic factor BCL2L1 (Margue et al., 2000; Medic et al., 2011). Thus, mutated melanocytes of extremely sun-exposed skin may be proliferative and resistant to apoptosis through PAX3 overexpression.

To summarise, *Pax3* has an early role in direction of neural crest cells toward a melanoblast fate in the neural crest staging area. As migration of specified neural crest precursors occurs within the developing embryo, *Pax3* has an indirect role in the survival of these cells linked to upregulation of *Mitf*, the master regulator of the survival of migratory melanoblasts. Germline mutations of *PAX3* that occur in melanoblasts affect upregulation of MITF such that melanoblast migration is perturbed; this results in characteristic pigmentary disorders such as those seen in persons affected with Waardenburg Syndromes I and III. In order for developmental melanoblasts to advance into the melanogenic-specific transcriptional program, *Pax3* inhibition of *Dct* must be lifted for subsequent upregulation of downstream melanogenic genes and thus, terminal differentiation of melanocytes. Finally, comparable to skeletal muscle tissue, a persistent population of *PAX3* expressant melanoblasts remains in adult skin as melanocyte progenitor cells. Once activated by epidermal injury or growth of the hair follicle, PAX3 functions as a molecular switch within melanocyte progenitor cells both to activate proliferation and to inhibit precocious differentiation while it primes the cell for differentiation.

1.9 How does *Pax3* govern the development of embryonic peripheral glioblasts?

In development of the peripheral nervous system, *Pax3* is known to be expressed in a characteristic, temporal pattern in peripheral glioblasts, or Schwann cells (Kioussi et al,

1995). While expression patterns of *Pax3* in embryonic and adult Schwann cells are reminiscent of myo- and melanogenetic expression patterns, little is known about *Pax3* function in both embryonic and adult gliogenesis. Thus, the impetus for this experimental work, namely, to identify and characterise cells that express *Pax3* in adult mouse peripheral nerve, was fueled by the scarcity of literature related to the function of *Pax3* in Schwann cells.

Schwann cells, one of the many cells types to arise from the neural crest (Le Douarin, 1986), are the supporting glia of peripheral nerve fibres. Gliogenesis begins with a wave of neural crest cell migration that proceeds ventrally, adjacent to the neural tube and within the anterior portion of the somite, where formation of the peripheral spinal ganglia and nerves occurs. In 10-12 day old mouse embryos, expression of *Pax3* delineates the bipotent glial/melanocyte precursor cells seen in the developing spinal ganglia (Goulding et al., 1991; Kioussi et al., 1995; Jessen & Mirsky, 1999). While the function of *Pax3* in these cells is unknown, an absence of the spinal ganglia is observed in the homozygous *Splotch* mice and indicates a role for Pax3 in the early generation and/or survival of the cells that form these structures. Similar to that seen in the *Pax3* regulation of somite patterning during early embryogenesis, where the loss of *Pax3* expression in skeletal myoblasts results in the malformation of the somite, so the loss of *Pax3* in neural crest cells results in the malformation of the developing spinal ganglia.

From embryonic day 11, specification of the bipotent (glial/melanocyte) neural crest cell in the ventral pathway is controlled by cellular contact with either nerve (followed by interactions with neuregulin/ErbB3 signals for adoption of glial fate) or contact with mesenchme (followed by insulin-like growth factor 1 and platelet-derived growth factor signals for melanocyte specification) (Thomas & Erickson, 2008; Adameyko et al.,

2009). Concurrent with glial specification, rapidly dividing precursor Schwann cells migrate along established ß-neuregulin-1 secreting axon tracts mediated by activation of tyrosine receptor kinase C signalling and low-affinity nerve growth factor receptor (p75NGFR) activity (Anton et al., 1994; Bhattacharyya et al., 1994; Mirsky et al, 1996; Bentley & Lee, 2000; Yamauchi et al., 2004; Yamauchi et al., 2005). At this stage, maintenance of the mitotic and chemotactic glial cell is regulated by transcription factor Sry-box 2 (*Sox2)* and *Sox10* (Kuhlbrodt et al, 1998; Peirano et al, 2000; Wegner, 2000; Britsch et al, 2001; Wakamatsu et al, 2004; Le et al, 2005). *Pax3* is also expressed in precursor Schwann cells at this stage (Blanchard et al., 1996) and based on knowledge of its function in migratory embryonic melanoblasts, it can be speculated that Pax3 cooperates with Sox10 to maintain the precursor Schwann cell via regulation of downstream target genes necessary for survival and/or migration. Support for this lies in the fact that when homozygous *Splotch* mice die at embryonic day 13.5, precursor Schwann cells cannot be detected (Franz, 1990). In homozygotes with the *Splotch-delayed* allele (which survive until embryonic day 18.5), a small number of glial-specified cells can be detected along peripheral nerve at embryonic day 13.5 although two days later, these cells cannot be detected (Moase & Trasler, 1990).

Transition from Schwann precursor to immature Schwann cell occurs between embryonic days 12 and 16 in the mouse, accompanied by a morphological change and the establishment of an autocrine survival circuit (Jessen & Mirsky, 1992; Jessen & Mirsky, 1994; Dong et al., 1995; Grinspan et al., 1996; Syroid et al., 1996; Murphy et al., 1996; Dong et al., 1999; Meier et al., 1999). In this independent state, immature Schwann cells undergo radial axonal sorting (Yu et al., 2005), a process by which they penetrate between axons to segregate them. Radial sorting is coupled to extensive Schwann cell mitotic and apoptotic activity so that the ratio of Schwann cells to axons

within the developing peripheral nerve trunk is specific (Friede and Samorajski, 1968; Stewart et al., 1993; Grinspan et al., 1996; Topilko et al. 1996; Nakao et al., 1997; Syroid et al., 1996; Carroll et al., 1997; Garratt et al. 2000). During this stage of Schwann cell development, *Pax3* is not expressed, thus, its marked downregulation from embryonic day 13.5-18.5 (Kioussi et al., 1995) indicates that it does not function to regulate cellular proliferation, survival or apoptosis during radial sorting by glioblasts (Fig. 7).

While survival of immature Schwann cells at this stage is not regulated by axonal factors, the signals for specification into myelinating or nonmyelinating cells are linked to dose dependent axonally secreted factors (Grinspan et al., 1996; Topilko et al. 1996; Carroll et al., 1997; Garratt et al. 2000). An undefined axonal-Schwann cell interaction signals for larger calibre axons to be ensheathed at a 1:1 axon-Schwann ratio (eventually to be myelinated) and the smaller calibre axons to be ensheathed at a 5-20:1 ratio (to remain nonmyelinated). From embryonic day 18.5 to postnatal day 5 there is a window of increased *Pax3* expression seen in immature Schwann cells where it is suggested to function for transcriptional repression of the myelination program (Kioussi et al., 1995). Around birth, Schwann cells determined to myelinate exit from the cell cycle and downregulate apoptotic factors (Zorick & Lemke, 1996; Jessen & Mirsky, 2002). Exit from the cell cycle leads to elevation of intracellular cyclic AMP levels, repression of immature Schwann genes *Pax3, L1 cell adhesion molecule (L1CAM), glial fibrillary acidic protein (GFAP)* and *p75NGFR* prior to upregulation of the genes required for construction of the myelin sheath (Kioussi et al, 1995; Zorick et al, 1999; Niemann et al, 2000; Parkinson et al, 2004; Le et al, 2005) (Fig. 5). Similar to other cell lineages, Pax3 expression is downregulated as myelinating Schwann cells terminally differentiate.

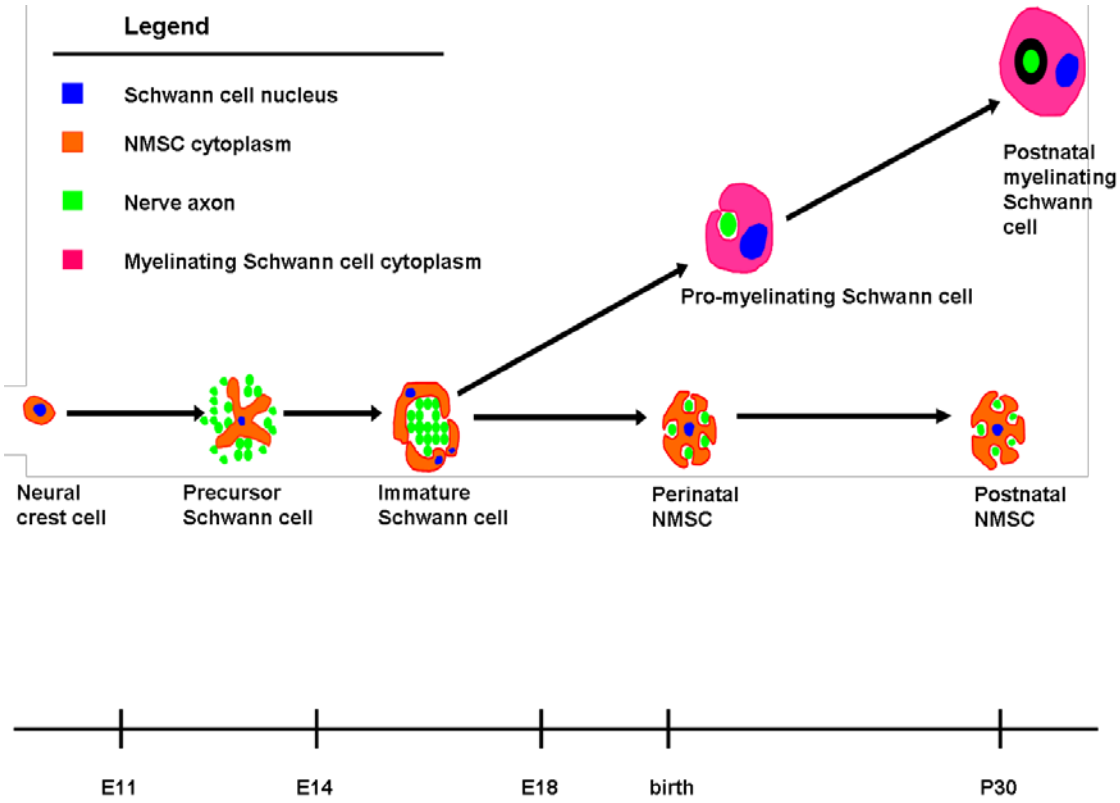

Figure 7. **Schwann cell development.** The diagram indicates the primary stages of Schwann cell development during embryogenesis and the divergence between nonmyelinating and myelinating Schwann cells that occur after birth. *Diagram adapted from Jessen, 2004.*

1.10 Why do nonmyelinating Schwann cells of adult peripheral nerve continue to express *Pax3?*

In the adult peripheral nervous system, C-fibre neurons are nonmyelinated and associate with nonmyelinating Schwann cells (NMSCs). Type C-fibres are subclassified into postganglionic sympathetics and dorsal root afferents which innervate viscera for homeostatic maintenance or conduction of peripheral afferent signals, respectively. Unmyelinated C-fibres are organised into a bundle in which many nerve fibres are ensheathed by one NMSC (Fig. 8); these bundles were originally described by Robert Remak (1838), hence postnatal NMSCs are often referred to as Remak Schwann cells and nonmyelinated bundles are referred to as Remak bundles. NMSCs have a characteristic morphology consisting of extraordinarily long branching networks of

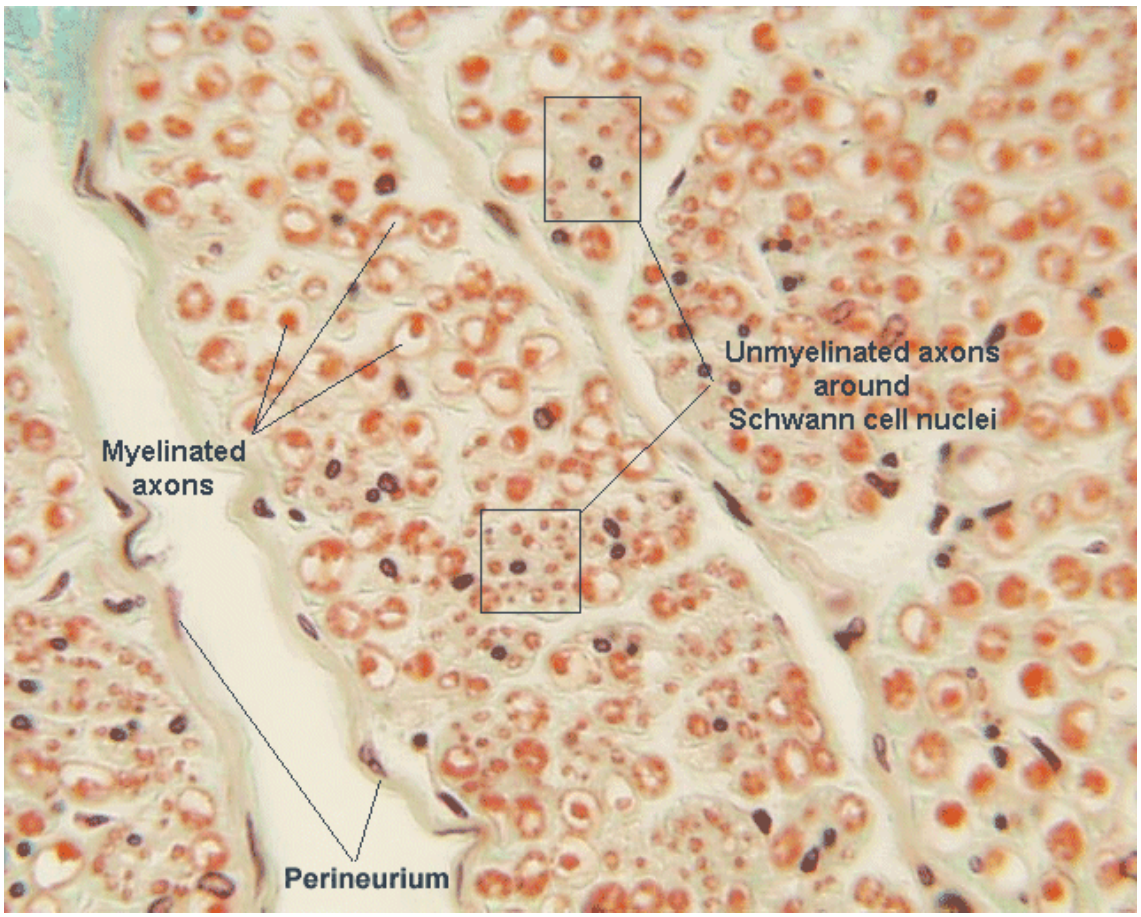

Figure 8. **Remak Schwann cells.** The micrograph shows a cross section through a peripheral nerve trunk. The areas indicated by the boxes are Remak bundles where the NMSC nuclei are associated with several unmyelinated C-fibres. *http://neuromedia.neurobio.ucla.edu/campbell/nervous/wp_images/182_TS_HP.gif*

cytoplasmic processes which form discontinuous syncytium and coalesce in a plexiform manner with adjacent Remak bundles (Carlsen & Behse, 1980; Murinson et al., 2005a) (Fig. 9). NMSCs are phenotypically contrasted to myelinating Schwann cells in that they continue to express immature Schwann genes such as *L1, GFAP, p75NGFR* (Kioussi et al, 1995). Kioussi and colleagues (1995) also report that *Pax3* RNA is associated with NMSCs of 30 day old mice sciatic nerve and suggest that Pax3 functions to maintain a nonmyelinating cell state through direct repression of myelination genes. Although it is unknown whether *Pax3* RNA is translated into protein and whether such protein is transcriptionally active in adult cells, the report indicates continued *Pax3* expression in an adult cell of neural crest origin, in a cell other than a stem or progenitor cell of adult tissue. It is interesting to note that exit from the cell

cycle in postnatal NMSCs does not cause repression of immature Schwann cell genes as it does in myelinating Schwann cells; moreover, postnatal NMSCs are maintained in a characteristically immature Schwann

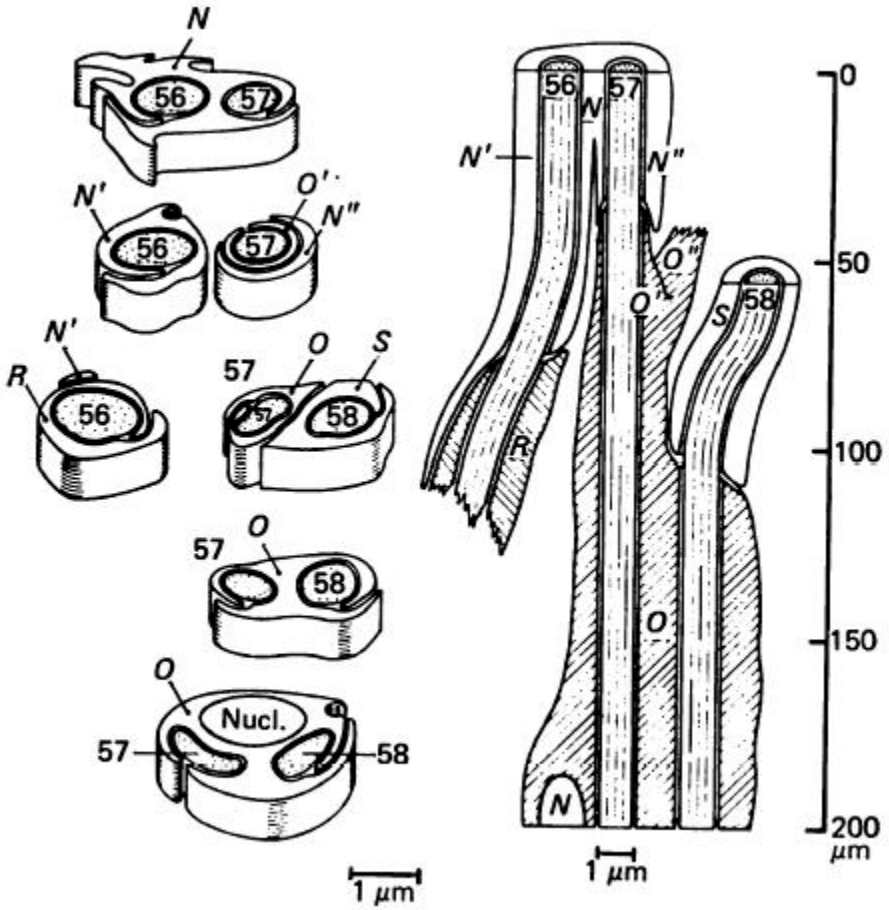

Figure 9. **The Organisation of Remak Schwann Cells in Peripheral Nerve Trunk.** The diagram shows axon-Schwann cell relations at different levels for two neighbouring subunits of a Remak bundle. At level 0 μm the subunit contains axons 56-57, embraced by the profile of the same Schwann cell N. At 40 μm the Schwann cell N is divided into two branches N' and N', each belonging to a different subunit. In addition, a profile from the contiguous Schwann cell 0 has entered and embraces axon 57. At 100 μm, axon 56 is embraced by a different contiguous Schwann cell R and Schwann cell N is only represented by a small profile. From 120 to 200 μm, the axons 57 and 58 are embraced by Schwann cell 0. *Diagram from Carlsen & Behse, 1980.*

phenotype. Thus, curiousity about the adult NMSC phenotype and expression of *Pax3* in adult nerve was the major driving force behind the development of the research methods to identify, visualise and characterise Pax3 expression in adult mouse peripheral nerve.

1.11 What is the role of *Pax3* in regenerative glioblasts of adult peripheral nerve?

Unlike other *Pax3* regulated tissue lineages, little is known about the *Pax3* expression observed in regenerative Schwann progenitor cells of adult peripheral nerve. In adult nerve regeneration, cells that express Pax3 are said to arise from myelinated cells that regress to an immature state (Kioussi et al., 1995; Harrisingh et al, 2004) rather than arise from a resident stem cell population such as in skeletal muscle and skin. While the function(s) of *Pax3* in progenitor Schwann cells of adult nerve remains unknown, that *Pax3* is upregulated after injury/disease may allude to its role in the maintenance of the progenitor cell state (Kioussi et al., 1995; Harrisingh et al, 2004).

Peripheral nerve injuries are varied but can be classified as those which produce localised conduction block (neuropraxia), interruption of axoplasm flow without severance of the nerve (axonotmesis) and those in which the nerve trunk is severed (neurotmesis). Conditions existing at the site of these various types of nerve injuries are different. For ease of understanding, *Pax3* expression in relation to Schwann cell responses to neurotmesis is discussed. Normally, the neuronal perikaryon maintains the axon through axoplasmic flow such that transection results in a series of biological alterations that lead to complete structural disintegration and chemical degradation of the segregated distal axon. The inflammatory response and effects of axonal separation from the nucleus are named Wallerian degeneration. A fundamental characteristic of Wallerian degeneration is the reported plasticity of adult myelinating Schwann cells that revert from the myelinogenic transcriptional program (or differentiated state) into the cell cycle and back (Salzer & Bunge, 1980). Typically, the phenotypic regression of a terminally differentiated mammalian cell is prevented in order to ensure cell-type specification, function and stability. During Wallerian degeneration, myelinating Schwann cell nuclei enter the DNA synthesis phase during which the myelin is

relatively intact (Stoll et al., 1989). Re-entry into the cell cycle, however, represents a commitment to demyelination (Griffin & Thompson, 2008). In the distal stump of the transected nerve, changes commence within cells as they discard degraded myelin into cytoplasmic ovoids and initialise autophagocytosis of myelin proteins and lipids (Perry & Brown, 1992; Fernandez-Valle et al., 1995). In terms of gene expression, the molecular mechanisms for the reversion of the quiescent myelinated Schwann cell to a proliferative state are linked to sustained signalling by the extracellular signal-regulated kinase-1 transduction pathway (Harrisingh et al, 2004) and *Pax3* expression remains silent (Kioussi et al., 1995).

Haematogenous macrophage infiltration of the degenerating distal trunk corresponds with maximal myelin degradation (Weinberg et al., 1978; Perry & Brown, 1992; Fernandez-Valle et al., 1995; Stoll & Muller, 1999) and concomitant inhibition of genes encoding for myelin structural proteins occurs within denervated demyelinating Schwann cells (Gupta et al, 1990; LeBlanc & Poduslo, 1990; Spreyer et al., 1990; Scherer et al, 1995). *Pax3* is upregulated at this stage followed by induction of the characteristic immature Schwann cell markers such as *GFAP*, *L1* and *p75NGFR* (Kioussi et al., 1995). Once the demyelinated phenotype is established, mitogens promote Schwann cell proliferation within the persisting distal Schwann cell basal lamina (Pellegrino et al., 1986; Baichwal et al., 1989) where internally multiplying Schwann cells form a longitudinal column, or Bungner band, which provides a pathway that proximally regenerating axons use to reach the original target tissue (Weinberg & Spencer, 1978; Ide, 1983; Salonen et al., 1987; Tona et al., 1993; Ara et al., 2005). As Schwann cells begin to produce and store myelin for remyelination of regenerating axons, *Pax3* levels temporally peak; in contrast, as myelination nears completion, *Pax3* is re-silenced (Kioussi et al., 1995). While theories for the function of *Pax3* in

myelinated nerve regeneration include prevention of premature myelogenesis and/or orchestration of Schwann progeny migration, development of efficacious methods for identification and visualisation of Pax3 expressant cells in adult peripheral nerve (a primary aim of this thesis) would facilitate future studies of the role of *Pax3* in peripheral nerve regeneration.

In summary, *Pax3* is expressed in dorsal regions of the neural fold from which neural crest cells originate. Development of the Schwann cell progresses from the neural crest cell to the bipotent precursor as early tissue patterning occurs during the formation of the spinal ganglia, during which time *Pax3* remains expressed. Precursor Schwann cells are specified through association with developing nerve and are dependent upon nerve-secreted mitogens and survival factors. They are highly motile and proliferative during peripheral growth and extension of the nerves and it is theorised that *Pax3* has a role in the survival and/or migration of these glioblasts. Radial sorting commences as the embryo grows rapidly; at this stage, immature Schwann cells survive by autocrine secreted factors and proliferate extensively while *Pax3* expression is silent. Nerve fibre associations are re-established with immature Schwann cells in a ratio-specific manner and terminal differentiation into the myelinating or nonmyelinating phenotype is initiated around birth. At this time, a brief window of *Pax3* re-expression is thought to prevent precocious myelination of cells via repression of target myelination genes (Kioussi et al., 1995). After birth, terminal differentiation of Schwann cells commences where downregulation of *Pax3* occurs in myelinating cells and expression is said to continue in nonmyelinating cells. In cases of peripheral nerve trauma or disease, myelinating Schwann cells re-express *Pax3* at a time when genes coding for myelin structural proteins are inhibited within denervated, demyelinating Schwann cells. A spike of *Pax3* expression occurs following successful reinnervation; during

reconstruction of the myelin sheath, *Pax3* expression is re-silenced. It should be mentioned that there is a paucity of studies that discuss the regeneration of nonmyelinated fibres and associative NMSCs.

1.12 Conclusion

PAX3/Pax3 has numerous integral functions in embryonic tissue morphogenesis and knowledge of its complex expression and function in cells of adult tissues continues to unfold. The roles of *PAX3/Pax3* are well defined across a variety of adult tissue lineages. From these studies, it can be concluded that the overarching purpose for continued expression of *PAX3/Pax3* in adult cells is primarily for maintenance of the progenitor cell state. In adult progenitor cells it is said that *PAX3/Pax3* protects the 'stemness' of the cell through regulation of downstream target genes involved in survival, apoptosis, migration and/or differentiation. This characteristic regulatory role is reminiscent of its embryonic function and appears conserved across an entire spectrum of cell and tissue types.

HYPOTHESES

The supposition that peripheral nerves harbour progenitor cells forms the basis for this research. The supposition is based on the fact that 30 day old mouse peripheral nerves express *Pax3* and that the function of *Pax3* in most adult tissues is for the maintenance of a progenitor cell population. Furthermore, a small body of literature has shown that, in the regenerative adult nerve trunk, NMSCs (that are reported to express *Pax3*) are proliferative, chemotactic and apoptotic in response to many forms of disease and injury, notably, those associated with loss of myelinated nerves. For example, in persons with Charcot-Marie Tooth disease type 1A, a disease linked to genetic pertubation of a gene that encodes a constitutive myelin protein, 'unaffected' NMSCs proliferate in the diseased nerve in response to lost myelinating cells affected by the mutation (Koike et al., 2007). Likewise, Murinson et al. (2005b) induced degeneration of distal myelinated fibres with a lesion of the ventral root and showed that normal, innervated NMSCs of the adjacent dorsal root ganglion enter the cell cycle while unaffected myelinating Schwann cells do not. Similarly, in specifically induced degeneration of myelinated fibres, intact NMSCs of adjacent Remak bundles extend cytoplasmic processes to temporarily ensheathe naked portions of neighbouring demyelinated fibres. Subsequently, a population of proliferative, NMSCs migrate through the endoneurium to overlie areas of demyelination. While the origin of the “supernumary” NMSCs remains unknown, it is suggested that they arise from adjacent Remak bundles (Griffin et al., 1987).

In addition, Neurofibromatosis Type 1 (NF1) affects 1 in 3500 newborns worldwide and is characterised by loss of the *NF1*gene that encodes neurofibromin (Gutmann, 2001; Le & Parada, 2007; Theos & Korf, 2006). Persons affected with NF1 are predisposed to develop benign peripheral nerve sheath tumours (or neurofibromas), myeloid leukemia,

hyperpigmentation of the skin and learning disabilities (Cichowski & Jacks, 2001; Riccardi, 2000; Zhu et al., 2002). Moreover, persons with a loss of heterozygosity of *NF1* alleles develop malignant peripheral nerve sheath tumours (Serra et al., 2000). Neurofibromas consist primarily of NMSCs (Rutkowski et al., 2000; Serra et al., 2000; Sheela et al., 1990) where malignant transformation is linked to loss of neurofibromin resulting in NMSC hyperproliferation and detrimental effects on adjacent cells (Zheng et al., 2008). Importantly, in neurofibroma, it has been found that tumours have a significant population of stem cells (Pongpudpunth et al., 2010) and although the origin of the stem cells remains unknown, Pongpudpunth et al (2010) proposed that "formation of neurofibromas may be linked to alterations in the self-renewal program of peripheral nerve progenitor cells".

Based on the above evidence and knowledge of the roles of *PAX3/Pax3* in stem and progenitor cell maintenance, it was hypothesised that a subset of adult NMSCs, reported to express *Pax3*, are early immature Schwann glioblasts that are retained along C-fibre tracts following birth and remain resident in the unmyelinated Remak bundles. In the research described in this thesis, the aims were to identify these cells *in vivo*, by the use of Pax3 (and other molecular markers) and to describe their morphology and location. Furthermore, it was hypothesised that cells that express Pax3 in adult mouse peripheral nerve would co-express early immature Schwann cell markers.

AIMS

1. It was a primary objective to develop foundational methods of labelling NMSC in the mouse species such that the studies could be compared and contrasted with future investigations undertaken using mutant mouse strains, in particular, *Pax3* mutant animals. Therefore, each of the aims was directed toward investigations using adult mice.

2. It was queried which transcripts of *Pax3* are expressed in the peripheral nerves of adult mice and queried whether knowledge of the *Pax3* transcriptome would give more understanding, based on the knowledge of functional differences of alternate *Pax3* transcripts, of its continued expression into adulthood in peripheral nerves. The first research aim thus became to determine the transcript profile of *Pax3* in normal adult mouse sciatic nerve.

3. Hundreds of studies have revealed the mechanisms of myelinated nerve regeneration and the role of the associated myelinated Schwann cells in peripheral nerve regeneration; however, few studies have investigated non-myelinated nerve regeneration and the role of associated NMSCs. It was thought important to develop methods with which to identify and visualise NMSCs *in vivo* using immunofluorescence; therefore, an important aim of the research became to develop immunofluorescent methods to label cell membrane bound low-affinty nerve growth factor receptor (p75Ngfr) on Remak bundles in normal adult mouse sciatic nerve and to assess the use of Pax3 as a marker of nonmyelinating Schwann cell nuclei in normal adult mouse sciatic nerve.

4. Finally, it was hypothesised that the *Pax3* expressing NMSCs may represent a population of Schwann glioblasts that are retained from embryogenesis; therefore, the final aim of the research became to develop immunofluorescent methods to double-label Pax3 and (early immature Schwann cell marker) Sox2 in normal adult mouse sciatic nerve in order to discern whether cells that express Pax3 retain a Schwann glioblast phenotype.

2

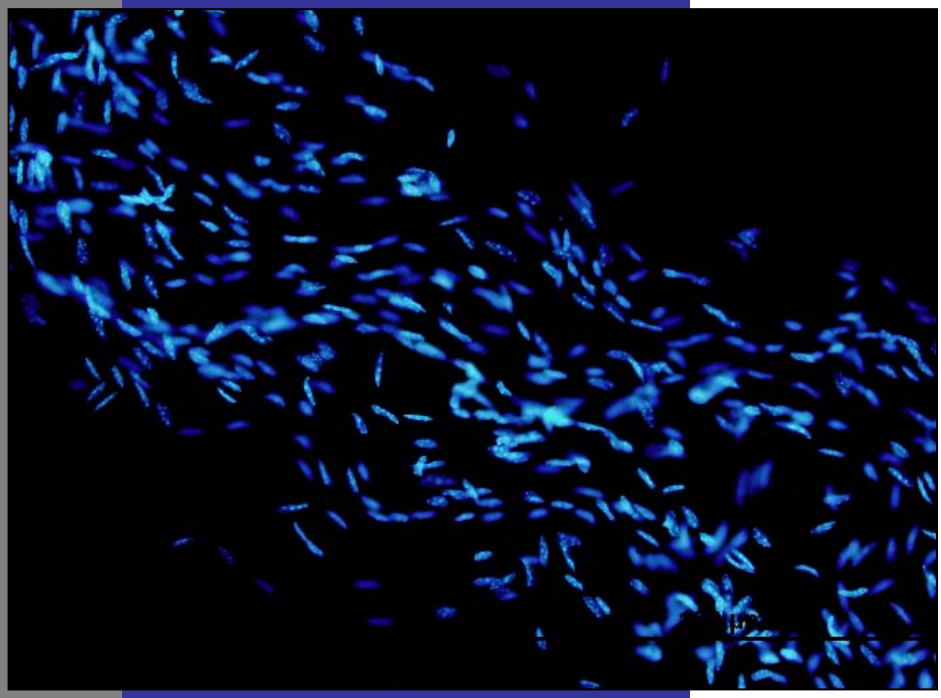

METHODS

2.1 Animals

Experimental procedures were carried out in accordance with the provisions of the National Health and Medical Research Council Australian Code for Responsible Conduct of Research (2007), the Australian code of practice for the care and use of animals for scientific purposes (2004) and the Animal Welfare Act (2002). Experimentation was approved by the Edith Cowan University Animal Ethics Committee (project code 06-A7 ZIMAN). Experiments were conducted using *Mus musculus* tissue. The age of the animals was chosen to reflect the cellular makeup of adult or mature tissue. All the investigations described were undertaken using 60 day old male mice that were provided by the Animal Resources Centre (Canning Vale, Western Australia), bar the C22 mice mentioned below.

Charcot-Marie-Tooth disease is a hereditary peripheral neuropathy classified as demyelinating (CMT1) or axonal (CMT2) forms. Subtype CMT1A is inherited as an autosomal dominant trait where partial duplication of the gene encoding peripheral myelin protein-22 leads to chronic demyelination and Schwann cell hyperplasia which results in progressive muscle weakness and hand and/or foot deformations (Chance & Fischbeck, 1994). Adult transgenic mice were generated by Huxley et al. (1996) by pronuclear injection of a yeast artificial chromosome containing the CMT1A duplication of *peripheral myelin protein-22*; the mutant mouse strain (C22) has phenotypic traits in common with persons affected with CMT1A (Huxley et al., 1996). C22 sciatic nerves were prepared and generously donated by the Genomé Humain et Développment, Faculté de Médecine de la Timone, France.

2.2 Isolation of RNA from sciatic nerve specimens

Mice were sacrificed by CO_2 narcosis at 20%/minute v/v and the sciatic nerves were

rapidly excised in an aseptic field. Nerves were dissected and ligated under a Leica Zoom 2000 dissecting microscope, with care taken to remove connective fascia from the epineurium. Freshly removed nerve tissue was immediately frozen by immersion in liquid nitrogen and stored at -80°C until further use. Total RNA was isolated from one individual sciatic nerve using TriReagent (Molecular Research Center, Inc.). Isolated tissues were homogenised using a glass-col mortar and pestle and incubated in TriReagent for 5 minutes at 25°C. Samples were shaken vigorously for 15 seconds and further incubated for 15 minutes. Samples were centrifuged at 12,000g for 15 minutes at 4°C before transfer of the aqueous phase to a fresh tube. 250 µl of isopropanol and 250 µl of 0.8 M sodium citrate/1.2 M Na Cl were added prior to incubation for 10 minutes at 25°C. Samples were centrifuged at 12,000g for 8 minutes at 4°C and supernatant was removed. The RNA pellet was washed with 1 ml of 75% v/v ethanol and vortexed prior to centrifugation at 12,000g for 8 minutes at 4°C. Ethanol was removed with a fine tube pipette without disruption of the RNA pellet. The RNA pellet was air-dried for 5 minutes prior to resuspension in 100 µl RNAse free water. Resuspended RNA was incubated at 60°C for 3 minutes to ensure complete dissolution of the RNA pellet. For each extraction, RNA purity and concentration were assessed using a Bioanalyzer (Agilent).

2.3 RT-PCR amplification of *Pax3* from whole nerve specimens

First strand cDNA was synthesised from 2 µg of isolated RNA using an OmniScript system (Qiagen) and an oligo$(dT)_{18}$ primer (10 µM) (Qiagen). Reverse transcription was carried out at 37°C for 1 hour in a total volume of 20 µl. Negative controls included reactions without Omniscript reverse transcriptase. PCR amplifications were performed using a TaqDNA Polymerase Kit (Qiagen). All solutions were kept on ice after complete thawing and vortexed prior to use. The PCR mix was prepared using the reagents shown

in Table 1 and a negative control (without template DNA) was included in every experiment.

Table 1. PCR Reaction Composition.

Component	**Volume/reaction**	**Final concentration**
10x PCR Buffer	2.0 µl	
dNTP mix	0.4 µl	10 mM each
Forward Primer	0.8 µl	0.5 µM
Reverse Primer	0.8 µl	0.5 µM
Taq DNA Polymerase	0.1 µl	
Q solution	4.0 µl	
Distilled water	9.9 µl	
Template DNA	2.0 µl	≤1 µg/reaction
Total volume	**20 µl**	

The PCR mix was kept on ice before being placed in the Eppendorf Mastercycler gradient thermal cycler. The PCR reaction was conducted with the following oligonucleotides, designed using OligoAnalyser 3.1 (Integrated DNA Technologies) and Primer-BLAST (NCBI):

Pax3c: (F) 5'-ACCAGGCATGGATTTTCAAG;

(R) 5'-AACGTCCAAGGCTTACTTTG

Pax3d: (F) 5'-CCTCAGGTAATGGGACTTCT;

(R) 5'-AATGAAAGGCACTTTGTCCA

Pax3^8: (F) 5'-CTGTGTCAGATCCCAGCA;

(R) 5'-GAGATAATGAAAGGCACCTGAG

Pax3f: (F) 5'-CAGATGAAGGCTCCGATATTGAC;

(R) 5'-CTGGCTTGAGATAATGAAAGGC

Internal controls for cDNA were performed using PCR amplification of mouse housekeeping gene *Gapdh* and the primers used were as follows:

Gapdh: (F) 5'-GTGAAGGTCGGTGTGAACG;

(R) 5'-ATTTGATGTTAGTGGGGTCTCG

Positive controls for primers were performed using total RNA isolated from embryonic day 11 mice and PCR negative controls eliminated cDNA as primer template from each PCR reaction. Thermocycling parameters are shown in Table 2.

Table 2. Thermal Cycler Conditions.

Initial denaturation	3 min	95°C
3-step cycling		
Denaturation	30 sec	94°C
Annealing	1 min	50°C *Gapdh* 48 °C *Pax3c* 48 °C *Pax3d* 50 °C *Pax3^8* 50 °C *Pax3f*
Extension	1 min	72°C
Number of cycles	39	
Final extension	10 min	72°C

PCR amplifications were performed using a thermocycler. PCR products were resolved on 1.5% w/v agarose gels and visualised under UV light using a Geldoc system. PCR products were sequenced using an ABI PRISM BigDye Terminator Cycle Sequencing Ready Reaction Kit (PE Biosystems) and an ABI Prism 3730 48 capillary sequencer. Sequences were aligned with known sequences in GenBank using the multiAlign tool in Angis, available on GenBank (http://blast.ncbi.nlm.nih.gov/Blast.cgi).

2.4 Preparation of frozen nerve sections

Wild-type and C22 frozen sections were fixed and prepared using an identical procedure; C22 nerves were harvested and fixed in the laboratory at Genomé Humain et

Développment, Faculté de Médecine de la Timone, France prior to overnight shipping on dry ice. To prepare fresh frozen sections of sciatic nerve, animals were sacrificed by cervical dislocation. The sciatic nerves were surgically excised, immersed in Tissue Tek O.C.T. (Sakura Finetek Europe) and frozen in liquid nitrogen cooled N-methyl butane (Sigma). Tissue blocks containing the entire length of a sciatic nerve were cryosectioned using a Thermos Shandon Cryotome E at 9 µm onto SuperFrost slides (Menzel-Gläser), dried and fixed in 4% w/v paraformaldehyde in 0.1 M phosphate buffer (PFA) for 30 minutes. Sections were washed in phosphate buffered saline (PBS) 3 times for 5 minutes prior to subsequent processing or storage at -80°C. To prepare pre-fixed frozen sections, animals were anaesthetised with Nembutal (Abbott) and transcardially perfused through the left ventricle; a constant flow (10 ml/min) of PBS (10ml) followed by ice cold PFA in 0.1M phosphate buffer at pH 7.4 (50ml) was established using a peristaltic pump. Sciatic nerves were surgically excised, post-fixed in PFA for 6 hours before immersion in 30% w/v sucrose for 48 hours. Individual sciatic nerves were rinsed in PBS, immersed in Tissue Tek O.C.T. and frozen in liquid nitrogen cooled N-methyl butane prior to cryosectioning of the entire length of nerve at 9 µm onto SuperFrost slides (Menzel-Gläser). Slides were dried prior to processing or storage at -80°C.

2.5 Preparation of teased nerve specimens

To prepare pre-fixed teased nerves, animals were anaesthetised with Nembutal (Abbott) 75 µg/g and perfused as described above. Sciatic nerves were surgically excised, separated into individual fascicles and cut into 2 mm segments. Subsets of these segments of nerve were post-fixed for either 2, 6 or 18 hours in PFA at 4°C prior to rinsing in PBS. All specimens were prepared onto Polysine slides (Menzel-Gläser) and individual nerve fibres along the 2 mm length were teased apart by 0.2 mm entomology

pins. Preparations were dried overnight before immunohistochemical processing or storage at -80°C. To prepare post-fixed teased nerves, animals were sacrificed by cervical dislocation. Sciatic nerves were immediately excised, separated into individual fascicles and cut into 2 mm segments. Subsets of these segments of nerve were postfixed in 4% w/v PFA for 2, 6 or 18 hours at 4°C or a fixative consisting of 35% v/v methanol, 5% v/v acetic acid, 25% v/v ddH_2O and 35% v/v acetone was used for 2 hours at 4°C (Blanchard et al., 1996). Nerves segments were rinsed in PBS and prepared onto Polysine slides (Menzel-Gläser) where individual nerve fibres were teased apart the entire 2 mm length by 0.2 mm entomology pins. Preparations were dried for 18 hours before immunohistochemical processing or storage at -80°C.

2.6 Preparation of whole mount nerve fascicle specimens

Whole mount preparations were prepared using freshly excised nerves which were obtained from animals sacrificed using CO_2 narcosis. Sciatic nerves were excised, placed on a glass slide (kept on ice) and kept moist with PBS at 4°C. These were teased into fascicles and cut into 2mm segments and mounted directly onto chilled Polysine slides. Slides were dried overnight, post-fixed in acetone for 10 minutes at -20°C and rinsed in PBS at pH 7.4, before immunohistochemical processing or storage at -80°C.

2.7 Antibodies used for immunohistochemistry and immunofluorescence

Primary antibodies used were mouse monoclonal IgG2a anti-quail Pax3 (1:10 v/v; Developmental Studies Hybridoma Bank); rabbit monoclonal anti-mouse Pax3 (1:250 v/v; Invitrogen); rabbit polyclonal anti-mouse Krox24 (1:250 v/v; Aviva Systems Biology); rabbit polyclonal anti-mouse Sox2 (1:200 v/v; Sapphire Bioscience) and rabbit polyclonal anti-mouse p75 nerve growth factor receptor (1:500 v/v; Chemicon). Species specific secondary antibodies used were AlexaFluor488-conjugated to goat anti-

mouse IgG2a (1:500 v/v; Molecular Probes); AlexaFluor546-conjugated to goat anti-rabbit IgG (1:500 v/v; Molecular Probes) and biotinylated goat anti-rabbit/mouse IgG (1:500; Dako). Tertiary antibody used was streptavidin-linked AlexaFluor 546 (1:500 v/v; Molecular Probes).

2.8 Procedure for immunofluorescent staining of frozen sections

Frozen sections were rehydrated in PBS and incubated in blocking buffer composed of 0.2% v/v Triton-X100 (TX100) (Sigma), 5% v/v normal goat serum (NGS) (Vector) in PBS at 25^{o}C for 2 hours. Primary antibodies with 3% v/v NGS and 0.2% v/v TX100 were incubated for 18 hours at 4^{o}C. Sections were washed in PBS 3 times for 5 minutes each. Secondary antibody incubation was performed at 25^{o}C for 2 hours using the appropriate fluorescent-conjugated goat anti-IgG in a solution containing 3% v/v NGS and 0.2% v/v TX100. Sections were washed in PBS 3 times for 5 minutes each where the last wash contained Hoechst DNA dye 33342 (1 ng/ml) (Thermo Fisher Scientific). Coverslips were mounted with FluorSave medium (Calbiochem). Negative controls were processed at the same time but were either not incubated with primary or secondary antibody.

2.9 Procedure for enzyme-linked immunohistochemical staining of frozen sections

Slides were rehydrated in PBS and 0.2% v/v TX100 for 10 min. Sections were then incubated in PBS containing 3% v/v H_2O_2 for 10 min, rinsed and blocked in buffer that contained 0.2% v/v TX100 and 5% v/v NGS in PBS at 25^{o}C for 2 hours. Samples were incubated with primary antibodies diluted in PBS containing 3% v/v NGS and 0.2% v/v TX100 for 18 hours at 4^{o}C. Sections were washed in PBS 3 times for 5 minutes each and incubated with biotinylated IgG that contained 3% v/v NGS and 0.2% v/v TX100 for 2 hours at 25^{o}C. Sections were then washed in PBS 3 times for 5 minutes each prior

to application of horseradish peroxidase-linked streptavidin for 10 min at 25°C. Following a wash in PBS, immunohistochemical staining was visualised using 3, 3-diaminobenzidine (Sigma) as chromogen, and mounted in DePeX (BDH Laboratory Supplies). Negative controls were processed at the same time but were either not incubated with primary or secondary antibody.

2.10 Procedure for immunofluorescent staining of teased nerve fibres

Teased nerve preparations were rehydrated in PBS prior to permeabilisation for 5, 10 or 20 minutes with either 0.2% v/v TX100 in PBS, 0.5% v/v Tween20 (Tw20) (Sigma-Aldrich) in PBS, acetone (Prolab), methanol (Prolab) or 10% w/v dimethyl sulphoxide (Sigma) in PBS (Table 3). Teased fibres were incubated in blocking buffer composed of 0.2% v/v TX100, 5% v/v NGS in PBS at 25°C for 2 hours. Primary antibodies diluted in PBS containing 3% v/v NGS and 0.2% v/v TX100, were incubated for 18 hours at 4°C. Slides were washed in 0.05% v/v Tris buffered saline (TBS)/Tw20, 6 times for 15 minutes each. Secondary antibody incubation was performed at 25°C for 20 minutes. Slides were washed in TBS/Tw20 6 times for 15 minutes each where the last wash contained Hoechst DNA dye (1 ng/ml). Coverslips were mounted with FluorSave medium. Negative controls were processed at the same time but were not incubated with primary antibody. Tissue integrity, intensity of nuclear labelling and non-specific staining were visually determined under a fluorescence microscope (see Microscopy Section) in order to evaluate each permeabilisation method according to the criteria in Table 4.

2.11 Procedure for double immunofluorescent staining of whole mount nerve

Slides were rehydrated in TBS and permeabilised in 0.01% v/v TX100 for 45 minutes at 25°C. Slides were washed in TBS 3 times for 10 minutes each prior to incubation in

10% v/v NGS for 6 hours at 25^{o}C. Primary antibodies were individually or simultaneously incubated with 0.2% v/v TX100 for 18 hours at 4^{o}C. Specimens were washed in 0.05% v/v TBS/Tw20, 6 times for 30 minutes each, using gentle agitation. Secondary antibody incubation was done thereafter at 25^{o}C for 20 minutes. Specimens were washed in TBS/Tween 20, 6 times for 30 minutes using gentle agitation where the last wash contained Hoechst DNA dye (1 ng/ml). Coverslips were mounted with FluorSave medium. Negative controls were processed at the same time but were either not incubated with primary antibody or secondary antibody.

2.12 Microscopy

Fluorescently labelled tissues were viewed with an Olympus BX51 microscope connected to an Olympus DP71 digital camera and digital images were collected in the Olympus analySIS FIVE program and transferred to the IrfanView program for montage construction. The contrast and brightness of these images were adjusted for optimal print quality, but the images were otherwise unaltered. Whole mount specimens were imaged with a BioRad MRC 1000/1024 UV laser scanning confocal microscope on a Nikon Diaphot 300 with either a 40X objective (with zoom) or 60X immersion objective (without zoom) using a 351- and 488-nanometer argon laser and a 543-nanometer helium/neon laser. Gain and black level adjustments were performed to improve analogue to digital signal conversion and background noise was eliminated using a KALMAN filter. Z-stacks were collected using various step-sizes and KALMAN averaging was performed manually for each step. Digital images were collected and compiled in greyscale and subsequently pseudocoloured with hues approximate to the fluorescence emission spectra of the respective fluorophores using the Confocal Assistant^{TM} (4.02) program. Images were transferred to Adobe Photoshop and IrfanView programs for montage construction. The images were unaltered.

3

RESULTS

3.1 *Pax3c* and *Pax3d* transcripts are expressed in 60 day old mouse sciatic nerve

At the onset of the literature review, it was noted that there were conflicting reports about the expression of *PAX3/Pax3* in Schwann cells of adult peripheral nerve. Kioussi et al., (1995) originally reported *Pax3* expression in 30 day old mouse sciatic nerve using *in situ* hybridisation with cDNA-binding probes (sequence data unavailable). In 1999 however, Padilla et al. reported that they were unable to label adult mouse peripheral nerve with a complete *Pax3* cDNA probe. Similarly, Gershon et al. (2005) reported that two widely used antibodies against PAX3, one developed by Grosveld's group at St. Jude's Children's Hospital in Memphis and one by Frederick's group at the Wistar Institute in Philadelphia, did not label glial cells of adult human peripheral nerve specimens. These antibodies target the paired/homeodomain of all Pax3 isoforms and the transactivation domain of the Pax3c and Pax3d isoforms, respectively. The initial aim of the research, therefore, was to investigate and report on the full spectrum of *Pax3* transcripts in normal mouse sciatic nerve. To identify all possible *Mus musculus* mRNA transcripts, the mouse genome sequence available on the NCBI was interrogated for all possible splice sites. Three mouse transcripts have been sequenced to date; *Pax3c* and *Pax3d* are expressed in embryonic cells of the myogenic and melanogenic lineages (Barber et al., 1999) and *Pax3^8*, which encodes a transcriptionally inactive isoform, is expressed in embryonic myogenic precursors (Pritchard et al., 2003). Barber et al. (1999) have reported a *Pax3f* transcript, expressed in the embryonic day 9.5 mouse and although exact sequence data is unavailable, it is thought that the transcript is generated by slicing exon 5 directly to exon 9 using the known splice donor and acceptor sequences (personal communication).

To delineate whether the production of additional mouse transcripts of *Pax3* is possible, a comparison of human and mouse nucleotide sequences was undertaken using the

NCBI BLAST database to search for mouse consensus donor and acceptor splice sequences contained within the *Pax3* locus. *PAX3a* (NCBI Reference Sequence: NM_000438.5) consists of four exons and include an alternate 400 base pair segment in the coding region of exon four which causes a frameshift in the encoded sequence and truncation before exon five (Tsukamoto et al., 1994). The resultant PAX3a isoform consists of 215 amino acids, lacks the homeodomain region and has a shorter and distinct C-terminus. *PAX3b* (NCBI Reference Sequence: NM_013942.4) consists of four exons and also encodes a transcript that causes truncation of the encoded protein before exon five (Tsukamoto et al., 1994). A comparison of the sequences of *PAX3a* and *PAX3b* indicates that they share 717 base-pair nucleotides and 196 amino acids (residues 1-196) at the NH_2 end. The amino acid sequence in the common region shows 100% homology with the amino acids encoded by exons 1-4 (residues 1-196) of the mouse Pax3 gene and intron-exon junctions of exons 1-3 are also conserved between the mouse and human genes (Goulding et al., 1991). The amino acid sequences from 197-215 of human PAX3a or 197-206 of PAX3b are not homologous to those of mouse Pax3 and there is no record of an alternate splice form of *Mus musculus Pax3* that encodes alternate transcripts *Pax3a* and *Pax3b*. Further analysis of the mouse Pax3 gene shows a lack of consensus splice site elements required for production of homologous *Pax3e, Pax3g* and *Pax3h* transcripts such as are produced in humans; moreover, the mouse Pax3 genomic sequence diverges from the human gene in the 3' region from which these transcripts are produced and shows less than 70% homology to the human sequence (Murine clone RP24-529B23 Chromosome 1).

Specific primers were designed therefore to amplify the mRNA of mouse *Pax3c*, *Pax3d*, *Pax3f* and *Pax3^8* transcripts with particular attention paid to the primer sets used to distinguish the *Pax3c* and *Pax3d* transcripts as these vary by 30 nucleotides in the 3'

region (Fig. 10). RT-PCR results confirmed that 2 alternate *Pax3* mRNA transcripts were expressed in 60 day old mouse sciatic nerve (n=6). *Pax3c* or *Pax3d* transcripts were detectable in 4/6 individual nerves, however co-expression of both transcripts was never observed in nerve samples utilised here. In 2/6 nerves analysed, *Pax3* mRNA was undetectable. In all nerves tested, PCR amplification of *Pax3^8* and *Pax3f* mRNA products were undetectable (Fig. 11).

AGGTAATGGG ACTCCTGACC AACCACGGTG GGGTACCTCA TCAGCCCCAG ACTGATTACG
CGCTCTCCCC TCTCACCGGG GGTCTGGAAC CTACCACCAC GGTGTCGGCC AGCTGCAGTC
AGAGACTAGA CCATATGAAG AGCTTGGACA GTCTGCCAAC ATCTCAGTCC TACTGTCCAC
CCACCTATAG CACCACAGGC TACAGTATGG ACCCTGTCAC AGGCTACCAA TATGGGCAGT
ATGGACAAAg taagccttgg acttttagg gggcaatttc tcctggaagg gagataaact
caactcttcc ttaagaaagg tgaattagag gcaagattaa gccacacatg ccggtatcaa
ttttttttt tgcaaagcca gctgactgtt ccagcagggg cttccttgtg taattatttt
cttaactgat gtcaacaaca tcttgcggtt attaattgtt gagacgtgaa acctgattgc
cactaggtaa aacacaaggg ttggccaaaa tgaaataatc cctgacatta gaaacacatg
ttcttaatga ggtcagctcc aggatcatat gggggataat cccagggaca caaagttgtg
tcaaacttgt ctcaggaata aaaatattag tctcaagcct ttgatagcac ggtattaaat
atgacattgt cagcctgtag ctgatcttgc ccctgactgt gaattgtccc agcatgacct
aaaaagctgc gtgtgtttcc ttacagGTGC CTTTCATTAT CTCAAGCCAG ATATCGCGTA
AGTGAACTGT CCACTTGGAG CTAAAACTGG CCCTGTTTCT GGTCTTCGCA GCCTAGATAT
GAAGAATCTG CTCTGAAAAC AAAAAAAAAT TACCCTTTTG TTGGGGGGGG TGGGGCAGTG
GTCCCAATAG GAGACAAAGG AGAGTGATTG ATTTTCTTCC TCCAATAGTT GGTTTCAAAT
CCTTTTGAAC ACGTTCGACA AAAGCAGTGG AGAAGAGGAA GACCTGGAGC AATAAA

Figure 10. **Generation of the *Pax3c* and *Pax3d* transcripts.** Shown here is the genomic sequence of *Pax3*, from exon 8. Exons 8 and 9 are denoted by UPPER case letters while the intronic region is denoted by lower case. In generation of the *Pax3c* pre-mRNA, splicing machinery recognises a signal for cleavage and adenylation located within the intronic region (indicated in red). In generation of the *Pax3d* pre-mRNA transcript, splicing machinery ignores the first signal for cleavage and polyadenylation used for *Pax3c* (in red) and continues transcription until the signal for cleavage and adenylation at the sequences indicated by pink lettering. This longer pre-mRNA will then be spliced at 5' and 3' consensus donor/acceptor sites (indicated in blue) utilising the branchpoint sequence and polypyrimidine tract indicated by green and orange lettering, respectively.

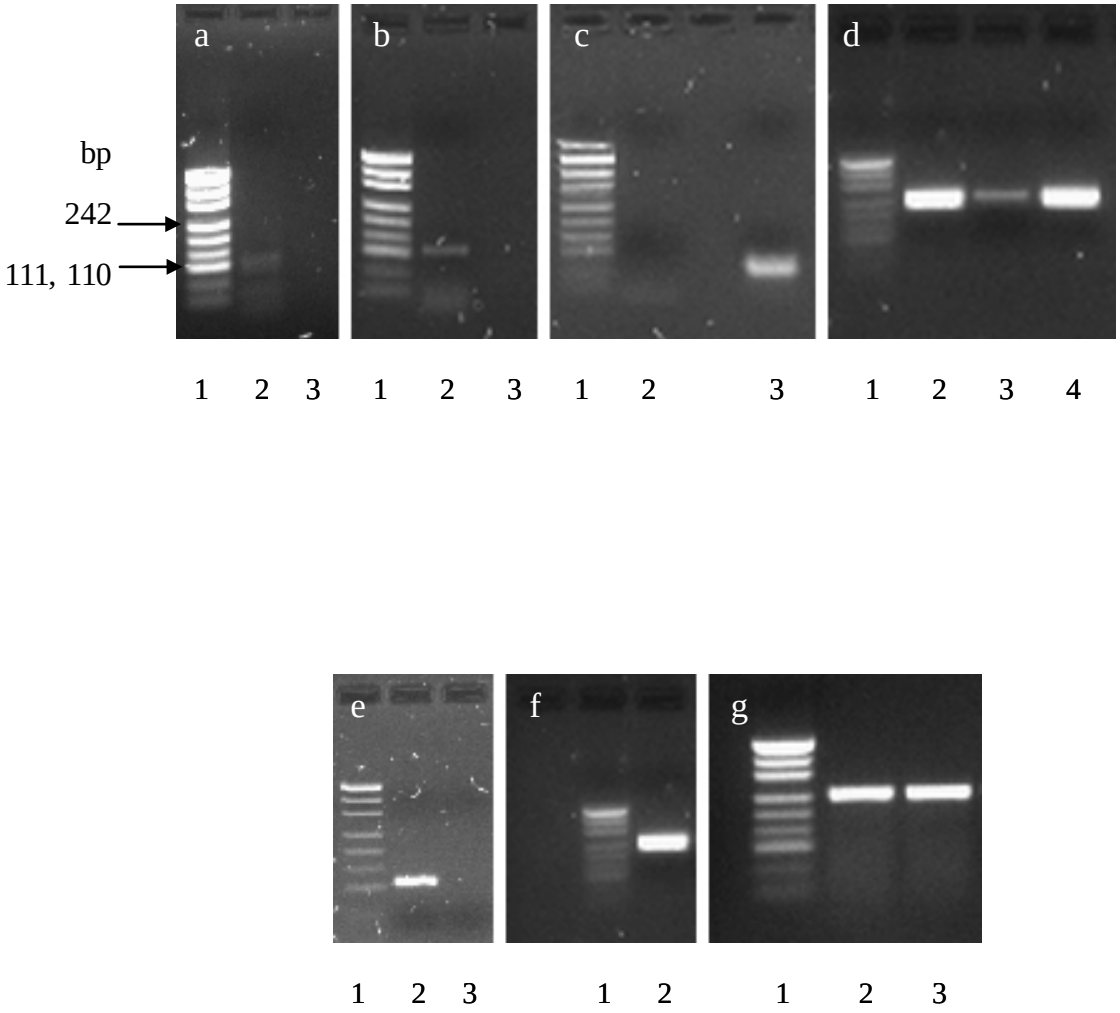

***Figure 11*. RT-PCR results.** Gel electrophoresis of PCR amplification products of Pax3 isoforms from normal mouse sciatic nerves. **a-g)** lane one shows pUC DNA ladder in all gels. Pax3c (117 bp) was expressed in 3/6 nerves tested (lane 2 in **a, b, e**) while Pax3d (97 bp) was expressed in 1/6 nerves tested (lane 3 in **c**). Pax3 products were not amplified in 2/6 nerves tested (data not shown). Positive (+ve) controls for relative amounts of *Gapdh* product amplified from the total RNA of the six nerve lysates are shown in lanes 2, 3, 4 of **d**, lane 2 of **f** and lanes 2, 3 of **g**. Negative controls that eliminated template DNA are shown in lane 3 of **a**, **b**, **e** and lane 2 of **c**. Images are unretouched.

3.2 The morphology of adult mouse NMSCs of sciatic nerve

The complexity of human NMSCs was revealed by Remak in 1838. To date, however, mouse NMSCs that make up Remak bundles have not been morphologically characterised. To observe these complex cells required the development of a variety of methods that preserve their morphological features. Preservation of overall nerve tissue morphology was superior in the whole mount nerve preparations post-fixed with acetone, so much so that the organisation of the cellular and endoneurial components

were readily visualised using fluorescence microscopy (Fig. 12).

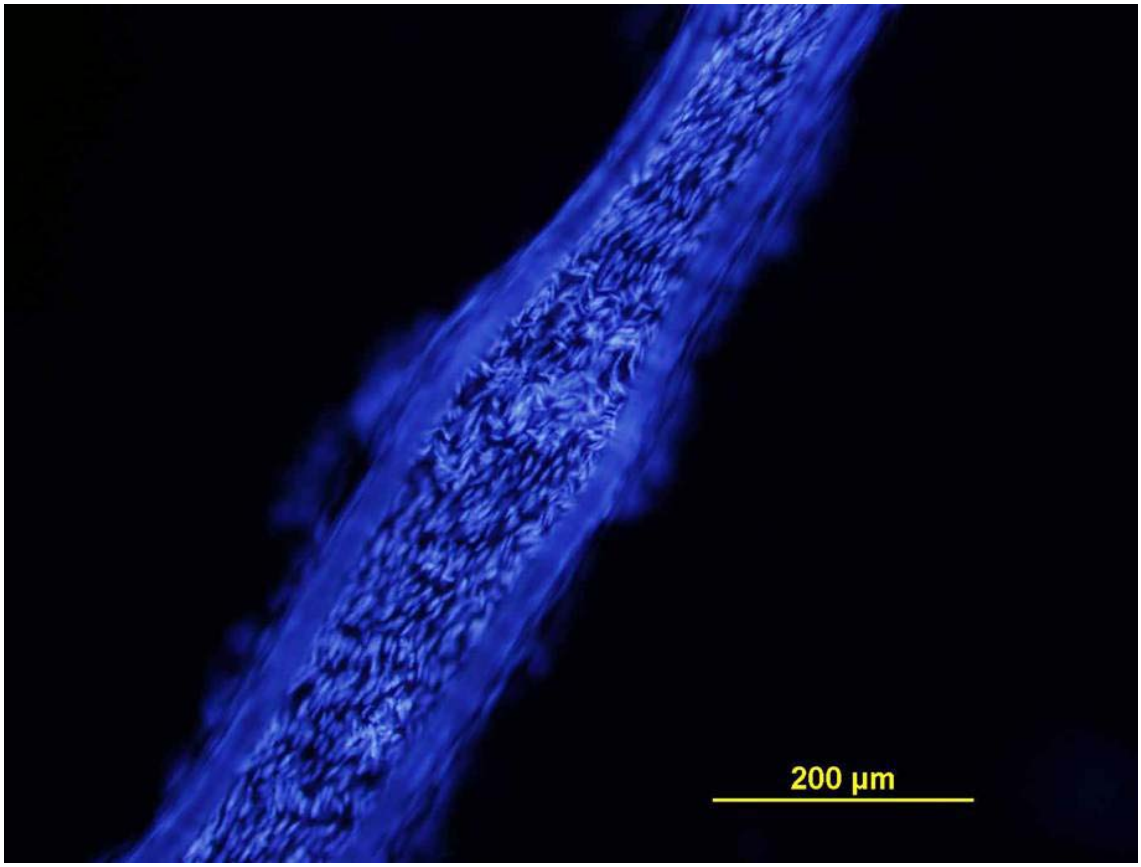

Figure 12. **Whole mount nerve morphology.** A paraformaldehyde perfused and post-fixed whole mount preparation of an eighth cervical posterior root that consists primarily of nonmyelinating Schwann cells is shown. The nuclei of the specimen are stained with Hoechst dye to show the characteristic spindle shape of NMSC nuclei.

Whole mount tissues post-fixed with acetone were not able to be teased into individual Schwann cells and associative axon(s) as cells were strongly adherent to one another and to the entomology pins used for teasing; nerves that had been fixed with paraformaldehyde, however, were efficiently teased into individual Remak bundles comprised of end-to-end NMSCs and associative axons. Analysis of the morphology of NMSCs in the teased fibre specimens showed that mouse NMSCs are 2-4 µm in diameter across the cytoplasmic extensions whereas the cells are 4-5 µm in diameter across the nuclear region (Figs. 13a & 13b, Fig 14). The length of the

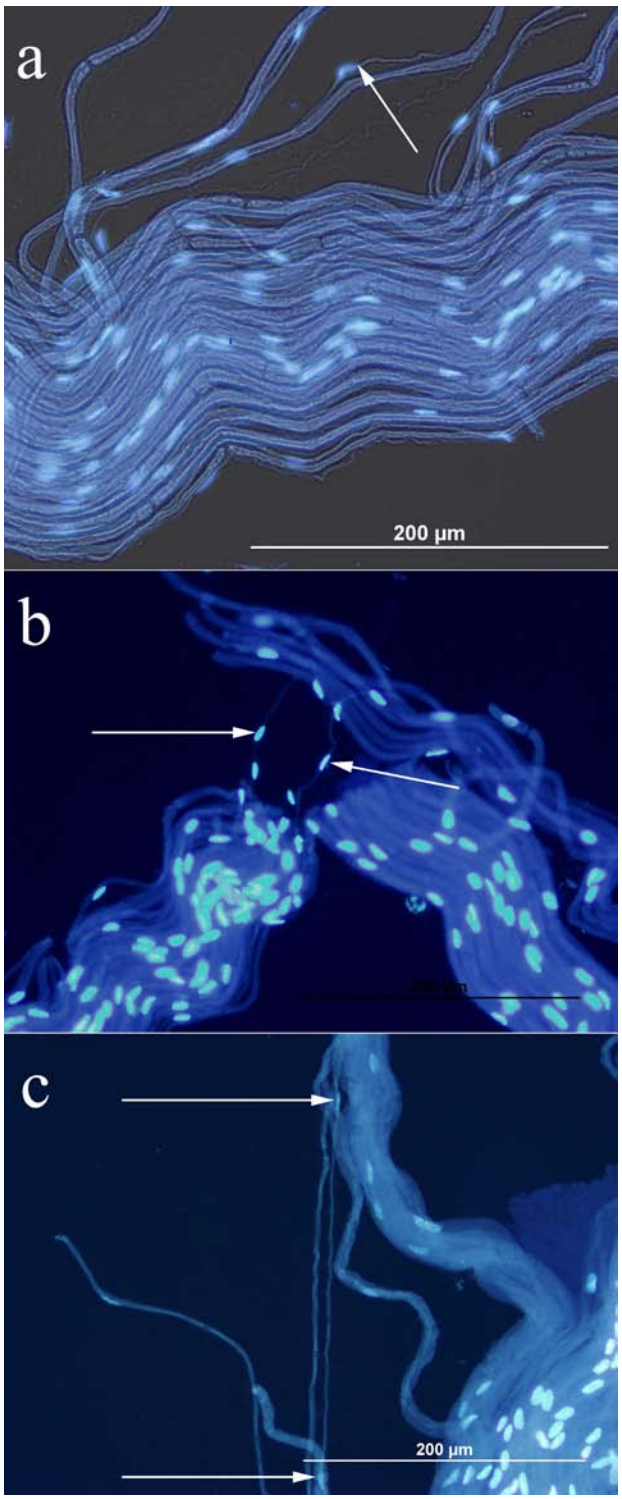

Figure 13. **Mouse nonmyelinating Schwann cell morphology.** Preparations were processed with Hoechst DNA dye to reveal the cell nuclei of the specimens. **a)** Tissues perfused and post-fixed for 2 hours in 4% paraformaldehyde retain superior morphology as evidenced by the retention of the wavelike organisation of the nerve trunk. The arrow indicates a small nonmyelinating Schwann cell juxtaposed to a large myelinating Schwann cell. **b)** Tissues solely post-fixed in 4% paraformaldehyde for 2 hours were difficult to tease, however cell morphology was retained as evidenced by the two small Schwann cells imaged (arrows). *Scale identical to* **13a** *and* **13c**. **c)** Two adjacent nonmyelinating Schwann cell nuclei are imaged (arrows) where the characteristic long cytoplasmic processes coalesce without an internode.

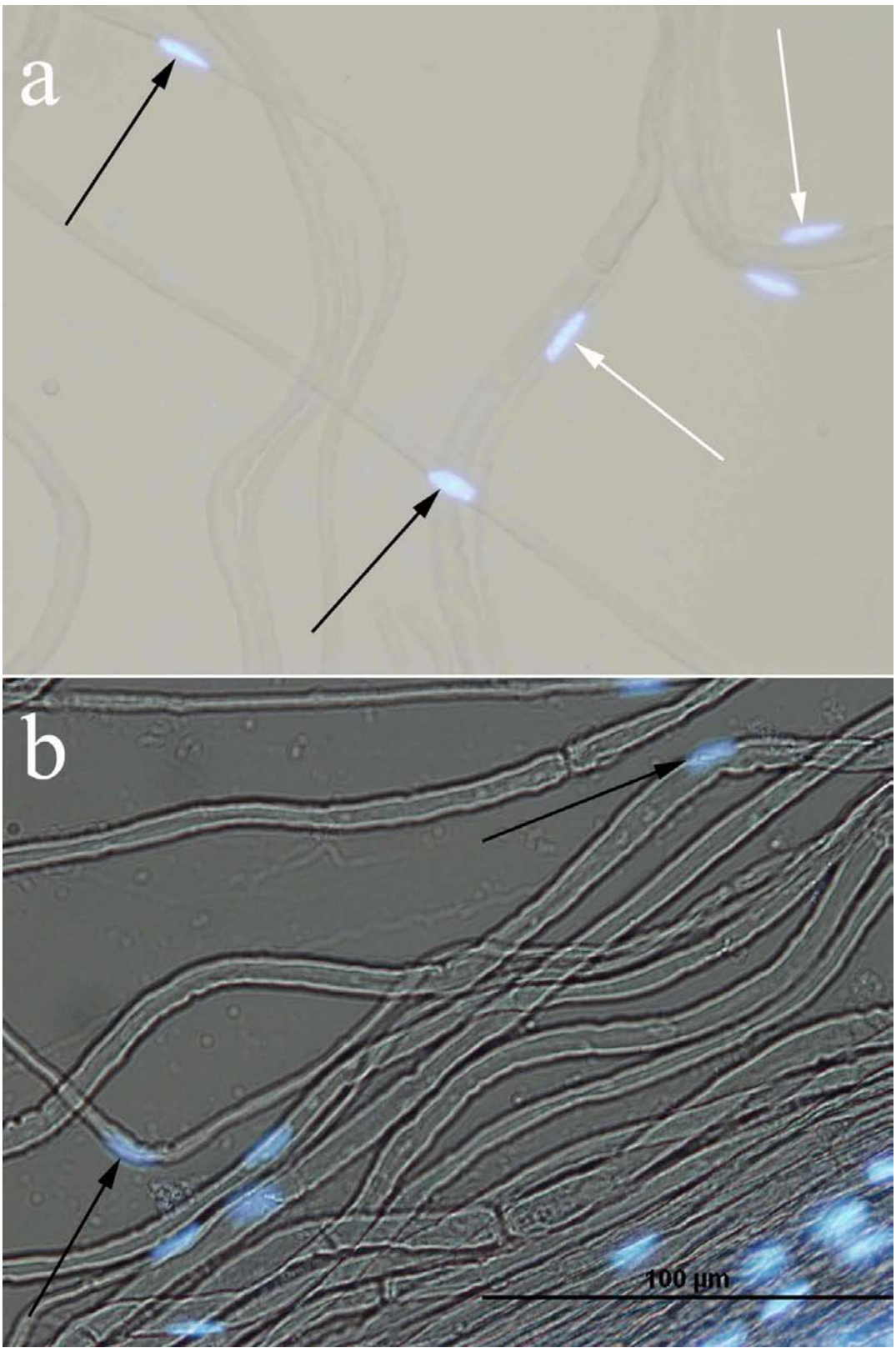

Figure 14. **Morphological characteristics of the nonmyelinating Schwann cell nucleus. a)** Nonmyelinating Schwann cell nuclei are centrally located within the cytoplasm (white arrows). **a, b)** Myelinating Schwann cell nuclei are situated on the periphery of the cell (black arrows). Note that the nonmyelinating Schwann cell nuclei are spindle shaped while the myelinating Schwann cell nuclei are oval or cupped around the fibre they myelinate. *Images are phase contrast merged with fluorescence. Scale bar is the same for both images*

cell is between 80 and 200 μm (Fig. 13c) and the nucleus is between 12 and 20 μm in length (Fig. 13). The nuclei of the NMSCs are centrally located (as opposed to the peripheral location of the nuclei of myelinating Schwann cells) (Fig. 14) and the unmyelinated C-fibres that traverse longitudinally across the NMSC nucleus form it into a characteristic spindle shape (Figs. 13b & 14a) such as has been described for rat NMSCs (Curtis et al., 1992).

3.3 p75Ngfr unveils the structural complexity of adult NMSCs *in vivo*

To distinguish a Remak bundle from the myelinating Schwann cells that associate with small caliber (δ) A fibres, a specific Remak bundle marker was required. Cytoplasmic proteins (e.g. GFAP) have been used in the past to label human NMSCs (Kwa et al, 2003); however, it was thought that a weak Pax3 nuclear label would be difficult to detect adjacent to a strong cytoplasmic signal in a double fluorescent labelling procedure on mouse tissue. There are two subsets of small caliber C-fibres present in adult peripheral nerve. Those which express the p75Ngfr are dependent upon nerve growth factor and synthesise peptidergic neurotransmitters (Averill et al.,1995; Bennett et al., 1996); those that are dependent on glial-derived neurotrophic factor synthesise nonpeptidergic neurotransmitters (Silverman & Kruger, 1988; Mulliver et al., 1997; Bradbury et al., 1998). It has been demonstrated that adult NMSCs simultaneously support both C-fibre types within the same Remak bundle (Murinson et al., 2005a). It is also known that p75Ngfr is expressed on the NMSC plasmalemma adjacent to the p75Ngfr dependent C-fibres it ensheathes (Guenard et al., 1996); therefore, the p75Ngfr was chosen to label Remak bundles and the subset of p75Ngfr expressant C-fibres within the bundle.

Endogenous peripheral nerve tissue autofluorescence (Reynolds et al., 1994) and autofluorescence arising as a result of certain fixation and permeabilisation procedures (Fig. 15), were minimised by the use of specific rinsing protocols (see Methods). Partially teased nerve specimens retained p75Ngfr cell membrane signals throughout the length of the cytoplasmic extensions (Fig. 16). The whole mount nerve fascicle specimens analysed using scanning laser confocal microscopy had superior retention of NMSC membrane integrity and intense p75Ngfr immunolabelling and the plexiform nature of Remak bundles, so aptly described by Carlsen & Behse (1980) in human and Murinson et al. (2005a) in rat, was seen for the first time in 60 day old mouse (Fig. 17)**.**

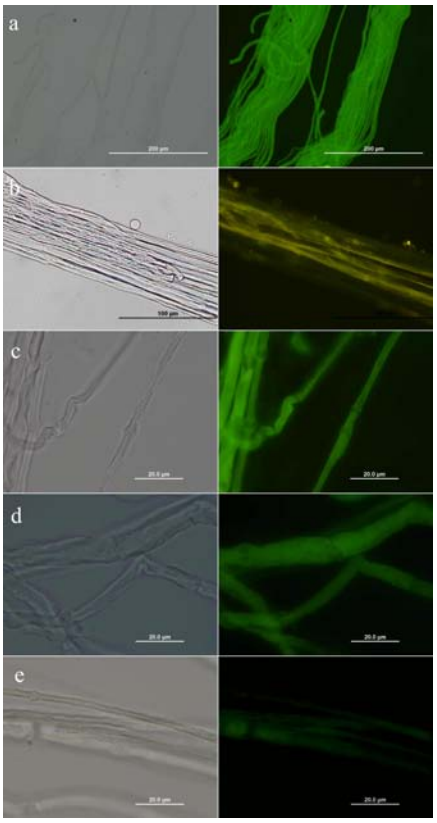

Figure 15. **Immunohistochemical methods affect tissue autofluorescence. a)** Nerves fixed with paraformaldehyde and permeabilised with methanol were difficult to tease and displayed autofluorescence emitted from the collagen of the endoneurium. **b)** Nerves fixed with a fixative that included acetic acid were strongly fluorescent in the 488nm emission range. **c)** Nerves fixed with paraformaldehyde and permeabilised with DMSO retained morphology however, myelin was highly fluorescent. **d)** Nerves perfused with paraformaldehyde and permeabilised with TritonX100 had a low level of autofluorescence, however cell morphology was degraded. **e)** Nerves simultaneously fixed and permeabilised with acetone had little autofluorescence but were unable to be efficiently teased. Specific rinsing methods were adapted to inhibit autofluorescence. *Left panel of images are phase contrast; right panels are fluorescent images.*

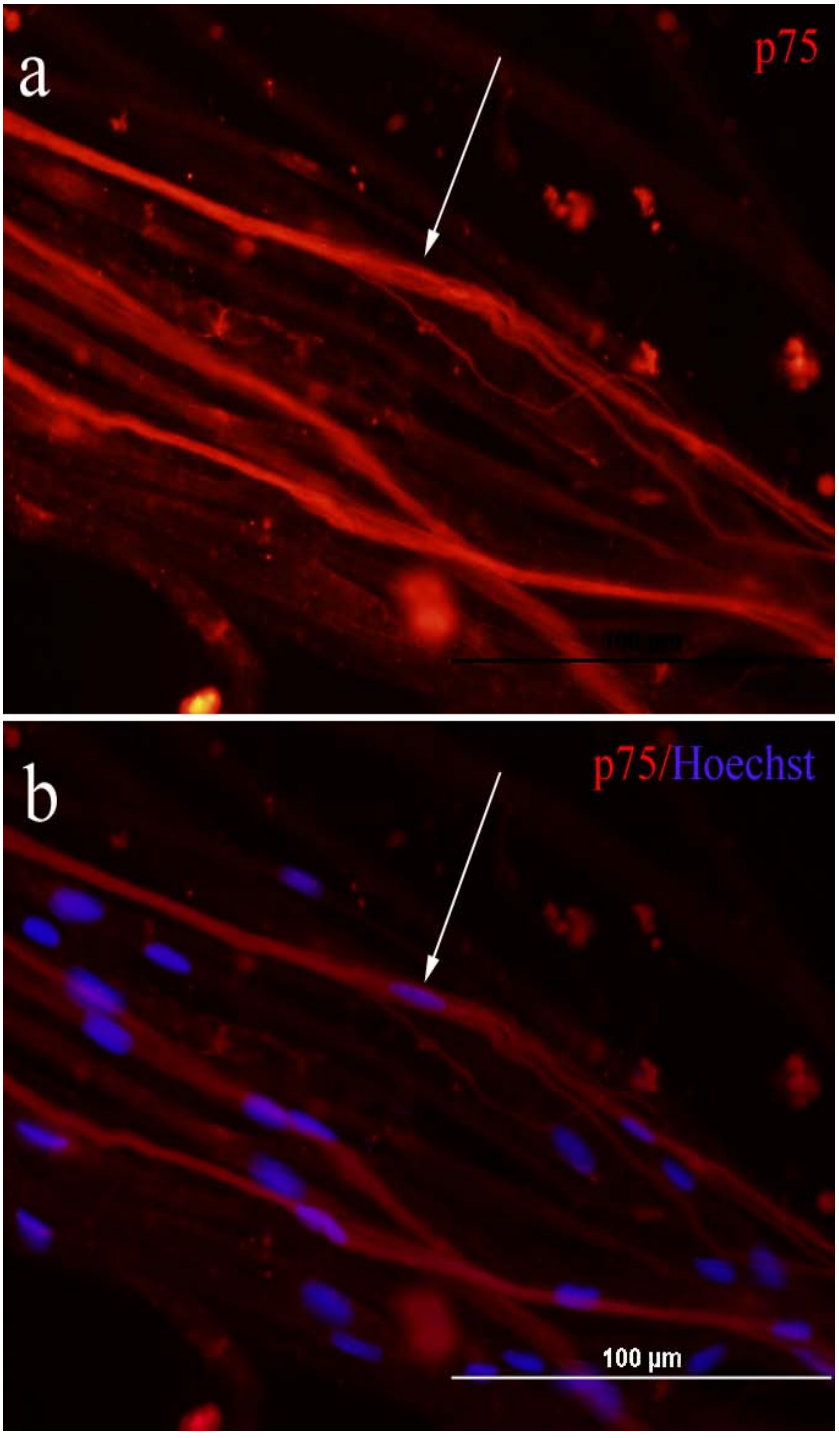

Figure 16. **p75Ngfr is a reliable marker for Remak bundles. a)** Antibodies targeted at the cell membrane receptor (p75) label Remak bundles (red). **b)** Counter-labelled with Hoechst DNA dye, it is evident that the indicated nonmyelinating Schwann cell nucleus (arrow) is associated with a Remak bundle that ensheathes several C-fibres. *Scale bar is the same for both images*

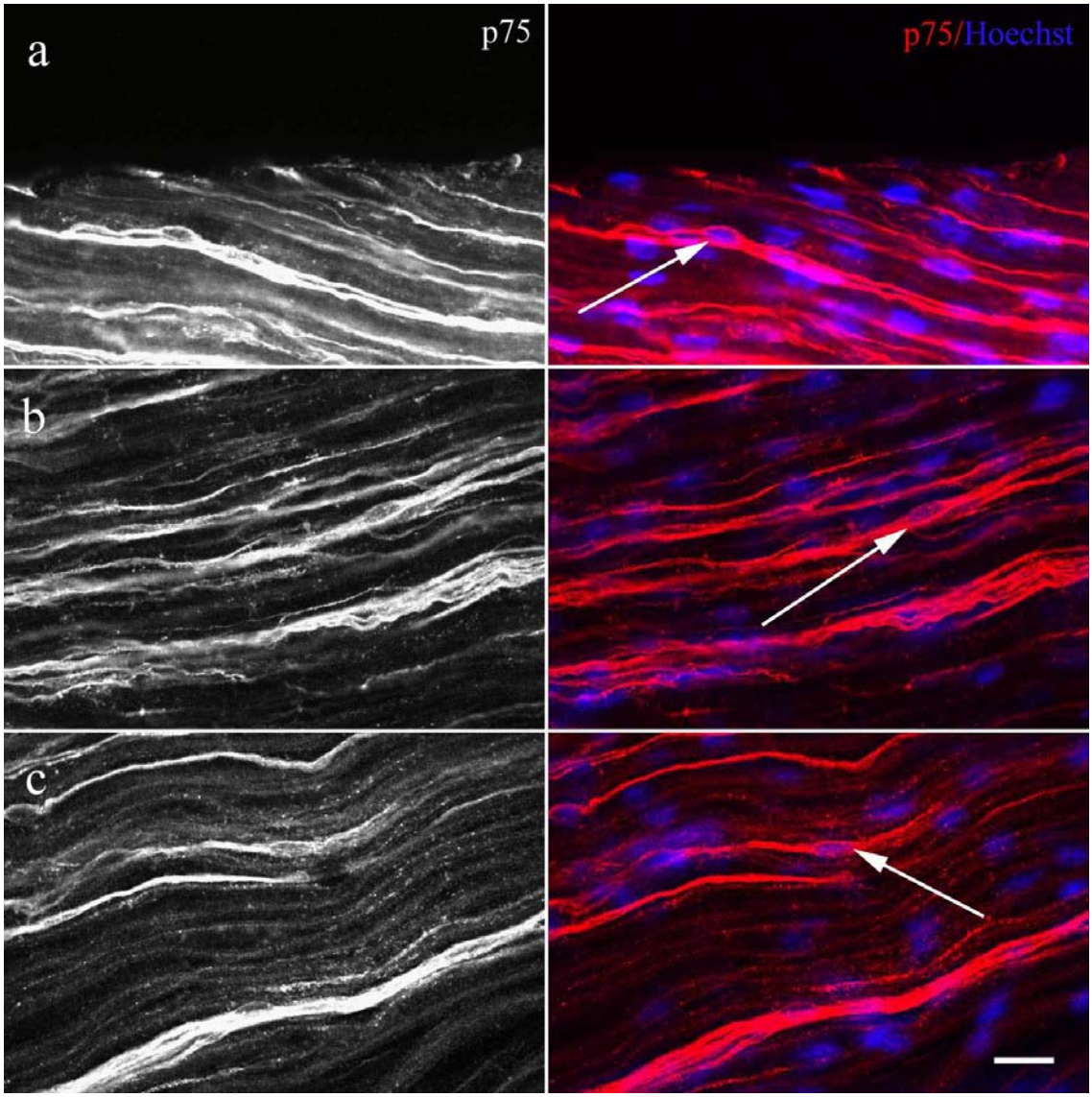

Figure 17. **The complex structure and distribution of Remak bundles in normal adult mouse peripheral nerve. a-c left panel)** Greyscale micrographs of whole mount nerve preparations labelled with anti-p75Ngfr (p75) reveal the plexiform comingling and exchange of p75Ngfr expressant C-fibres between adjacent Remak bundles. **a-c right panel)** Whole mount nerve preparations co-labelled with anti-p75Ngfr and Hoechst DNA dye reveal the *in vivo* distribution of p75Ngfr positive mouse Remak NMSCs (arrows). Note the centralised nuclei of the cells indicated. Images were acquired using scanning laser confocal microscopy. *Pinhole aperture= 3.0. Optical plane = 1.5 μm. Scale bar represents 20 μm.*

3.4 The use of Pax3 as a marker of NMSCs in adult mouse sciatic nerve

One of the principle aims of the work was to develop methods with which to describe the expression pattern of Pax3 protein in adult mouse peripheral nerve with the specific

aim of identifying cells with Pax3 expression. Knowing that *Pax3* has the ability to temporally produce alternatively spliced gene products, it was necessary to determine which *Pax3* transcripts are produced in adult mouse nerve, as the commercially available Pax3 antibodies target epitopes of different domains of the variable protein isoforms.

RT-PCR results verified that *Pax3c* and *Pax3d* transcripts were present in 60 day old mouse sciatic nerve (Fig. 11), thus, it remained to confirm the presence of the proteins encoded by these transcripts in the mouse tissue. Multiple Pax3 antibodies are available; of these, a mouse monoclonal IgG2a isotype-specific antibody directed at amino acids that form the transactivation domain of the quail Pax3 protein (Venters et al., 2004) was employed. Although the quail Pax3 protein has more homology with the human protein than it does with the mouse, the specific amino acids to which the antibody is directed are also present in the mouse Pax3c and Pax3d isoforms. A rabbit monoclonal antibody directed at the paired and homeodomain of human PAX3 was also used; the amino acids to which the antibody is directed are present in all mouse isoforms. When the mouse monoclonal Pax3 antibody was used with the isotype-specific anti-mouse IgG2a secondary antibody, optimal results were obtained and non-specific background staining of endogenous mouse tissue IgGs and other components was minimised.

Pax3 labelling was initially performed using frozen sections of nerve. Antibody-concentration titration experiments were performed and monitored using an indirect immunofluorescent staining procedure. In tangental sections, a nuclear Pax3 label was undetectable (Fig. 18); moreover, longitudinal sections had an indiscriminate labelling (Fig. 19), where specificity of the label was questionable due to the peri-nuclear localisation of the signal. As indicated by the RT-PCR results, Pax3 expression levels

were expected to be relatively low in the sciatic nerves tested. Therefore, a tertiary (avidin/biotin) indirect immunofluorescence procedure was also performed in an

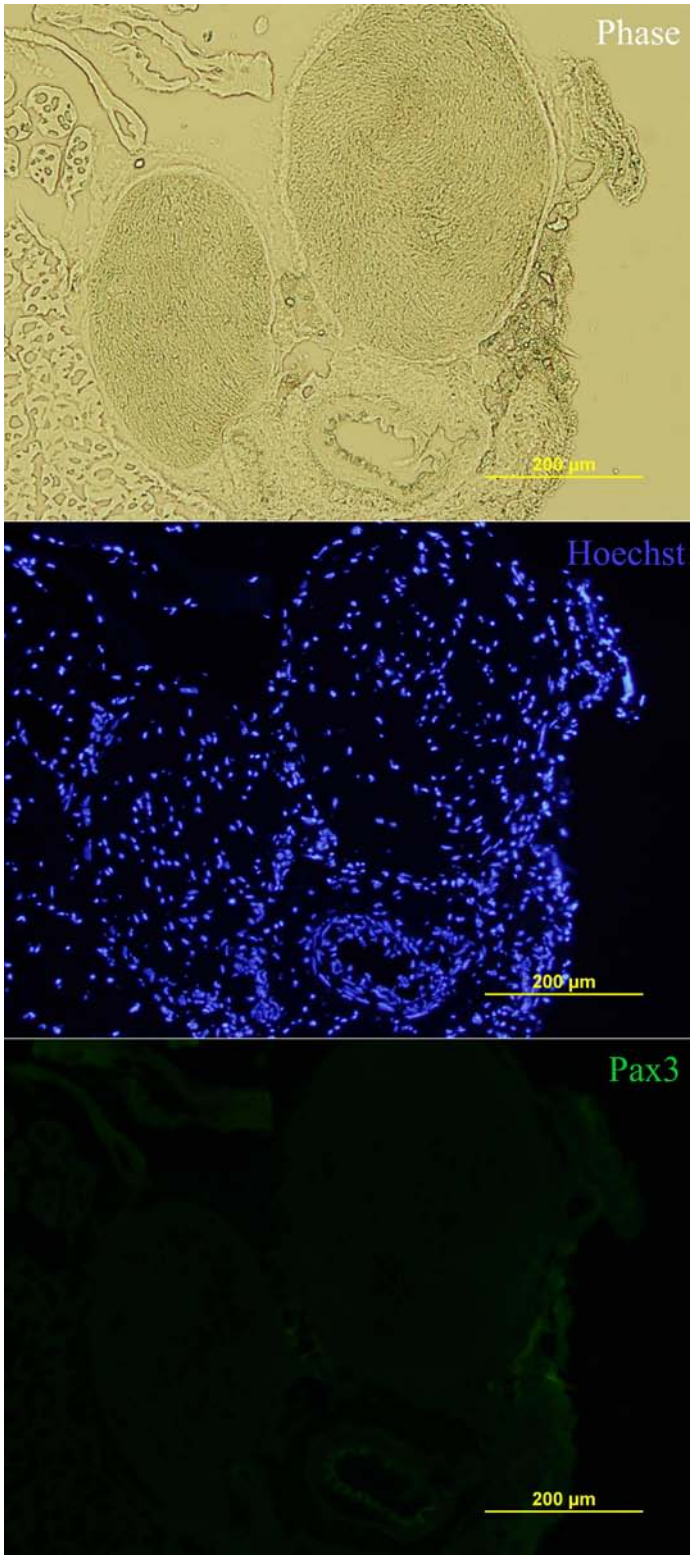

Figure 18. **Pax3 is undetectable in frozen cross sections.** A single indirect immunohistochemical protocol processed on transverse frozen sections using an anti-Pax3 immunoglobulin did not reveal Pax3 positivity (green) in any cells throughout the length of the nerve trunk.

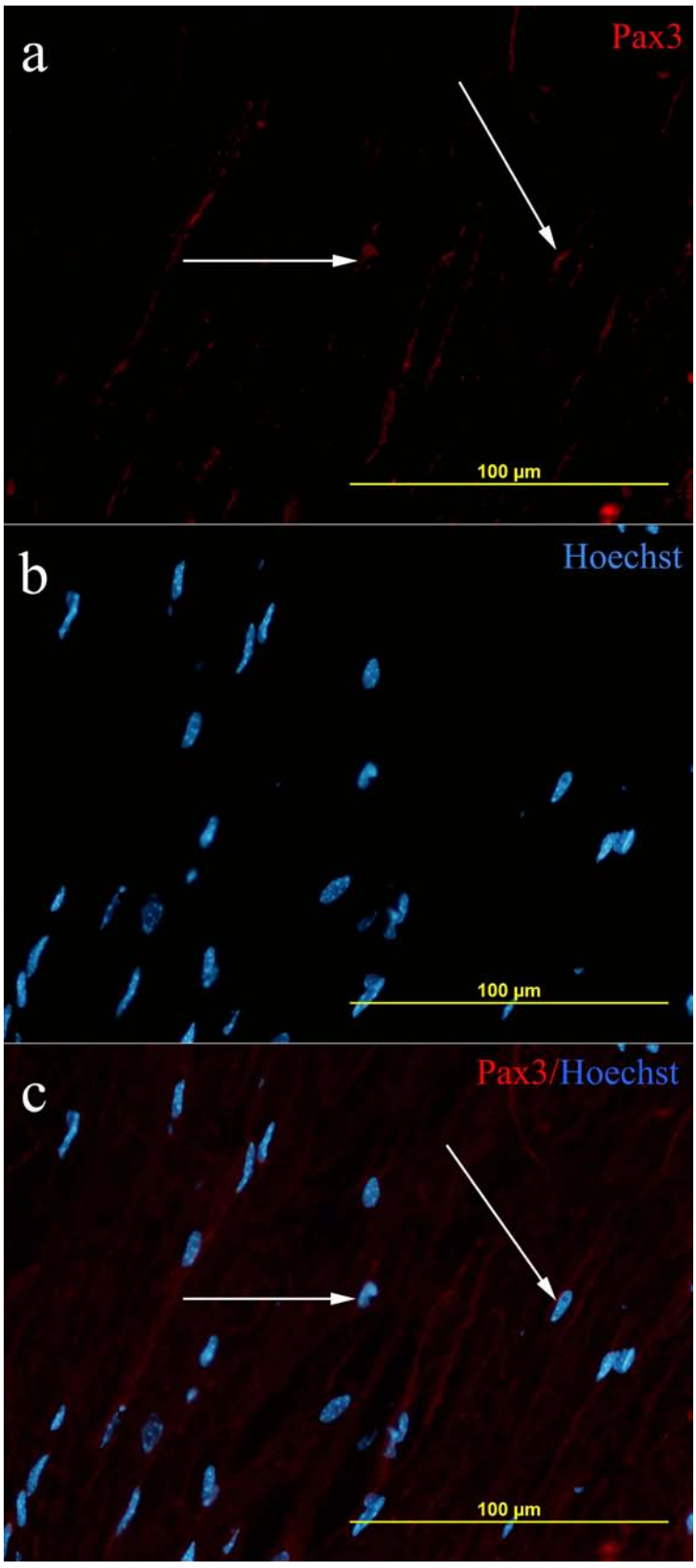

Figure 19. **The Pax3 immunolabel of frozen longitudinal sections. a)** Nuclear Pax3 expression (red) as indicated by the arrows is negligible in longitudinal frozen sections. **b)** When nuclei of the specimen are counterstained with Hoechst DNA dye **c)** co-localisation is difficult to detect (arrows).

attempt to amplify the Pax3 signal which could otherwise be below the level of detection. When this method was analysed, levels of non-specific background staining were high and a nuclear Pax3 label continued to be undetectable regardless of the primary antibody used (data not shown).

It remained necessary to determine whether cells of adult sciatic nerve that express Pax3 could be immunohistochemically labelled using the chosen Pax3 antibodies. It was reasoned that Pax3 protein levels would be increased in transgenic mouse C22 sciatic nerves, where the phenotype results in increased numbers of Pax3 expressant NMSCs (Huxley et al., 1996); therefore, frozen sections of sciatic nerves of 60 day old C22 mutant mice were obtained and used for Pax3 labelling. In these experiments, mutant and normal nerves were fixed, prepared and immunohistochemically processed using an identical enzyme-linked procedure to eliminate the fluorescence-based difficulties associated with fluorophore photobleaching and quenching during attempts to detect very low levels of fluorescent labelling at a high magnification. The C22 frozen sections were consistently immunolabelled using both the Pax3 antibodies. Moreover, the specificity of the Pax3 label to the nuclei of the cells was apparent (Fig. 20a, 20b, 20c). Repeatedly, Pax3 expression was not detected in cells of the wild-type frozen nerve sections processed in the same experiment (Fig. 20d). The significance of the Pax3 expression seen in C22 tissue will be discussed later in light of other results (see Discussion, pg. 78).

At this stage, it was not understood whether the lack of detection of a Pax3 label in wild-type nerve was linked to expression levels or the immunohistochemical procedure on the frozen sections. Therefore, individually teased Schwann cells were next employed in an attempt to label Pax3 in the nuclei of these cell preparations. Penetration

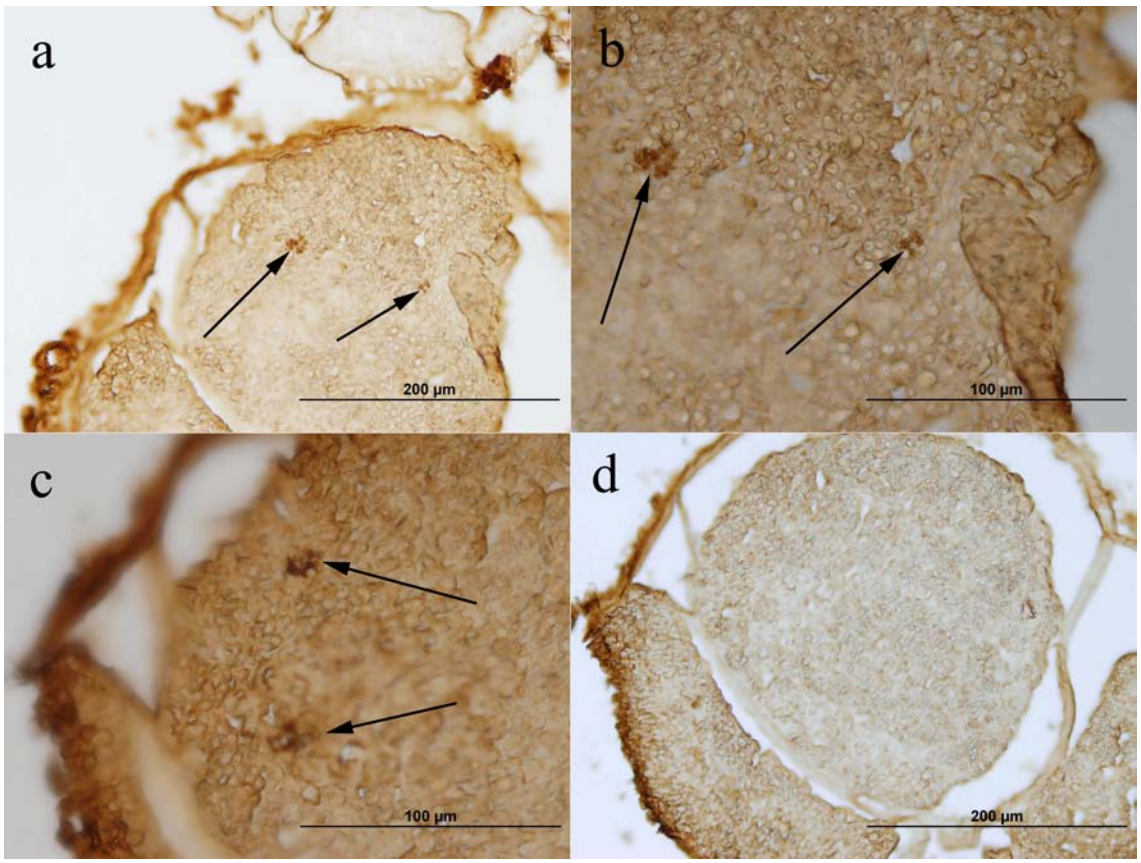

Figure 20. **Pax3 expression in transgenic C22 sciatic nerve**. **a)** The mouse monoclonal anti-Pax3 immunoglobulin, directed at the C-terminus of the Pax3 protein, labelled clusters of expressant cells throughout the trunk of transgenic nerves affected with the C22 mutation (arrows). **b)** Magnification of section a. **c)** The rabbit monoclonal anti-Pax3 immunoglobulin, directed at the paired-box region of the Pax3 protein also labelled clusters of expressant cells in an adjacent, distal section of the same nerve. **d)** The frozen sections of wild-type sciatic nerve processed at the same time with an identical procedure did not reveal Pax3 protein expression.

of the antibodies through the paraformaldehyde fixed endoneurial collagen surrounding the individual NMSCs was thought problematic (Fig.21); therefore, various permeabilisation techniques were used to assess their effects on cellular and extracellular integrity, nonspecific staining and intensity of nuclear label (Tables 3 and 4). In these experiments, cells post-fixed by paraformaldehyde and permeabilised with Tw20 did have a nuclear Pax3 label; these specimens, however, retained little other cellular morphology (Fig. 22c). Cells fixed similarly but with a permeabilisation with TX100 had a Pax3 label of low intensity (Fig. 22b). Tissues perfused with paraformaldehyde and permeabilised with methanol had a Pax3 label, however, cell

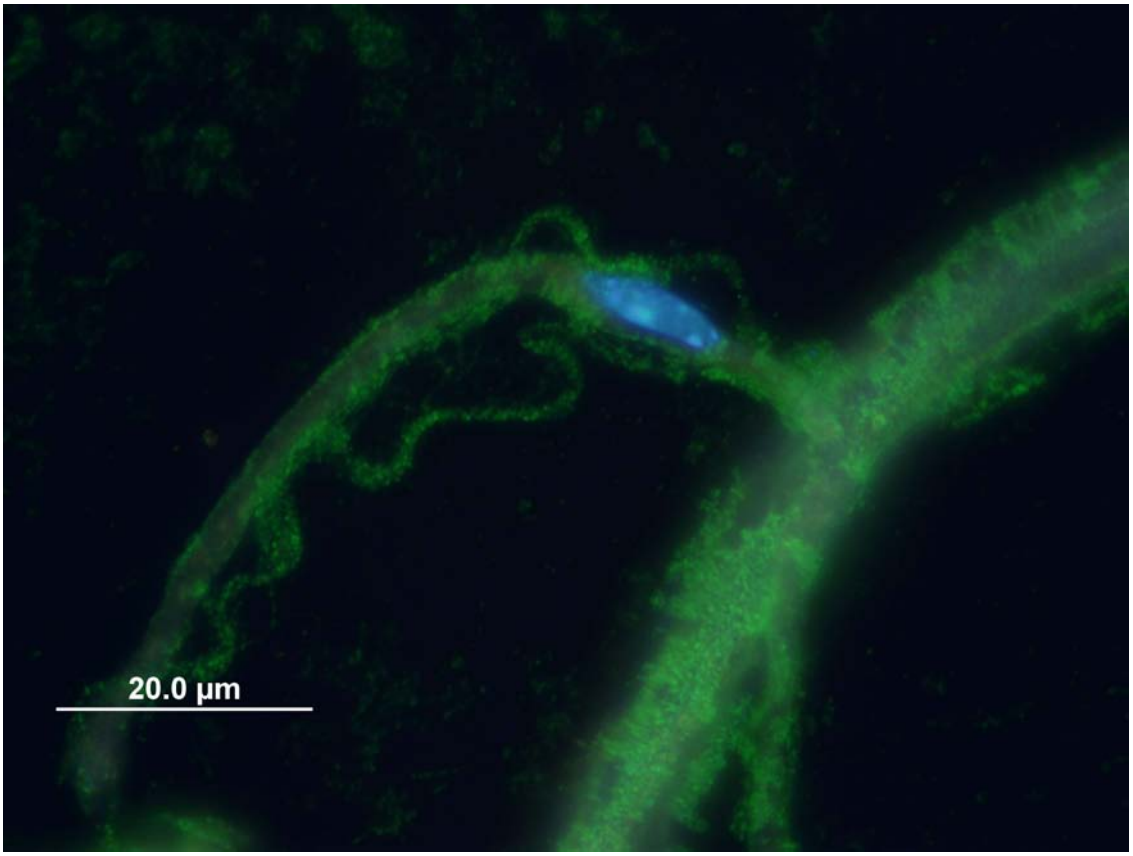

Figure 21. **Endoneurial collagen.** The image shows an individual Schwann cell that was taken through a 20 minute permeabilisation procedure with TX100 before being counterstained with Hoechst DNA dye. The highly autofluorescent endoneurial collagen (green) is seen to be disassociated from the cell.

structure was again severely degraded (Fig. 22a). Few individual cell specimens were able to be prepared using the fascicles post-fixed in acetone; as stated previously, this tissue was difficult to tease into individual cells. Of those acetone post-fixed specimens able to be teased into individual cells, a nuclear Pax3 signal and good quality cell morphology were observed (Fig. 22d).

Consistent among all the teased cell preparations analysed was the demonstration that relatively 2% of cell nuclei were immunolabelled with Pax3. Therefore, a further panel of individual Schwann cells was processed using the various permeabilisation methods and an alternate primary antibody against Krox24, a transcription factor reported expressed in Schwann cells of adult peripheral nerve (Topilko et al., 1997; Kury et al., 2002) was used to confirm the efficacy and consistency of the techniques. The

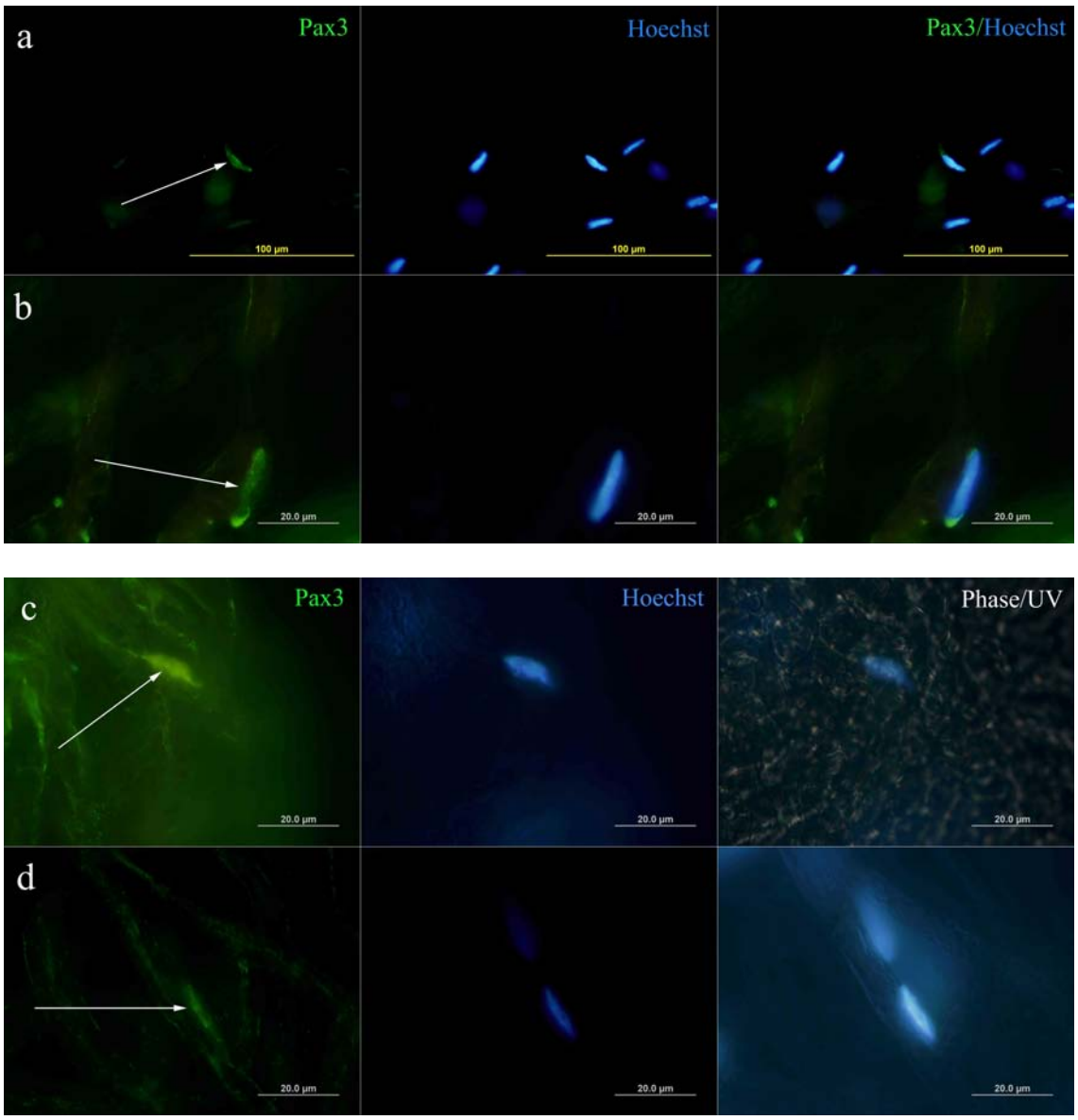

Figure 22. **Optimisation of the Pax3 immunofluorescent histochemistry. a)** Normal tissues fixed by perfusion with 4% paraformaldehyde followed by a permeabilisation step in methanol showed Pax3 positivity (green) in cells as indicated by the arrow, however, fibre integrity was severely degraded in the teasing process. **b)** Tissues processed with a 2 hour post-fixation in 4% paraformaldehyde followed by a permeabilisation step in TX100 revealed nuclei with Pax3 positivity (arrow). **c)** Tissues post-fixed with 4% paraformaldehyde followed by a permeabilisation step in Tw20 showed Pax3 positivity in cells (arrow), however fibre integrity was destroyed as seen in the phase-contrast image (Phase/UV panel). **d)** Tissues simultaneously fixed and permeabilised with acetone demonstrated Pax3 positivity in cell nuclei (arrow) with the advantage of superior tissue morphology as seen in the phase-contrast image.

experiments ncorporated identical reagents and procedures as those employed in the Pax3 permeabilisation trials described above. In these trials, the loss of cellular structure due to the various reagents was similar to that described in the Pax3 trials. Here, the

nuclei that expressed Krox24 were clearly distinguishable and although relatively 2% in number, were strongly immunofluorescent. Moreover, the Krox24 labelled cells appeared, by morphology, to be myelinating Schwann cells (Fig. 23). It was therefore concluded that the paraformaldehyde fixation method, rather than the permeabilisation process, was linked to the difficulties associated with the Pax3 immunofluorescent labelling procedure experienced during this study.

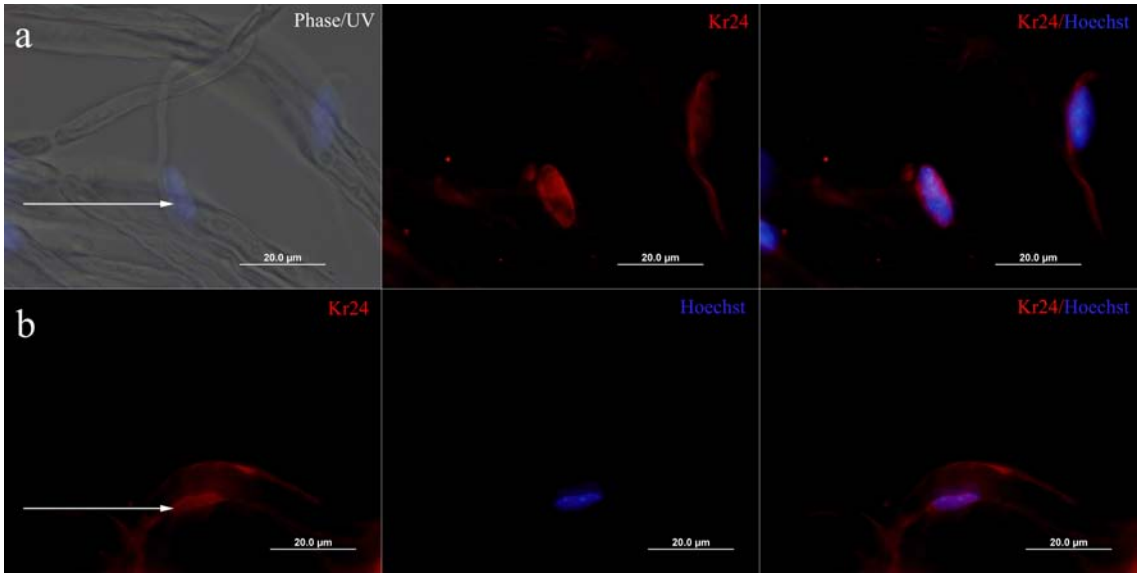

Figure 23. **Verification of nuclear immunofluorescent histochemistry. a)** Tissues post-fixed for 2 hours in 4% paraformaldehyde were labelled with an antibody targeted at the Krox24 transcription factor protein. In this preparation, a myelinating Schwann cell nucleus shows Krox24 positivity. **b)** Tissue fixed by 4% paraformaldehyde perfusion with a permeabilisation step using TX100 shows a Krox24 expressant nucleus (arrow) that is associated with a large myelinated fibre.

3.5 The expression of Pax3 protein in normal adult mouse sciatic nerve

Nerves post-fixed in acetone retained superior morphology and Pax3 antigenicity, thus, a procedure for immunofluorescent labelling of Pax3 was next developed using the whole mount preparations that had been post-fixed in acetone. The adult mouse sciatic nerve has many fascicles, each with a variant diameter, therefore, the smallest fascicles were used to optimise penetration of the Pax3 antibodies through the tissue. The optimal procedure was similar to that used for the p75Ngfr labelling of whole mount tissue and included tissue permeabilisation with a dilute concentration (0.2% TX100) of detergent

in the primary antibody solution together with stringent, lengthy rinsing steps following all antibody incubations (see Methods-section 2.11). The immunofluorescently labelled specimens were then imaged using scanning laser confocal microscopy. Results showed that strong Pax3 immunoreactivity was identified in cell nuclei randomly distributed along the length of the 60 day old nerve trunk. In all the whole mount specimens analysed, relatively 2% of the cell nuclei were positive for Pax3 when compared to the total number of Hoechst stained nuclei visible along the length of the nerve. Moreover, results showed that Pax3 expressing nuclei did not have the characteristic spindle shape of the Remak NMSCs, rather, they were distinctly oval or round (Fig. 24b & 24c). Relatively 5% of the Pax3 positive cells displayed perinuclear Pax3 expression (Fig. 24a & 24c) which may be indicative of a post-translational modification of the transcription factor (Topilko et al., 1997).

3.6 Characterisation of cells that express Pax3 in normal adult mouse sciatic nerve

The development of methods for co-localisation of p75Ngfr and Pax3 in the nerve revealed that relatively 98% of Schwann cells that make up the Remak bundles of normal adult sciatic nerve did not express Pax3 and were distinct from the Pax3 labelled cells. All of the Pax3 positive cells were closely adjacent to p75Ngfr labelled Remak bundles (Figs. 25-27), had a round nucleus, a lack of p75Ngfr positive cell membrane extensions (Figs. 25c, 26 & 27) and a nuclear and perinuclear p75Ngfr expression pattern (Figure 27).

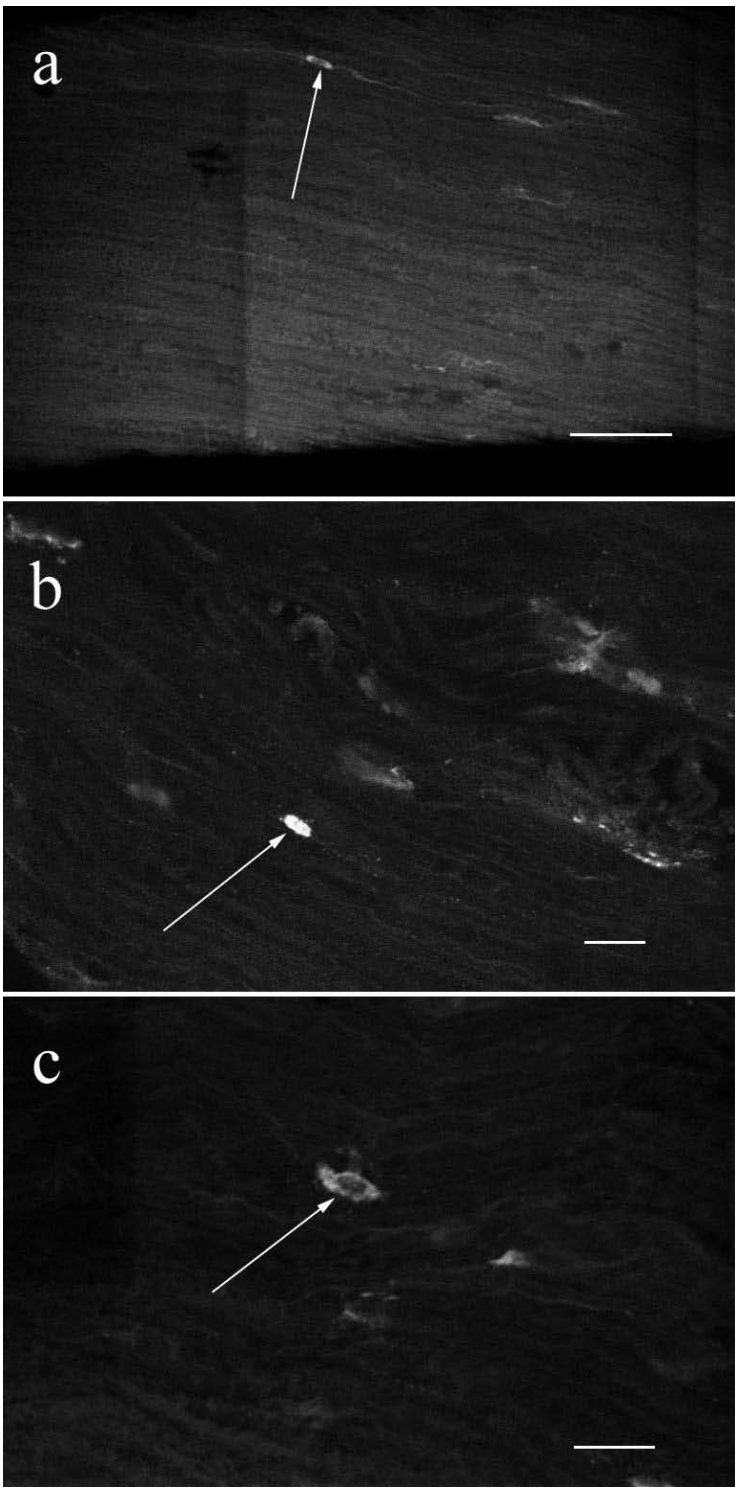

Figure 24. **The distribution of Pax3 protein in adult mouse sciatic nerve.** Whole mount tissue reveals Pax3 labelled cells randomly distributed throughout the trunk of the nerve (arrows); images were acquired using scanning laser confocal microscopy. **a)** In this optical plane of view, the Pax3 protein appears to have a perinuclear locale (arrow). *Pinhole aperture= 3.5. Optical plane= 1.0 μm. Scale bar represents 50 μm.* ***b)*** In this optical plane, the nucleus that is strongly immunolabelled with anti-Pax3 is notably rounded. *Pinhole aperture= 3.5. Optical plane= 1.0 μm. Scale bar represents 20 μm.* **c)** The cell indicated by the arrow has a distinctly perinuclear localisation of Pax3 protein. *Pinhole aperture= 3.5. Optical plane= 1.0 μm. Scale bar represents 20 μm.*

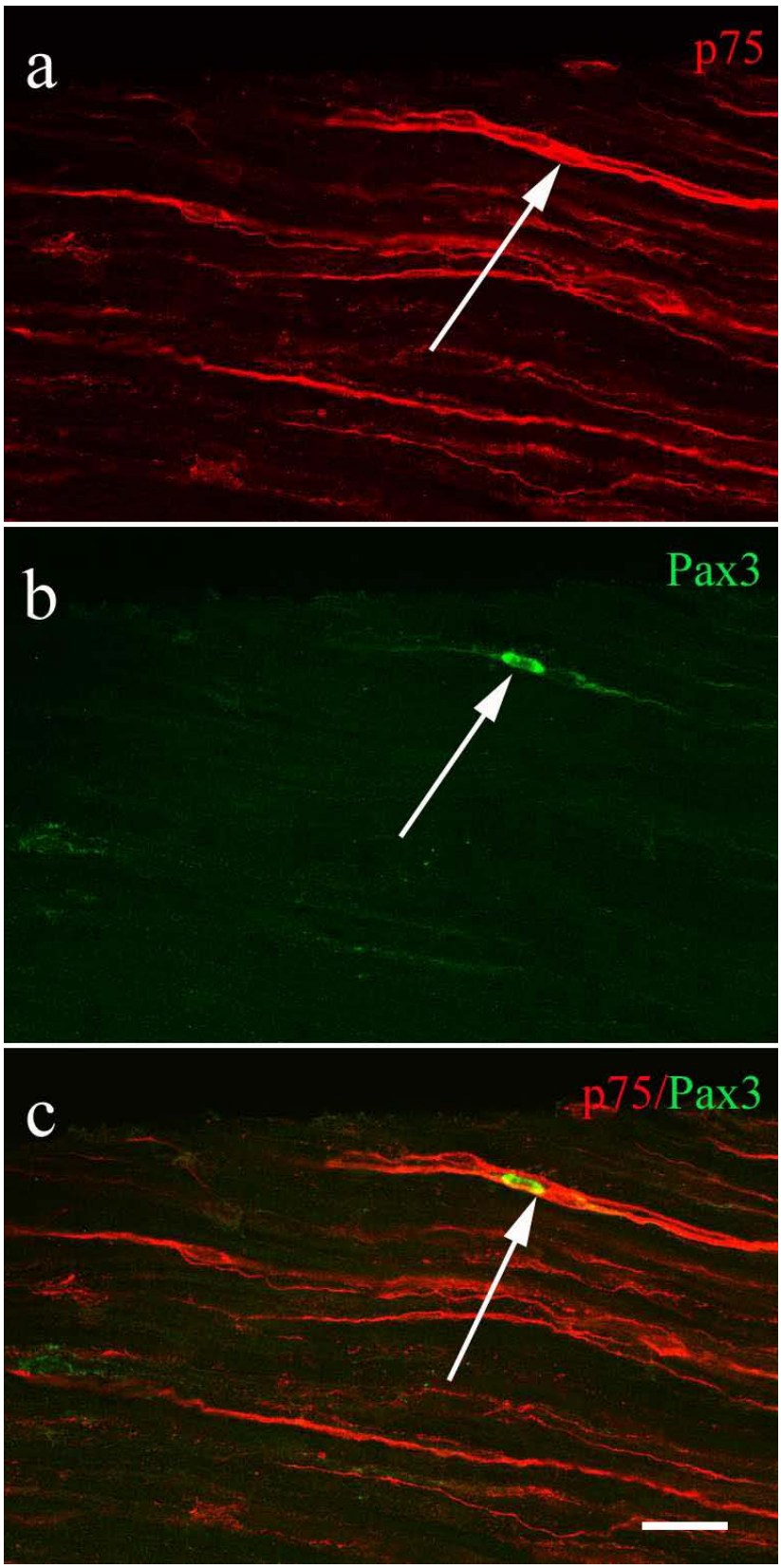

Figure 25. **A Pax3 expressant cell *in situ*.** a) Whole mount tissue reveals the p75Ngfr labelled Remak bundles (arrow). b) A Pax3 expressing cell is indicated by the arrow. c) Co-localisation analysis of p75Ngfr and Pax3 demonstrates that the Pax3 expressant cell is in close proximity to the Remak bundle indicated (arrow) but does not appear associated with it. Images were acquired using scanning laser confocal microscopy. *Pinhole aperture= 3.5. Optical plane= 1.5 µm. Scale bar represents 20 µm.*

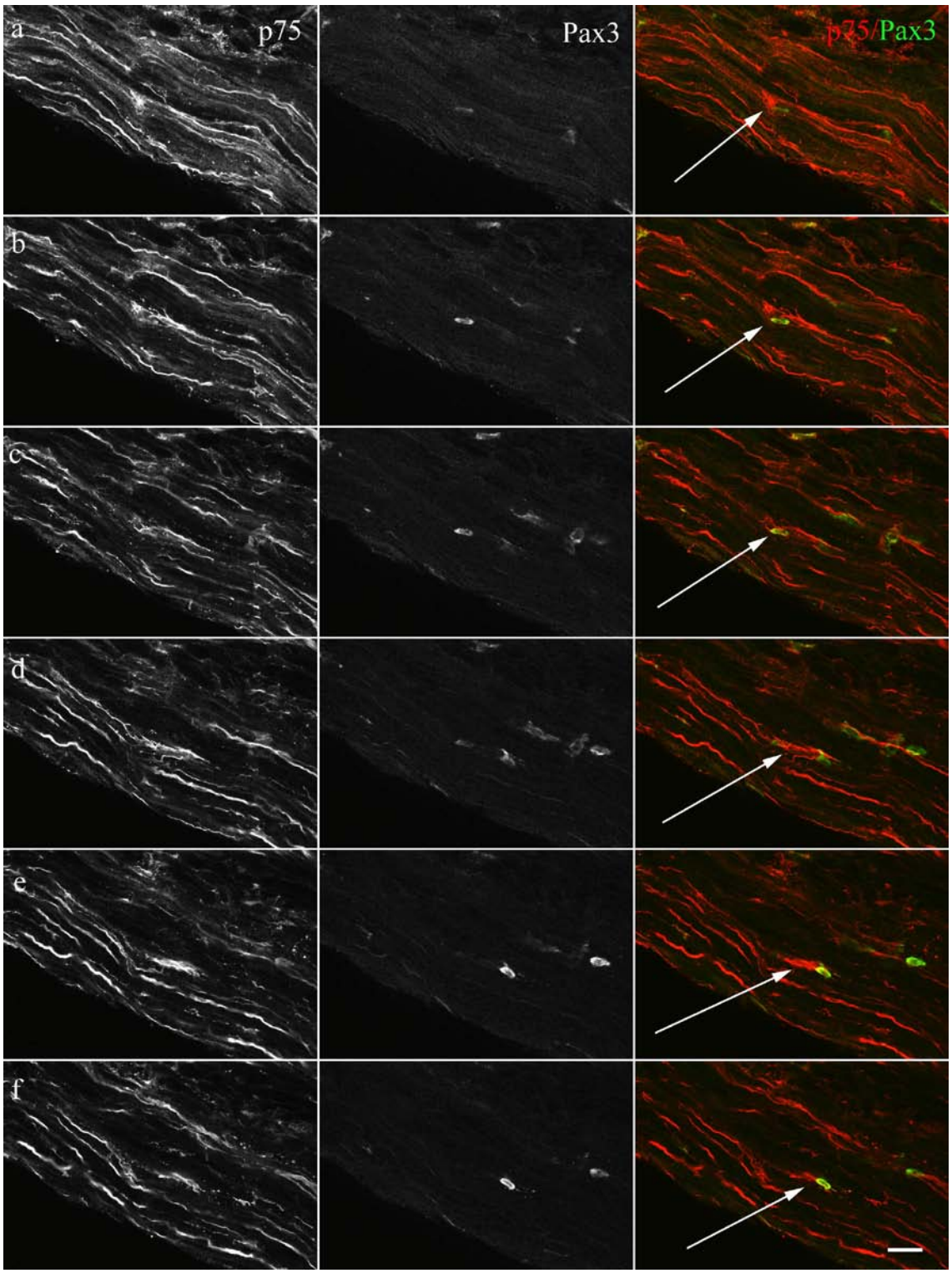

Figure 26. **p75Ngfr and Pax3 co-Localisation in adult nerve.** Whole mount preparations were co-immunolabelled for p75Ngfr and nuclear Pax3. **(a-f)** Consecutive scanning laser confocal images through the nerve trunk are shown where each optical plane is 1 *μm*. Greyscale images reveal p75Ngfr or Pax3 signals, respectively, as indicated. Co-localisation of p75Ngfr (red) and Pax3 (green) reveals that Pax3 expressing cells are closely associated with Remak bundles (arrows). *Pinhole aperture= 3.5. Scale bar represents 20 μm.*

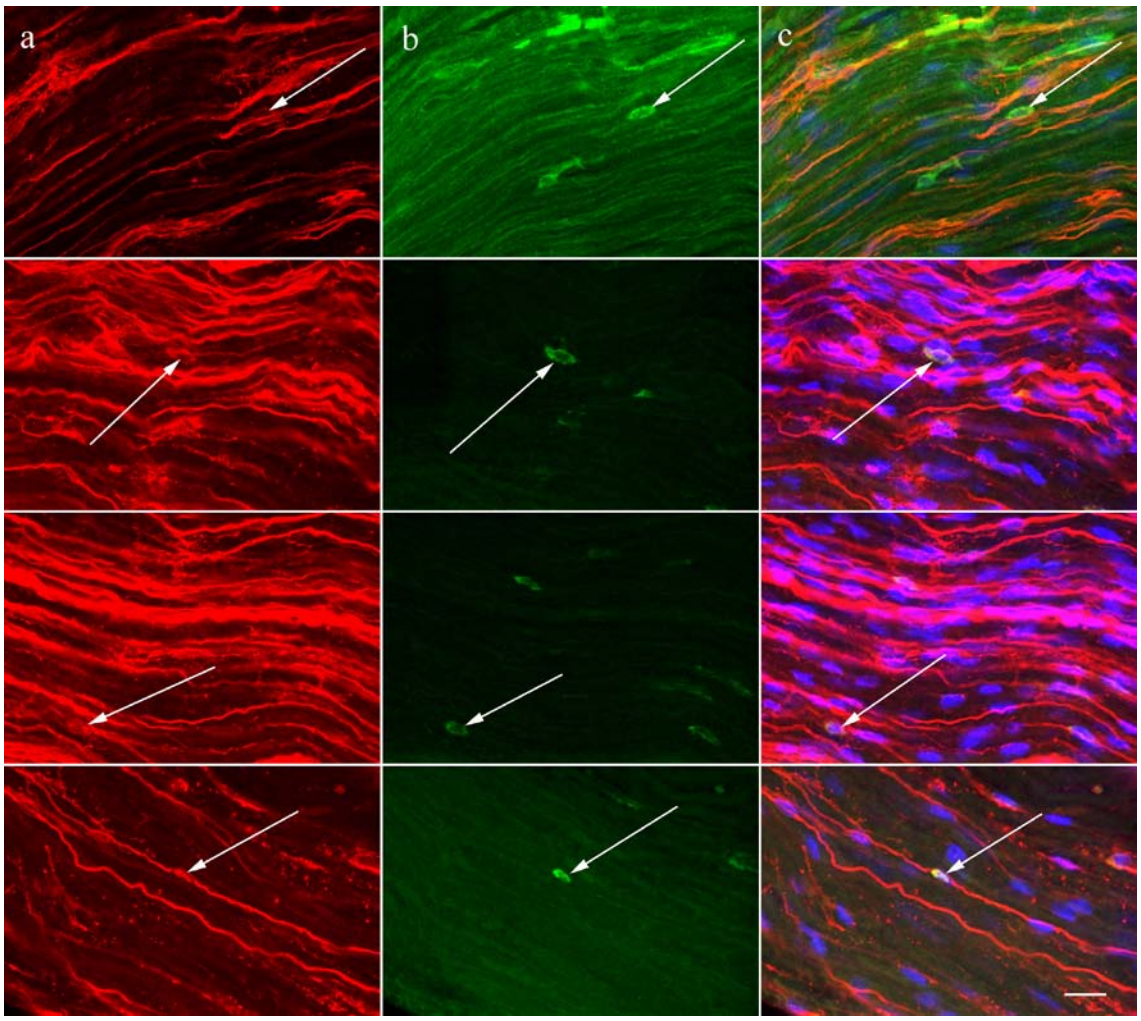

Figure 27. **Pax3 is expressed in a subset of nonmyelinating Schwann cells of adult nerve. a-c)** Whole mount tissues co-immunolabelled with anti-p75Ngfr, anti-Pax3 and Hoechst DNA dye reveal that Pax3 expressing cells are distinct from the majority of Remak bundles. **a)** The arrows indicate nuclear and perinuclear p75Ngfr expression seen on Pax3 expressant cells indicated in panel **b**. **b)** The Pax3 positive cells are indicated by the arrows. **c)** The merged images demonstrate co-localisaton of p75Ngfr and Pax3 expression. Images were acquired using scanning laser confocal microscopy. *Pinhole aperture= 3.5, Optical Plane= 1.5 μm. Scale bar represents 20 μm.*

It was hypothesised that cells of adult nerve that express Pax3 would co-express other early immature Schwann cell markers. The final aim of the project, therefore, was to perform immunofluorescent co-localisation studies using antibodies against Pax3 and a marker of early neural crest cells, Sox2. These studies were undertaken using labelling of whole mount nerve preparations and analyses by scanning laser confocal microscopy. While Sox2 expression has been demonstrated in Schwann cells of embryonic 17 day old mice (Le et al, 2005), it was shown here for the first time detected in mouse sciatic

nerve of 60 day old animals. In all of the Pax3 and Sox2 co-labelled whole mount specimens examined, nuclear Pax3 expression co-localised with that of Sox2 in a distinct subset of cells within the nerve (Fig. 28).

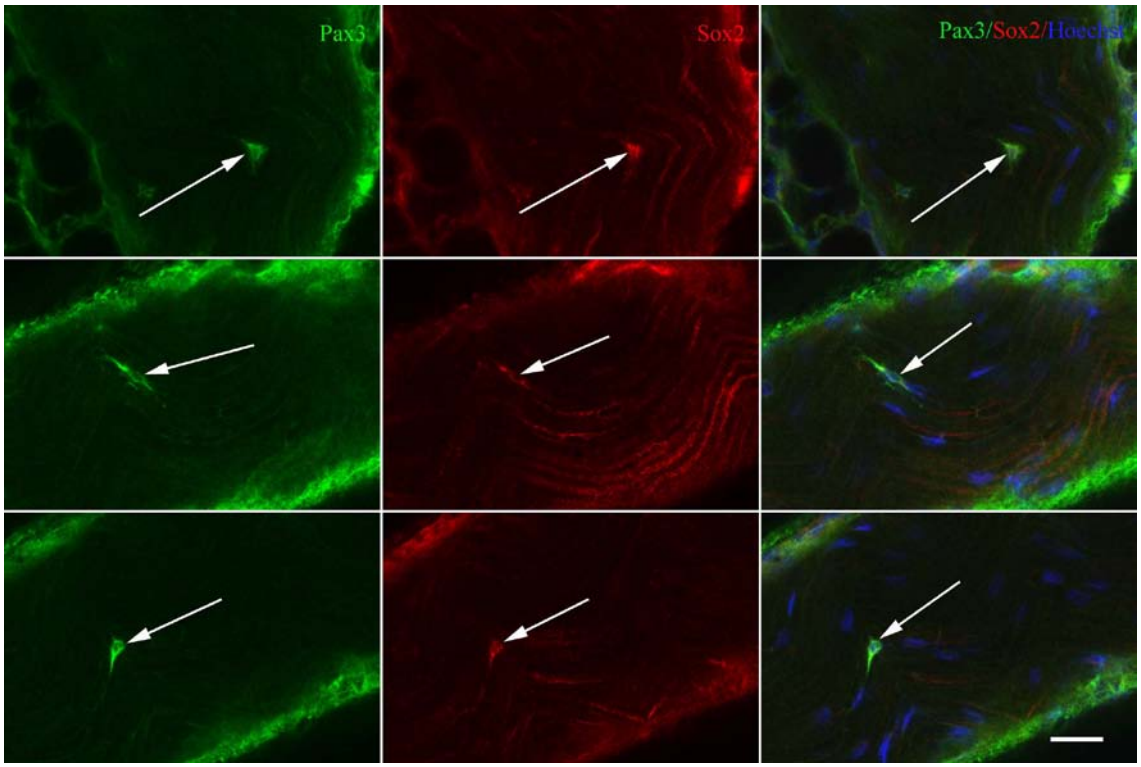

Figure 28. **Transcription factors Pax3 and Sox2 co-localise in cells of adult nerve.** Whole mount tissues co-immunolabelled with anti-Pax3, anti-Sox2 and Hoechst DNA dye reveal that all Pax3 expressant cells co-express with stem cell marker Sox2 (indicated by the arrows). Images were acquired using scanning laser confocal microscopy. *Pinhole aperture= 3.5, Optical Plane= 1.5 µm. Scale bar represents 20 µm.*

3.7 Summary of the results

Methods were developed that allowed characterisation of NMSCs of normal 60 day old mouse peripheral nerve. To date, neurological studies of this kind have been performed on larger animals such as frog, rat, cat and dog. The intricate and complex morphological characteristics of mouse NMSCs are described here for the first time and novel images of the cell *in vivo* within the mouse sciatic nerve trunk are demonstrated. A novel finding was that NMSCs associated with p75Ngfr positive (with bipolar cytoplasmic extensions) labelling did not express Pax3 and were distinct from the small population of cells that expressed Pax3. Cells that expressed Pax3 were closely adjacent

to the labelled Remak bundles. Importantly, the findings that p75Ngfr is expressed on the abaxonal cell membrane of Pax3 positive cells and that expression coincided with stem cell marker Sox2 provides compelling evidence for the existence of a progenitor cell population in adult mouse sciatic nerve.

4

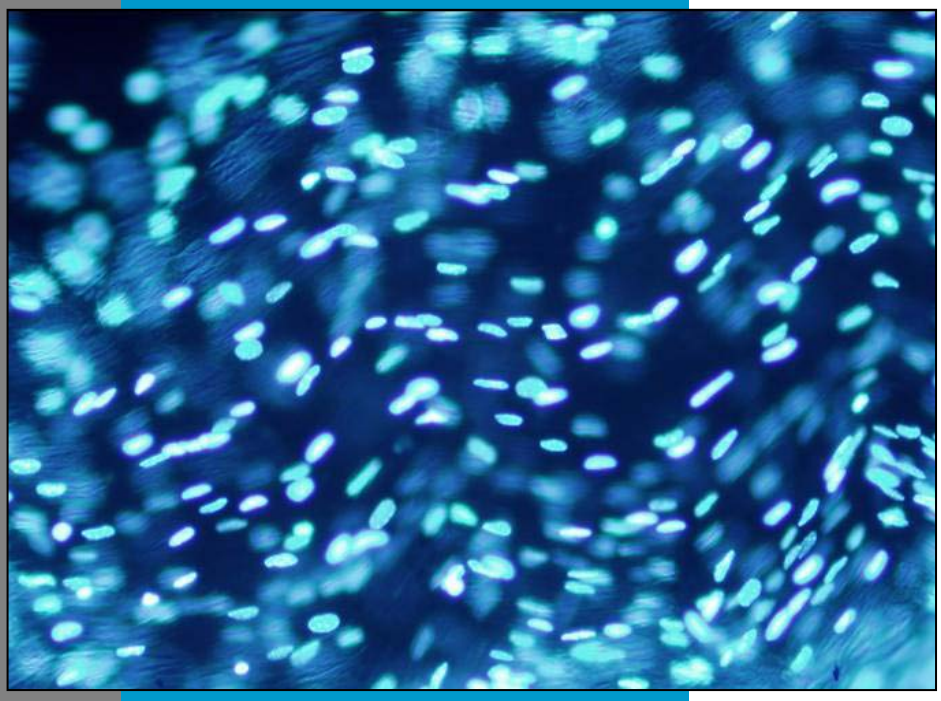

DISCUSSION

4.1 A distinct population of Pax3 expressing cells in adult mouse peripheral nerve

Based on the evidence and knowledge of the role of Pax3 in other adult tissue stem and progenitor cells, and taken together with evidence that a population of cells exist in adult peripheral nerve that express Pax3 (Kioussi et al., 1995), it was hypothesised that the population of cells that express Pax3 in adult peripheral nerve are Schwann glioblasts. Therefore, the aims of the research focused on identification, visualisation and initial characterisation of the cells of adult nerve that express Pax3. The most significant finding of these investigations is that a subset of stem/progenitor cells that express transcription factors Pax3 and Sox2 have been identified in adult mouse peripheral nerve. These transcription factors are commonly expressed in multipotent cells in a variety of tissues and while the role of Pax3 in Schwann cells remains largely undetermined, its overarching role in other tissues is maintenance of progenitor cells across the life span. In Schwann cells, *Sox2* has been shown conclusively to increase responsiveness to proliferative stimuli, prevent myelin gene expression and inhibit differentiation (Wakamatsu et al., 2004; Le et al., 2005). *SOX2* is one of the four Yamanaka factors, or genes whose expression is artificially forced to induce non-pluripotent adult somatic cells into pluripotent stem cells (iPSCs) *in vitro*. In the progress toward clinical application of iPSCs, both *SOX2* and *PAX3* have key roles in the generation, identification and maintenance of patient-specific iPSCs *in vitro* (Takahashi &Yamanaka, 2006; Masui et al., 2007; Ohta et al., 2011). Therefore, the identification of cells in these investigations that co-express the putative stem cell markers Pax3 and Sox2 is initial, sound evidence of the existence of Schwann progenitor cells in adult mouse peripheral nerve trunk. It should be stated here that investigation of a progenitor Schwann cell population in adult peripheral nerve has not been performed in any other animal, to date.

A principle aim of this research was to assess the distribution of Pax3 protein in adult mouse peripheral nerve. At the start of the investigations, it was conceived that the Pax3 expression pattern would be similar to that seen in adult skeletal muscle where Pax3/7 expressing progenitor cells account for 1-4% of the total myonuclei (Bischoff & Franzini-Armstrong, 2004). That *Pax3* transcripts were below the level of detection in some of the nerves tested here by RT-PCR, was confirmed by the fact that only a minute population of cells within the nerve trunk express *Pax3* mRNA at age 60 days. These findings are in agreement with other studies which failed to label *Pax3*/Pax3 in adult peripheral nerve. The low levels of these cells in adult nerves may be linked to a limited physiological need for progenitor Schwann cells in normal peripheral nerve, as compared to the need for progenitor myoblasts in normal skeletal muscle. Regrettably, confirmation of the limited number of cells that expressed Pax3 at this age in mouse nerve quelled cell sorting methodologies for a more in-depth characterisation of their phenotype in this research. With the development of rare cell sorters, future experiments are now possible.

4.2 The characterisation of Pax3 expressing cells and Remak NMSCs

Another primary aim of the research was to develop methods of imaging NMSCs *in vivo*, as little is known about mouse NMSCs. Here, development of the Pax3/p75Ngfr and Pax3/Sox2 double immunohistochemical labelling procedures allowed several morphological and phenotypic distinctions to be made between Pax3 expressing cells and other Remak bundle NMSCs. Firstly, it was seen that the Pax3 positive cells were not bipolar and had a p75Ngfr nuclear and perinuclear expression pattern which is indicative of a progenitor cell (Wong et al., 2006) and is similar to denervated Schwann cells *in vitro*. When Schwann cells are released from axonal contact *in vitro* they express p75Ngfr on the cell surface, secrete nerve growth factor for autocrine survival

(Sobue, 1990), do not exit the cell cycle and retain an early immature Schwann phenotype (Salzer & Bunge, 1980).

Not only have distinct morphologic characteristics of the two diverse subsets of adult NMSCs been described, but also, distinct phenotypic differences lend credence to the theory that early immature Schwann cells are retained in peripheral nerve after birth. It is important to remember that transition from the embryonic Schwann precursor to the 'committed', or immature Schwann phenotype, progresses at embryonic day 12, at which time changes are associated with the establishment of an autocrine survival circuit. Where precursor Schwann cells undergo apoptosis in the absence of axonal trophic support, immature Schwann cells survive via autocrine secretion of growth factors such as neurotrophin-3, a ligand of p75NGFR (Jessen & Mirsky, 1992; Jessen & Mirsky, 1994; Dong et al., 1995; Grinspan et al., 1996; Syroid et al., 1996; Murphy et al., 1996; Dong et al., 1999; Meier et al., 1999). At this stage, the early, fated Schwann cells express *Pax3, p75Ngfr* and *Sox2* and are capable of self-survival. This author suggests that a population of these cells are retained into adulthood and are the Pax3/Sox2/p75Ngfr positive cells seen in this study (Fig. 30).

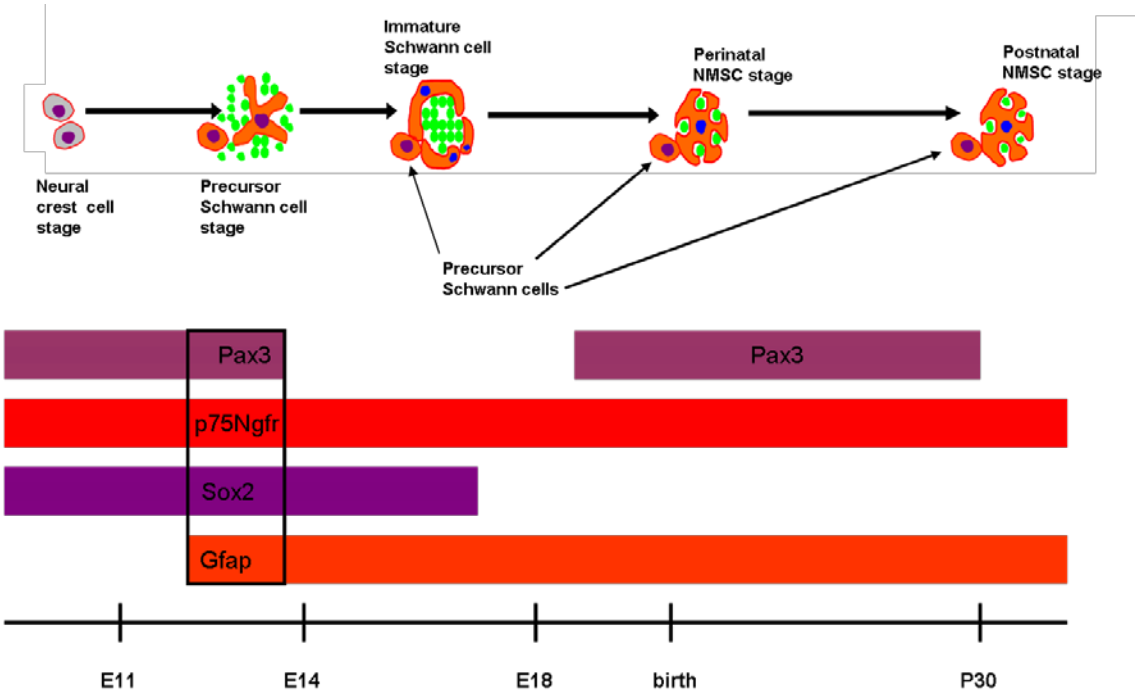

Figure 29. **The proposed retention of peripheral nerve progenitor cells from embryogenesis.** NMSCs that form the Remak bundles of adult peripheral nerve down-regulate Pax3 after P30 but continue to express p75Ngfr and Gfap. A subset of Schwann cells juxtaposed to Remak bundles have been identified that express Pax3, Sox2 and p75Ngfr; it is proposed that these cells represent progenitor cells that persist from embryogenesis into adulthood (indicated by arrows) and continue to express the late precursor/early immature Schwann phenotype.

After birth, the subset of Schwann cells that associate with C-fibres differentiate toward a nonmyelinating phenotype, re-establish dependency on p75NGFR signalling for survival (Chen et al., 2003) and form the peripheral Remak bundles. Of note is the finding that 60 day old NMSCs that form the Remak bundles did not express Pax3, which indicates that expression is down-regulated from postnatal day 30 when Kioussi et al. (1995) last report its expression. Thus, Pax3 appears to have a temporal postnatal role in the suppression of myelination genes in NMSCs much the same as it does in myelinating Schwann cells. Therefore, terminally differentiated NMSCs of Remak bundles such as those seen in these investigations have a phenotype characterised by *p75Ngf* and *Gfap* expression and a lack of *Pax3* and *Sox2* expression (Fig. 29).

4.3 Pax3 expression in C22 adult mouse peripheral nerve

Given the relatively small amount of *Pax3* transcripts amplified in these investigations, it is interesting to note that the *Pax3d* transcript was found expressed in adult sciatic nerve as functional analyses have demonstrated that, in melanocytes, *Pax3d* promotes cell proliferation and migration. Throughout the investigations, it was critically queried whether the observed Pax3 positive cells could represent NMSCs undergoing a normal cell turnover, despite the fact that studies in rat and mouse have shown that normal adult Schwann cells have a low cell turnover and are mitotically quiescent (Lubinska, 1961; Martin and Webster, 1973; Muller et al, 1996; Murinson et al, 2005b). When the rare NMSC turnover has been observed in adult nerve, there is evidence that mitosis occurs while the cell maintains the unmyelinated cytoplasmic processes that wrap around axons even after the nuclear membrane has dissolved (Murinson et al., 2005b). Above dispute is the fact that, although the number of Pax3 positive cells seen in these investigations was low, the number seen in one area of tissue, should they be construed as mitotic, far exceeds that which the literature states are present in normal adult nerve (Griffin et al., 1987, 1990). Griffin et al. (1987) showed that mitosis of adult rat Schwann cells is so rare that less than one Schwann cell per 15000 fibres can be labelled with mitotic marker [3H] thymidine.

Rather, the present findings suggest that the cells labelled with Pax3, Sox2 and p75Ngfr may represent peripheral nerve progenitor cells that were 'poised' for proliferation and migration, similar to Pax3 positive melanoblast progenitors of skin described by Lang et al (2005). Other studies have described how, in demyelinating injury or disease, normal unaffected NMSCs proliferate asymmetrically (Griffin et al., 1987, 1990, 2008; Rambukkana et al, 2002; Murinson et al., 2005b; Koike et al., 2007) and are suggested to migrate to areas of demyelination (Griffin et al., 1987). The “supernumary” Schwann

cells visualised and described by Griffin et al (1987) had the same morphology as the Pax3 positive cells seen in these investigations in that they were round, had little cytoplasm and did not ensheathe nerve fibres. This denervated, progenitor morphology was also seen in the experiments here that employed the C22 mouse sciatic nerve where Pax3 expressing cells were sporadically clustered in groups along the length of the diseased nerve trunk (Fig. 20); these Pax3 positive cells were smaller than the average NMSC and had a round nucleus. Undoubtedly, future studies need to be undertaken to isolate and confirm properties of self-renewal in the proposed Schwann progenitor cells; use of the immunohistochemical labelling techniques developed in this research and the tissues of *Pax3* mutant animals could prove efficacious for investigations of the role of Pax3 in Schwann cell responses to neuropathy.

4.4 Immunohistochemical hurdles

Paraformaldehyde is a common fixative employed in peripheral neurology and various methods of paraformaldehyde fixation were assessed here for preservation of the nerve tissue, individual cell morphology and antigenicity of the target proteins. While a p75Ngfr cell membrane antigen was retained in most of the paraformaldehyde fixed preparations, a reliable nuclear Pax3 antigen was not. Initially, it was reasoned that the number of Pax3 expressing cells in normal nerve was extremely low (as supported by RT-PCR results) such that they may be unidentifiable along the length of the nerve trunk (the proverbial needle in a haystack). Therefore, C22 transgenic nerves were acquired and used for Pax3 labelling investigations as C22 nerves are reported to have, by virtue of regeneration, an increased number of NMSCs that were conceptualised to strongly express Pax3. Interestingly, C22 tissues that were fixed with a paraformaldehyde perfusion did reveal Pax3 positive cells, whereas, wild-type tissues immunohistochemically processed in the same experiment did not.

It was reasoned that DNA and/or protein binding may mask targeted Pax3 epitopes in normal NMSCs, whereas Pax3 epitopes were accessible to antibodies in the C22 tissue due to an altered state of DNA/protein binding in those cells. To investigate the possibility, a fixative that included acetic acid was trialled on teased individual Schwann cells as this agent is commonly used for *in situ* hybridisation studies to break DNA/protein bonds; the acetic acid fixative was employed according to a published protocol for the labelling of transcription factors in mouse sciatic nerve (Blanchard et al., 1996). The nerves fixed in this way were not only difficult to tease but also highly autofluorescent across a wide spectrum of emissions that clashed with both the secondary fluorophores employed. Moreover, the highly soluble myelin proteins were extracted by the fixative to the detriment of the tissue. Thus; there were no optimal results for Pax3 detection using this procedure.

After close inspection of individual, teased Schwann cells under high magnification, it was thought that the immunohistochemical antibodies were not reaching the nucleus due to the paraformaldehyde cross-linking of the nuclear envelope, surrounding cytoplasmic and endoneurial structures. A checkerboard approach to experimentation was therefore employed where combinations of paraformaldehyde fixation times and various permeabilisation methods were tested on individual teased cell preparations in a further attempt to detect a Pax3 nuclear label in these specimens. In identical procedures, primary antibodies targeting the Krox24 transcription factor clearly labelled the nuclei of the Schwann cells while the anti-Pax3 label continued to be undetectable. It was concluded after this panel of experiments that the antibodies were able to penetrate the extra- and intracellular structures into the nuclei of the teased cells and although the morphology of the individually teased Schwann cells prepared by fixation

with paraformaldehyde were exquisite, the specimens were not conducive to anti-Pax3 immunolabelling.

An alternate method, consisting of a short post-fixation of dried whole mount sciatic nerve fascicles with 4ºC acetone was found to preserve both tissue morphology and Pax3 antigenicity. As specimens postfixed with acetone were not able to be efficiently teased, methods were developed using preserved whole mounted nerve fascicles. The next hurdle to contend with was development of a double-labelling immunofluorescent procedure that combined the optimal components of the plasmalemma labelling with the optimal labelling of the nucleus. The acetone-fixed whole fascicles did not require much permeabilisation for an optimal nuclear label; therefore, TX100 and Tw20 detergents were able to be used conservatively as preservation of p75Ngfr membrane bound antigens was contingent upon gentle detergent permeabilisation and rinsing methods. The ability of the acetone to solely extract the non-polar lipids of the myelin undoubtedly contributed to adequate penetration of the antibodies into the cell nuclei and subsequent, intense Pax3 signals. Repeatedly, the double-labelling procedure described above preserved the intimate comingling of myelinated and unmyelinated fibres and optimally labelled both nuclear Pax3 and p75Ngfr membrane proteins within well preserved Remak bundles. The indirect double labelling procedure was also optimal for the co-localisation of Pax3 and Sox2, which eventuated in the characterisation of the proposed peripheral nerve Schwann progenitor cells.

4.5 The significance of the research findings

NF1 is a heritable genetic disorder affecting 1 in 3,500 individuals worldwide. Patients develop numerous neurofibromas (benign peripheral nerve sheath tumors), café-au-lait spots (due to defects in pigmentation) and benign lesions of the iris. They are also

predisposed to development of malignant peripheral nerve sheath tumors (Kleihues, 1994). The devastating effects that neurofibromatosis and malignant peripheral nerve sheath tumors have on persons affected by NF1 have been an impetus for the establishment of the cell of origin of these tumors. During neurofibroma formation, cell-cell interactions are disrupted, leading to loss of the normal nerve structure. The most abundant cell type in neurofibromas is NMSCs, which comprise 60-80% of the cell population (Peltonen et al., 1988) and are found without apparent contact with axons (Waggener, 1966; Poirier et al., 1968; Stefansson et al., 1982; Cichowski & Jacks, 2001). Neurofibroma formation correlates with a disruption of normal axon-glial interactions in Remak bundles, the development of hypertrophy throughout peripheral nerves and an enhancement of mast cell recruitment into these nerves. The hypertrophied peripheral nerves and neurofibromas contain large numbers of cells similar to immature Schwann cells (Wu et al., 2008) and it has been further suggested that the neurofibroma progenitor cell corresponds to cells at the boundary between Schwann cell precursors and immature Schwann cells (Wu et al, 2008). As stated previously, it has also been found that tumours have a significant population of nestin expressant stem cells (Pongpudpunth et al., 2010). Up until now, progenitor cells have not been identified in normal adult peripheral nerves (Bixby et al., 2002). Thus, it has been previously hypothesised that the possible mechanism underlying neurofibroma formation was that NF1 deficiency inhibits differentiation of neural crest/ precursor Schwann cells in the embryo which leads to the persistence of undifferentiated cells into adult nerves and the formation of tumors at later stages. Zheng et al. (2008) demonstrated however, that Nf1-deficient fetal stem/progenitor cells differentiate according to a normal time course into NMSCs.

An interesting clue into the cell of origin of neurofibromatosis may lie in the

demonstration that transformed Schwann/neural crest cells in neurofibroma and malignant peripheral nerve sheath tumours have pigmented melanosomes in the cytoplasm as well as fully differentiated melanocytes within peripheral nerve trunk and dorsal root ganglion (Anderson et al, 1979; Kanno et al, 1987; Hess et al, 1988; Kuhnen et al, 2002; Motoi et al, 2005). This finding alludes to a process of dedifferentiation of Schwann cells into a bipotent 'melanocyte/Schwann cell progenitor' during clonal propogation (Real et al, 2005), such as was first proposed by Nichols and Weston in 1977 and demonstrated *in vitro* in avian cultures (Sherman et al, 1993; Nataf et al, 2000). Of note then, is that the early immature Pax3 expressing Schwann cells described herein are poised phenotypically one step from the bipotent melanocyte/Schwann cell precursor seen in the ventral neurogenic pathway of embryogenesis at around E12. Should further studies confirm the existence of these Pax3 expressing cells as adult peripheral nerve progenitor cells, it could be theorised that the chronic neurofibrotic milieu of the nerve trunk may be a possible mechanism of the transformation of peripheral nerve progenitor cells and the ensuing development of neurofibromatosis.

Finally, millions of people suffer from peripheral nerve degeneration due to chemotherapy, infection, diabetes, congenital and chronic demyelinating disorders. In the regeneration of damaged peripheral nerve, Pax3 expression in regenerative Schwann cells is constitutive. The capacity to manipulate the proliferation of endogenous Pax3 expressing replacement cells would greatly enhance the development of cell replacement therapies for disease treatment. Here, the development of a procedure to label and image Pax3 positive cells of peripheral nerve *in vivo,* may be used for future investigations study mechanisms of Remak bundle regeneration with an objective to advance therapies that alleviate the clinical symptoms of C-fibre degeneration.

4.6 Research conclusion

In 2008, the prominent neuroscientists Griffin and Thompson stated that “the possibility of a population of Schwann cell precursors in adult nerves is largely unexplored” (Griffin & Thompson, 2008). The current investigations were intended to build on the previous work of others who showed that *Pax3*, a classic progenitor cell marker, is detected in adult peripheral nerve trunk. In accord with the hypotheses and aims proposed at the onset of this research, successful co-localisation of progenitor cell markers Pax3, Sox2, and p75Ngfr in the nerve specimens investigated, provides initial evidence for the existence of peripheral nerve Schwann progenitor cells in adult mouse nerves. Furthermore, the novel phenotypic subclassification of Pax3 expressing cells as separate from those of the terminally differentiated Remak NMSC, similarly supports the long held tenet that developmental progenitor Schwann cells are retained in adult nerve much the same as other adult tissue progenitor cells, and Pax3 plays a principle role in maintenance of these cells.

REFERENCES

Abdel-Malek, Z. A., A. L. Kadekaro, et al. (2010). "Stepping up melanocytes to the challenge of UV exposure." Pigment cell & melanoma research **23**(2): 171-186.

Adameyko, I. and F. Lallemend (2010). "Glial versus melanocyte cell fate choice: Schwann cell precursors as a cellular origin of melanocytes." Cellular and molecular life sciences : CMLS **67**(18): 3037-3055.

Anton, E. S., G. Weskamp, et al. (1994). "Nerve growth factor and its low-affinity receptor promote Schwann cell migration." Proceedings of the National Academy of Sciences of the United States of America **91**(7): 2795-2799.

Ara, J., P. Bannerman, et al. (2005). "Schwann cell-autonomous role of neuropilin-2." Journal of neuroscience research **79**(4): 468-475.

Baichwal, R. R. and G. H. DeVries (1989). "A mitogen for Schwann cells is derived from myelin basic protein." Biochemical and biophysical research communications **164**(2): 883-888.

Bajard, L., F. Relaix, et al. (2006). "A novel genetic hierarchy functions during hypaxial myogenesis: Pax3 directly activates Myf5 in muscle progenitor cells in the limb." Genes & development **20**(17): 2450-2464.

Barber, T. D., M. C. Barber, et al. (1999). "PAX3 gene structure, alternative splicing and evolution." Gene **237**(2): 311-319.

Barr, F. G., J. C. Fitzgerald, et al. (1999). "Predominant expression of alternative PAX3 and PAX7 forms in myogenic and neural tumor cell lines." Cancer research **59**(21): 5443-5448.

Bennicelli, J. L., W. J. Fredericks, et al. (1995). "Wild type PAX3 protein and the PAX3-FKHR fusion protein of alveolar rhabdomyosarcoma contain potent, structurally distinct transcriptional activation domains." Oncogene **11**(1): 119-130.

Bentley, C. A. and K. F. Lee (2000). "p75 is important for axon growth and schwann cell migration during development." The Journal of neuroscience : the official journal of the Society for Neuroscience **20**(20): 7706-7715.

Bhattacharyya, A., R. Brackenbury, et al. (1994). "Axons arrest the migration of Schwann cell precursors." Development **120**(6): 1411-1420.

Bischoff, R. and C. Franzini-Armstrong (2004). Satellite and stem cells in muscle regeneration. New York: McGraw Hill.

Blake, J. A. and M. R. Ziman (2005). "Pax3 transcripts in melanoblast development." Development, growth & differentiation **47**(9): 627-635.

Blanchard, A. D., A. Sinanan, et al. (1996). "Oct-6 (SCIP/Tst-1) is expressed in Schwann cell precursors, embryonic Schwann cells, and postnatal myelinating Schwann cells: comparison with Oct-1, Krox-20, and Pax-3." Journal of neuroscience research **46**(5): 630-640.

Bober, E., T. Franz, et al. (1994). "Pax-3 is required for the development of limb muscles: a possible role for the migration of dermomyotomal muscle progenitor cells." Development **120**(3): 603-612.

Bolognia, J. L. and J. M. Pawelek (1988). "Biology of hypopigmentation." Journal of the American Academy of Dermatology **19**(2 Pt 1): 217-255.

Bondurand, N., V. Pingault, et al. (2000). "Interaction among SOX10, PAX3 and MITF, three genes altered in Waardenburg syndrome." Human molecular genetics **9**(13): 1907-1917.

Borycki, A. G., J. Li, et al. (1999). "Pax3 functions in cell survival and in pax7 regulation." Development **126**(8): 1665-1674.

Botchkareva, N. V., M. Khlgatian, et al. (2001). "SCF/c-kit signaling is required for cyclic regeneration of the hair pigmentation unit." The FASEB journal : official

publication of the Federation of American Societies for Experimental Biology **15**(3): 645-658.
Britsch, S., D. E. Goerich, et al. (2001). "The transcription factor Sox10 is a key regulator of peripheral glial development." Genes & development **15**(1): 66-78.
Buckingham, M., L. Bajard, et al. (2006). "Myogenic progenitor cells in the mouse embryo are marked by the expression of Pax3/7 genes that regulate their survival and myogenic potential." Anatomy and embryology **211 Suppl 1**: 51-56.
Burri, M., Y. Tromvoukis, et al. (1989). "Conservation of the paired domain in metazoans and its structure in three isolated human genes." The EMBO journal **8**(4): 1183-1190.
Cairns, D. M., M. E. Sato, et al. (2008). "A gradient of Shh establishes mutually repressing somitic cell fates induced by Nkx3.2 and Pax3." Developmental biology **323**(2): 152-165.
Cao, Y. and C. Wang (2000). "The COOH-terminal transactivation domain plays a key role in regulating the in vitro and in vivo function of Pax3 homeodomain." The Journal of biological chemistry **275**(13): 9854-9862.
Carlsen, F. and F. Behse (1980). "Three dimensional analysis of Schwann cells associated with unmyelinated nerve fibres in human sural nerve." Journal of anatomy **130**(Pt 3): 545-557.
Carroll, S. L., M. L. Miller, et al. (1997). "Expression of neuregulins and their putative receptors, ErbB2 and ErbB3, is induced during Wallerian degeneration." The Journal of neuroscience : the official journal of the Society for Neuroscience **17**(5): 1642-1659.
Chance, P. F. and K. H. Fischbeck (1994). "Molecular genetics of Charcot-Marie-Tooth disease and related neuropathies." Human molecular genetics **3 Spec No**: 1503-1507.
Charge, S. B. and M. A. Rudnicki (2004). "Cellular and molecular regulation of muscle regeneration." Physiological reviews **84**(1): 209-238.
Charytonowicz, E., C. Cordon-Cardo, et al. (2009). "Alveolar rhabdomyosarcoma: is the cell of origin a mesenchymal stem cell?" Cancer letters **279**(2): 126-136.
Charytonowicz, E., I. Matushansky, et al. (2011). "Alternate PAX3 and PAX7 C-terminal isoforms in myogenic differentiation and sarcomagenesis." Clinical & translational oncology : official publication of the Federation of Spanish Oncology Societies and of the National Cancer Institute of Mexico **13**(3): 194-203.
Chen, S., C. Rio, et al. (2003). "Disruption of ErbB receptor signaling in adult non-myelinating Schwann cells causes progressive sensory loss." Nature neuroscience **6**(11): 1186-1193.
Cichowski, K. and T. Jacks (2001). "NF1 tumor suppressor gene function: narrowing the GAP." Cell **104**(4): 593-604.
Corry, G. N. and D. A. Underhill (2005). "Pax3 target gene recognition occurs through distinct modes that are differentially affected by disease-associated mutations." Pigment cell research / sponsored by the European Society for Pigment Cell Research and the International Pigment Cell Society **18**(6): 427-438.
Cramer, S. F. (2009). "Stem cells for epidermal melanocytes--a challenge for students of dermatopathology." The American Journal of dermatopathology **31**(4): 331-341.
Crist, C. G., D. Montarras, et al. (2009). "Muscle stem cell behavior is modified by microRNA-27 regulation of Pax3 expression." Proceedings of the National Academy of Sciences of the United States of America **106**(32): 13383-13387.

da-Silva, E. O. (1991). "Waardenburg I syndrome: a clinical and genetic study of two large Brazilian kindreds, and literature review." American journal of medical genetics **40**(1): 65-74.
Daston, G., E. Lamar, et al. (1996). "Pax-3 is necessary for migration but not differentiation of limb muscle precursors in the mouse." Development **122**(3): 1017-1027.
Dastur, D. K. and G. L. Porwal (1979). "Lepromatous leprosy as a model of Schwann cell pathology and lysosomal activity." Clinical and experimental neurology **16**: 277-293
Dastur, D. K. (1983). "Pathology and pathogenesis of predilective sites of nerve damage in leprous neuritis. Nerves in the arm and the face." Neurosurgical review **6**(3): 139-152.
Davids, L. M., E. du Toit, et al. (2009). "A rare repigmentation pattern in a vitiligo patient: a clue to an epidermal stem-cell reservoir of melanocytes?" Clinical and experimental dermatology **34**(2): 246-248.
Dong, Z., A. Brennan, et al. (1995). "Neu differentiation factor is a neuron-glia signal and regulates survival, proliferation, and maturation of rat Schwann cell precursors." Neuron **15**(3): 585-596.
Dong, Z., A. Sinanan, et al. (1999). "Schwann cell development in embryonic mouse nerves." Journal of neuroscience research **56**(4): 334-348.
Dottori, M., M. K. Gross, et al. (2001). "The winged-helix transcription factor Foxd3 suppresses interneuron differentiation and promotes neural crest cell fate." Development **128**(21): 4127-4138.
Epstein, D. J., D. Malo, et al. (1991). "Molecular characterization of a deletion encompassing the splotch mutation on mouse chromosome 1." Genomics **10**(1): 89-93.
Epstein, J. A., D. N. Shapiro, et al. (1996). "Pax3 modulates expression of the c-Met receptor during limb muscle development." Proceedings of the National Academy of Sciences of the United States of America **93**(9): 4213-4218.
Epstein, J. A., J. Li, et al. (2000). "Migration of cardiac neural crest cells in Splotch embryos." Development **127**(9): 1869-1878.
Farin, H. F., A. Mansouri, et al. (2008). "T-box protein Tbx18 interacts with the paired box protein Pax3 in the development of the paraxial mesoderm." The Journal of biological chemistry **283**(37): 25372-25380.
Fernandes, K. J., I. A. McKenzie, et al. (2004). "A dermal niche for multipotent adult skin-derived precursor cells." Nature cell biology **6**(11): 1082-1093.
Fernandez-Valle, C., R. P. Bunge, et al. (1995). "Schwann cells degrade myelin and proliferate in the absence of macrophages: evidence from in vitro studies of Wallerian degeneration." Journal of neurocytology **24**(9): 667-679.
Fortin, A. S., D. A. Underhill, et al. (1997). "Reciprocal effect of Waardenburg syndrome mutations on DNA binding by the Pax-3 paired domain and homeodomain." Human molecular genetics **6**(11): 1781-1790.
Foy, C., V. Newton, et al. (1990). "Assignment of the locus for Waardenburg syndrome type I to human chromosome 2q37 and possible homology to the Splotch mouse." American journal of human genetics **46**(6): 1017-1023.
Franz, T. (1990). "Defective ensheathment of motoric nerves in the Splotch mutant mouse." Acta anatomica **138**(3): 246-253.
Franz, T., R. Kothary, et al. (1993). "The Splotch mutation interferes with muscle development in the limbs." Anatomy and embryology **187**(2): 153-160.
Friede, R. L. and T. Samorajski (1968). "Myelin formation in the sciatic nerve of the rat. A quantitative electron microscopic, histochemical and radioautographic study." Journal of neuropathology and experimental neurology **27**(4): 546-570.

Galili, N., R. J. Davis, et al. (1993). "Fusion of a fork head domain gene to PAX3 in the solid tumour alveolar rhabdomyosarcoma." Nature genetics **5**(3): 230-235.
Garratt, A. N., O. Voiculescu, et al. (2000). "A dual role of erbB2 in myelination and in expansion of the schwann cell precursor pool." The Journal of cell biology **148**(5): 1035-1046.
Gershon, T. R., O. Oppenheimer, et al. (2005). "Temporally regulated neural crest transcription factors distinguish neuroectodermal tumors of varying malignancy and differentiation." Neoplasia **7**(6): 575-584.
Ghazizadeh, S. and L. B. Taichman (2001). "Multiple classes of stem cells in cutaneous epithelium: a lineage analysis of adult mouse skin." The EMBO journal **20**(6): 1215-1222.
Gibbels, E., U. Henke-Lubke, et al. (1988). "Unmyelinated nerve fibres in leprosy. A qualitative and quantitative study of sural nerve biopsies in 2 cases of lepromatous leprosy." Leprosy review **59**(2): 153-162.
Goulding, M. D., G. Chalepakis, et al. (1991). "Pax-3, a novel murine DNA binding protein expressed during early neurogenesis." The EMBO journal **10**(5): 1135-1147.
Goulding, M., S. Sterrer, et al. (1993). "Analysis of the Pax-3 gene in the mouse mutant splotch." Genomics **17**(2): 355-363.
Goulding, M., A. Lumsden, et al. (1994). "Regulation of Pax-3 expression in the dermomyotome and its role in muscle development." Development **120**(4): 957-971.
Grichnik, J. M. (2008). "Melanoma, nevogenesis, and stem cell biology." The Journal of investigative dermatology **128**(10): 2365-2380.
Griffin, J. W., N. Drucker, et al. (1987). "Schwann cell proliferation and migration during paranodal demyelination." The Journal of neuroscience : the official journal of the Society for Neuroscience **7**(3): 682-699.
Griffin, J. W., E. A. Stocks, et al. (1990). "Schwann cell proliferation following lysolecithin-induced demyelination." Journal of neurocytology **19**(3): 367-384.
Griffin, J. W. and W. J. Thompson (2008). "Biology and pathology of nonmyelinating Schwann cells." Glia **56**(14): 1518-1531.
Grinspan, J. B., M. A. Marchionni, et al. (1996). "Axonal interactions regulate Schwann cell apoptosis in developing peripheral nerve: neuregulin receptors and the role of neuregulins." The Journal of neuroscience : the official journal of the Society for Neuroscience **16**(19): 6107-6118.
Gros, J., M. Manceau, et al. (2005). "A common somitic origin for embryonic muscle progenitors and satellite cells." Nature **435**(7044): 954-958.
Guenard, V., D. Montag, et al. (1996). "Onion bulb cells in mice deficient for myelin genes share molecular properties with immature, differentiated non-myelinating, and denervated Schwann cells." Glia **18**(1): 27-38.
Gupta, S. K., J. F. Poduslo, et al. (1990). "Myelin-associated glycoprotein gene expression in the presence and absence of Schwann cell-axonal contact." Developmental neuroscience **12**(1): 22-33.
Gutmann, D. H., A. C. Hirbe, et al. (2001). "Functional analysis of neurofibromatosis 2 (NF2) missense mutations." Human molecular genetics **10**(14): 1519-1529.
Harrisingh, M. C., E. Perez-Nadales, et al. (2004). "The Ras/Raf/ERK signalling pathway drives Schwann cell dedifferentiation." The EMBO journal **23**(15): 3061-3071.
He, S. J., G. Stevens, et al. (2005). "Transfection of melanoma cells with antisense PAX3 oligonucleotides additively complements cisplatin-induced cytotoxicity." Molecular cancer therapeutics **4**(6): 996-1003.

Hirobe, T. (1984). "Effects of genic substitution at the brown locus on the differentiation of epidermal melanocytes in newborn mouse skin." The Anatomical record **209**(4): 425-432.
Hornyak, T. J., D. J. Hayes, et al. (2001). "Transcription factors in melanocyte development: distinct roles for Pax-3 and Mitf." Mechanisms of development **101**(1-2): 47-59.
Hoth, C. F., A. Milunsky, et al. (1993). "Mutations in the paired domain of the human PAX3 gene cause Klein-Waardenburg syndrome (WS-III) as well as Waardenburg syndrome type I (WS-I)." American journal of human genetics **52**(3): 455-462.
Hu, P., K. G. Geles, et al. (2008). "Codependent activators direct myoblast-specific MyoD transcription." Developmental cell **15**(4): 534-546.
Huxley, C., E. Passage, et al. (1996). "Construction of a mouse model of Charcot-Marie-Tooth disease type 1A by pronuclear injection of human YAC DNA." Human molecular genetics **5**(5): 563-569.
Hyatt, J. P., G. E. McCall, et al. (2008). "PAX3/7 expression coincides with MyoD during chronic skeletal muscle overload." Muscle & nerve **38**(1): 861-866.
Ide, C., K. Tohyama, et al. (1983). "Schwann cell basal lamina and nerve regeneration." Brain research **288**(1-2): 61-75.
Ishikiriyama, S. (1993). "Gene for Waardenburg syndrome type I is located at 2q35, not at 2q37.3." American journal of medical genetics **46**(5): 608.
Jessen, K. R. and R. Mirsky (1992). "Schwann cells: early lineage, regulation of proliferation and control of myelin formation." Current opinion in neurobiology **2**(5): 575-581.
Jessen, K. R. and R. Mirsky (1994). "Neural development. Fate diverted." Current biology : CB **4**(9): 824-827.
Jessen, K. R. and R. Mirsky (1999). "Schwann cells and their precursors emerge as major regulators of nerve development." Trends in neurosciences **22**(9): 402-410.
Jessen, K. R. and R. Mirsky (2002). "Signals that determine Schwann cell identity." Journal of anatomy **200**(4): 367-376.
Jimbow, K., S. I. Roth, et al. (1975). "Mitotic activity in non-neoplastic melanocytes in vivo as determined by histochemical, autoradiographic, and electron microscope studies." The Journal of cell biology **66**(3): 663-670.
Jordan, S. A. and I. J. Jackson (2000). "A late wave of melanoblast differentiation and rostrocaudal migration revealed in patch and rump-white embryos." Mechanisms of development **92**(2): 135-143.
Jun, S. and C. Desplan (1996). "Cooperative interactions between paired domain and homeodomain." Development **122**(9): 2639-2650.
Kassar-Duchossoy, L., E. Giacone, et al. (2005). "Pax3/Pax7 mark a novel population of primitive myogenic cells during development." Genes & development **19**(12): 1426-1431.
Keller, C., B. R. Arenkiel, et al. (2004a). "Alveolar rhabdomyosarcomas in conditional Pax3:Fkhr mice: cooperativity of Ink4a/ARF and Trp53 loss of function." Genes & development **18**(21): 2614-2626.
Keller, C., M. S. Hansen, et al. (2004b). "Pax3:Fkhr interferes with embryonic Pax3 and Pax7 function: implications for alveolar rhabdomyosarcoma cell of origin." Genes & development **18**(21): 2608-2613.
Kioussi, C., M. K. Gross, et al. (1995). "Pax3: a paired domain gene as a regulator in PNS myelination." Neuron **15**(3): 553-562.

Koike, H., M. Iijima, et al. (2007). "Nonmyelinating Schwann cell involvement with well-preserved unmyelinated axons in Charcot-Marie-Tooth disease type 1A." Journal of neuropathology and experimental neurology **66**(11): 1027-1036.
Krauss, S., T. Johansen, et al. (1991). "Zebrafish pax[zf-a]: a paired box-containing gene expressed in the neural tube." The EMBO journal **10**(12): 3609-3619.
Kuhlbrodt, K., B. Herbarth, et al. (1998). "Sox10, a novel transcriptional modulator in glial cells." The Journal of neuroscience : the official journal of the Society for Neuroscience **18**(1): 237-250.
Kumar, V., R. B. Narayanan, et al. (1992). "An ultrastructural study of Schwann cells in peripheral nerves of leprosy patients." Indian journal of leprosy **64**(1): 81-87.
Kury, P., R. Greiner-Petter, et al. (2002). "Mammalian achaete scute homolog 2 is expressed in the adult sciatic nerve and regulates the expression of Krox24, Mob-1, CXCR4, and p57kip2 in Schwann cells." The Journal of neuroscience : the official journal of the Society for Neuroscience **22**(17): 7586-7595.
Kwa, M. S., I. N. van Schaik, et al. (2003). "Autoimmunoreactivity to Schwann cells in patients with inflammatory neuropathies." Brain : a journal of neurology **126**(Pt 2): 361-375.
Lang, D., M. M. Lu, et al. (2005). "Pax3 functions at a nodal point in melanocyte stem cell differentiation." Nature **433**(7028): 884-887.
Le Douarin, N. M. (1980). "The ontogeny of the neural crest in avian embryo chimaeras." Nature **286**(5774): 663-669.
Le Douarin, N. M. (1986). "Cell line segregation during peripheral nervous system ontogeny." Science **231**(4745): 1515-1522.
Le, N., R. Nagarajan, et al. (2005). "Analysis of congenital hypomyelinating Egr2Lo/Lo nerves identifies Sox2 as an inhibitor of Schwann cell differentiation and myelination." Proceedings of the National Academy of Sciences of the United States of America **102**(7): 2596-2601.
Le, L. Q. and L. F. Parada (2007). "Tumor microenvironment and neurofibromatosis type I: connecting the GAPs." Oncogene **26**(32): 4609-4616.
LeBlanc, A. C. and J. F. Poduslo (1990). "Axonal modulation of myelin gene expression in the peripheral nerve." Journal of neuroscience research **26**(3): 317-326.
Lepper, C., S. J. Conway, et al. (2009). "Adult satellite cells and embryonic muscle progenitors have distinct genetic requirements." Nature **460**(7255): 627-631.
Levy, V., C. Lindon, et al. (2005). "Distinct stem cell populations regenerate the follicle and interfollicular epidermis." Developmental cell **9**(6): 855-861.
Levy, V., C. Lindon, et al. (2007). "Epidermal stem cells arise from the hair follicle after wounding." The FASEB journal : official publication of the Federation of American Societies for Experimental Biology **21**(7): 1358-1366.
Li, L., M. Fukunaga-Kalabis, et al. (2010). "Human dermal stem cells differentiate into functional epidermal melanocytes." Journal of cell science **123**(Pt 6): 853-860.
Liu, T. C., Z. M. Ji, et al. (1989). "Light- and electron-microscopic study of M. leprae-infected armadillo nerves." International journal of leprosy and other mycobacterial diseases : official organ of the International Leprosy Association **57**(1): 65-72.
Lubinska, L. (1961). "Sedentary and migratory states of Schwann cells." Experimental cell research **Suppl 8**: 74-90.
Mak, S. S., M. Moriyama, et al. (2006). "Indispensable role of Bcl2 in the development of the melanocyte stem cell." Developmental biology **291**(1): 144-153.
Margue, C. M., M. Bernasconi, et al. (2000). "Transcriptional modulation of the anti-apoptotic protein BCL-XL by the paired box transcription factors PAX3 and PAX3/FKHR." Oncogene **19**(25): 2921-2929.

Martin, J. R. and H. D. Webster (1973). "Mitotic Schwann cells in developing nerve: their changes in shape, fine structure, and axon relationships." Developmental biology **32**(2): 417-431.
Masui, S., Y. Nakatake, et al. (2007). "Pluripotency governed by Sox2 via regulation of Oct3/4 expression in mouse embryonic stem cells." Nature cell biology **9**(6): 625-635.
Medic, S. and M. Ziman (2010). "PAX3 expression in normal skin melanocytes and melanocytic lesions (naevi and melanomas)." PloS one **5**(4): e9977.
Medic, S., H. Rizos, et al. (2011). "Differential PAX3 functions in normal skin melanocytes and melanoma cells." Biochemical and biophysical research communications **411**(4): 832-837.
Mehta, L. N. and N. H. Antia (1984). "Ultrastructure of sciatic nerve of armadillo infected with Mycobacterium leprae." Indian journal of leprosy **56**(3): 540-554.
Mehta, L. N., V. P. Shetty, et al. (1975). "Quantitative, histologic and ultrastructural studies of the index branch of the radial cutaneous nerve in leprosy and its correlation with electrophysiologic study." International journal of leprosy and other mycobacterial diseases : official organ of the International Leprosy Association **43**(3): 256-264.
Meier, C., E. Parmantier, et al. (1999). "Developing Schwann cells acquire the ability to survive without axons by establishing an autocrine circuit involving insulin-like growth factor, neurotrophin-3, and platelet-derived growth factor-BB." The Journal of neuroscience : the official journal of the Society for Neuroscience **19**(10): 3847-3859.
Mirsky, R., H. J. Stewart, et al. (1996). "Development and differentiation of Schwann cells." Revue neurologique **152**(5): 308-313.
Moase, C. E. and D. G. Trasler (1990). "Delayed neural crest cell emigration from Sp and Spd mouse neural tube explants." Teratology **42**(2): 171-182.
Moase, C. E. and D. G. Trasler (1992). "Splotch locus mouse mutants: models for neural tube defects and Waardenburg syndrome type I in humans." Journal of medical genetics **29**(3): 145-151.
Muller, L. J., L. Pels, et al. (1996). "Ultrastructural organization of human corneal nerves." Investigative ophthalmology & visual science **37**(4): 476-488.
Muratovska, A., C. Zhou, et al. (2003). "Paired-Box genes are frequently expressed in cancer and often required for cancer cell survival." Oncogene **22**(39): 7989-7997.
Murinson, B. B., D. R. Archer, et al. (2005). "Degeneration of myelinated efferent fibers prompts mitosis in Remak Schwann cells of uninjured C-fiber afferents." The Journal of neuroscience : the official journal of the Society for Neuroscience **25**(5): 1179-1187.
Murphy, P., P. Topilko, et al. (1996). "The regulation of Krox-20 expression reveals important steps in the control of peripheral glial cell development." Development **122**(9): 2847-2857.
Nakao, J., J. Shinoda, et al. (1997). "Apoptosis regulates the number of Schwann cells at the premyelinating stage." Journal of neurochemistry **68**(5): 1853-1862.
Ng, V., G. Zanazzi, et al. (2000). "Role of the cell wall phenolic glycolipid-1 in the peripheral nerve predilection of Mycobacterium leprae." Cell **103**(3): 511-524.
Niemann, S., M. W. Sereda, et al. (2000). "Uncoupling of myelin assembly and schwann cell differentiation by transgenic overexpression of peripheral myelin protein 22." The Journal of neuroscience : the official journal of the Society for Neuroscience **20**(11): 4120-4128.
Nishimura, E. K., S. A. Jordan, et al. (2002). "Dominant role of the niche in melanocyte stem-cell fate determination." Nature **416**(6883): 854-860.

Nishimura, E. K., S. R. Granter, et al. (2005). "Mechanisms of hair graying: incomplete melanocyte stem cell maintenance in the niche." Science **307**(5710): 720-724.
Ohta, S., Y. Imaizumi, et al. (2011). "Generation of human melanocytes from induced pluripotent stem cells." PloS one **6**(1): e16182.
Ohyama, M., A. Terunuma, et al. (2006). "Characterization and isolation of stem cell-enriched human hair follicle bulge cells." The Journal of clinical investigation **116**(1): 249-260.
Olguin, H. C. and B. B. Olwin (2004). "Pax-7 up-regulation inhibits myogenesis and cell cycle progression in satellite cells: a potential mechanism for self-renewal." Developmental biology **275**(2): 375-388.
Osawa, M., G. Egawa, et al. (2005). "Molecular characterization of melanocyte stem cells in their niche." Development **132**(24): 5589-5599.
O'Shea, K. S. and L. H. Liu (1987). "Basal lamina and extracellular matrix alterations in the caudal neural tube of the delayed Splotch embryo." Brain research **465**(1-2): 11-20.
Oshima, H., A. Rochat, et al. (2001). "Morphogenesis and renewal of hair follicles from adult multipotent stem cells." Cell **104**(2): 233-245.
Oustanina, S., G. Hause, et al. (2004). "Pax7 directs postnatal renewal and propagation of myogenic satellite cells but not their specification." The EMBO journal **23**(16): 3430-3439.
Owens, D. M. and F. M. Watt (2003). "Contribution of stem cells and differentiated cells to epidermal tumours." Nature reviews. Cancer **3**(6): 444-451.
Padilla, F., R. Marc Mege, et al. (1999). "Upregulation and redistribution of cadherins reveal specific glial and muscle cell phenotypes during wallerian degeneration and muscle denervation in the mouse." Journal of neuroscience research **58**(2): 270-283.
Parker, C. J., S. G. Shawcross, et al. (2004). "Expression of PAX 3 alternatively spliced transcripts and identification of two new isoforms in human tumors of neural crest origin." International journal of cancer. Journal international du cancer **108**(2): 314-320.
Parkinson, D. B., A. Bhaskaran, et al. (2004). "Krox-20 inhibits Jun-NH2-terminal kinase/c-Jun to control Schwann cell proliferation and death." The Journal of cell biology **164**(3): 385-394.
Pawelek, J. M. (1976). "Factors regulating growth and pigmentation of melanoma cells." The Journal of investigative dermatology **66**(4): 201-209.
Peirano, R. I., D. E. Goerich, et al. (2000). "Protein zero gene expression is regulated by the glial transcription factor Sox10." Molecular and cellular biology **20**(9): 3198-3209.
Pellegrino, R. G., M. J. Politis, et al. (1986). "Events in degenerating cat peripheral nerve: induction of Schwann cell S phase and its relation to nerve fibre degeneration." Journal of neurocytology **15**(1): 17-28.
Perry, V. H. and M. C. Brown (1992). "Role of macrophages in peripheral nerve degeneration and repair." BioEssays : news and reviews in molecular, cellular and developmental biology **14**(6): 401-406.
Peters, E. M., D. J. Tobin, et al. (2002). "Migration of melanoblasts into the developing murine hair follicle is accompanied by transient c-Kit expression." The journal of histochemistry and cytochemistry : official journal of the Histochemistry Society **50**(6): 751-766.
Petronic-Rosic, V., C. R. Shea, et al. (2004). "Pagetoid melanocytosis: when is it significant?" Pathology **36**(5): 435-444.
Pharis, D. B. and J. A. Zitelli (2003). "The management of regional lymph nodes in cancer." The British journal of dermatology **149**(5): 919-925.

Plettenberg, A., C. Ballaun, et al. (1995). "Human melanocytes and melanoma cells constitutively express the Bcl-2 proto-oncogene in situ and in cell culture." The American journal of pathology **146**(3): 651-659.
Plummer, R. S., C. R. Shea, et al. (2008). "PAX3 expression in primary melanomas and nevi." Modern pathology : an official journal of the United States and Canadian Academy of Pathology, Inc **21**(5): 525-530.
Pongpudpunth, M., J. Bhawan, et al. (2010). "Nestin-positive stem cells in neurofibromas from patients with neurofibromatosis type 1-tumorigenic or incidental?" The American Journal of dermatopathology **32**(6): 574-577.
Potterf, S. B., M. Furumura, et al. (2000). "Transcription factor hierarchy in Waardenburg syndrome: regulation of MITF expression by SOX10 and PAX3." Human genetics **107**(1): 1-6.
Pritchard, C., G. Grosveld, et al. (2003). "Alternative splicing of Pax3 produces a transcriptionally inactive protein." Gene **305**(1): 61-69.
Ptashne, M. (1988). "How eukaryotic transcriptional activators work." Nature **335**(6192): 683-689.
Qualman, S. J., C. M. Coffin, et al. (1998). "Intergroup Rhabdomyosarcoma Study: update for pathologists." Pediatric and developmental pathology : the official journal of the Society for Pediatric Pathology and the Paediatric Pathology Society **1**(6): 550-561.
Rambukkana, A., G. Zanazzi, et al. (2002). "Contact-dependent demyelination by Mycobacterium leprae in the absence of immune cells." Science **296**(5569): 927-931.
Reeves, F. C., G. C. Burdge, et al. (1999). "Induction of antisense Pax-3 expression leads to the rapid morphological differentiation of neuronal cells and an altered response to the mitogenic growth factor bFGF." Journal of cell science **112 (Pt 2)**: 253-261.
Relaix, F., D. Rocancourt, et al. (2005). "A Pax3/Pax7-dependent population of skeletal muscle progenitor cells." Nature **435**(7044): 948-953.
Relaix, F., D. Montarras, et al. (2006). "Pax3 and Pax7 have distinct and overlapping functions in adult muscle progenitor cells." The Journal of cell biology **172**(1): 91-102.
Remak, R. (1838). Observationes anatomicae et microscopicae de system-atis nervosi structura. Berlin : Suptibus formis Reimerianis.
Reynolds, R. J., G. J. Little, et al. (1994). "Imaging myelinated nerve fibres by confocal fluorescence microscopy: individual fibres in whole nerve trunks traced through multiple consecutive internodes." Journal of neurocytology **23**(9): 555-564.
Riccardi, V. M. (2000). "Histogenesis control genes: embryology, wound-healing, and NF1." Teratology **62**(1): 4.
Roeb, W., A. Boyer, et al. (2007). "PAX3-FOXO1 controls expression of the p57Kip2 cell-cycle regulator through degradation of EGR1." Proceedings of the National Academy of Sciences of the United States of America **104**(46): 18085-18090.
Rutkowski, J. L., K. Wu, et al. (2000). "Genetic and cellular defects contributing to benign tumor formation in neurofibromatosis type 1." Human molecular genetics **9**(7): 1059-1066.
Salonen, V., J. Peltonen, et al. (1987). "Laminin in traumatized peripheral nerve: basement membrane changes during degeneration and regeneration." Journal of neurocytology **16**(5): 713-720.
Salzer, J. L. and R. P. Bunge (1980). "Studies of Schwann cell proliferation. I. An analysis in tissue culture of proliferation during development, Wallerian degeneration, and direct injury." The Journal of cell biology **84**(3): 739-752.

Scherer, S. S., Y. T. Xu, et al. (1995). "Periaxin expression in myelinating Schwann cells: modulation by axon-glial interactions and polarized localization during development." Development **121**(12): 4265-4273.
Scholl, F. A., J. Kamarashev, et al. (2001). "PAX3 is expressed in human melanomas and contributes to tumor cell survival." Cancer research **61**(3): 823-826.
Schubert, F. R., P. Tremblay, et al. (2001). "Early mesodermal phenotypes in splotch suggest a role for Pax3 in the formation of epithelial somites." Developmental dynamics : an official publication of the American Association of Anatomists **222**(3): 506-521.
Seo, H. C., B. O. Saetre, et al. (1998). "The zebrafish Pax3 and Pax7 homologues are highly conserved, encode multiple isoforms and show dynamic segment-like expression in the developing brain." Mechanisms of development **70**(1-2): 49-63.
Serra, E., T. Rosenbaum, et al. (2000). "Schwann cells harbor the somatic NF1 mutation in neurofibromas: evidence of two different Schwann cell subpopulations." Human molecular genetics **9**(20): 3055-3064.
Sheela, S., V. M. Riccardi, et al. (1990). "Angiogenic and invasive properties of neurofibroma Schwann cells." The Journal of cell biology **111**(2): 645-653.
Shetty, V. P., L. N. Mehta, et al. (1980). "Study of the evolution of nerve damage in leprosy. Part I--Lesions of the index branch of the radial cutaneous nerve in early leprosy." Leprosy in India **52**(1): 5-18.
Shetty, V. P. (1993). "Animal model to study the mechanism of nerve damage in leprosy--a preliminary report." International journal of leprosy and other mycobacterial diseases : official organ of the International Leprosy Association **61**(1): 70-75.
Shetty, V. P. and N. H. Antia (1996). "A semi quantitative analysis of bacterial load in different cell types in leprous nerves using transmission electron microscope." Indian journal of leprosy **68**(1): 105-108.
Shetty, V. P. and N. H. Antia (2002). "Light and ultrastructural study of sciatic nerve lesions induced using intraneural injection of viable Mycobacterium leprae in normal and immunosuppressed Swiss white mice." International journal of leprosy and other mycobacterial diseases : official organ of the International Leprosy Association **70**(1): 25-33.
Sorensen, P. H., J. C. Lynch, et al. (2002). "PAX3-FKHR and PAX7-FKHR gene fusions are prognostic indicators in alveolar rhabdomyosarcoma: a report from the children's oncology group." Journal of clinical oncology : official journal of the American Society of Clinical Oncology **20**(11): 2672-2679.
Spreyer, P., H. Schaal, et al. (1990). "Regeneration-associated high level expression of apolipoprotein D mRNA in endoneurial fibroblasts of peripheral nerve." The EMBO journal **9**(8): 2479-2484.
Stewart, H. J., L. Morgan, et al. (1993). "Changes in DNA synthesis rate in the Schwann cell lineage in vivo are correlated with the precursor--Schwann cell transition and myelination." The European journal of neuroscience **5**(9): 1136-1144.
Stoll, G., J. W. Griffin, et al. (1989). "Wallerian degeneration in the peripheral nervous system: participation of both Schwann cells and macrophages in myelin degradation." Journal of neurocytology **18**(5): 671-683.
Stoll, G. and H. W. Muller (1999). "Nerve injury, axonal degeneration and neural regeneration: basic insights." Brain pathology **9**(2): 313-325.
Syroid, D. E., P. R. Maycox, et al. (1996). "Cell death in the Schwann cell lineage and its regulation by neuregulin." Proceedings of the National Academy of Sciences of the United States of America **93**(17): 9229-9234.

Tajbakhsh, S., D. Rocancourt, et al. (1997). "Redefining the genetic hierarchies controlling skeletal myogenesis: Pax-3 and Myf-5 act upstream of MyoD." Cell **89**(1): 127-138.

Takahashi, K. and S. Yamanaka (2006). "Induction of pluripotent stem cells from mouse embryonic and adult fibroblast cultures by defined factors." Cell **126**(4): 663-676.

Tapinos, N. and A. Rambukkana (2005). "Insights into regulation of human Schwann cell proliferation by Erk1/2 via a MEK-independent and p56Lck-dependent pathway from leprosy bacilli." Proceedings of the National Academy of Sciences of the United States of America **102**(26): 9188-9193.

Tassabehji, M., A. P. Read, et al. (1992). "Waardenburg's syndrome patients have mutations in the human homologue of the Pax-3 paired box gene." Nature **355**(6361): 635-636.

Tassabehji, M., A. P. Read, et al. (1993). "Mutations in the PAX3 gene causing Waardenburg syndrome type 1 and type 2." Nature genetics **3**(1): 26-30.

Taylor, G., M. S. Lehrer, et al. (2000). "Involvement of follicular stem cells in forming not only the follicle but also the epidermis." Cell **102**(4): 451-461.

Theos, A. and B. R. Korf (2006). "Pathophysiology of neurofibromatosis type 1." Annals of internal medicine **144**(11): 842-849.

Thomas, A. J. and C. A. Erickson (2008). "The making of a melanocyte: the specification of melanoblasts from the neural crest." Pigment cell & melanoma research **21**(6): 598-610.

Tobin, D. J., A. Slominski, et al. (1999). "The fate of hair follicle melanocytes during the hair growth cycle." The journal of investigative dermatology. Symposium proceedings / the Society for Investigative Dermatology, Inc. [and] European Society for Dermatological Research **4**(3): 323-332.

Tobin, D. J. (2008). "Human hair pigmentation--biological aspects." International journal of cosmetic science **30**(4): 233-257.

Toma, J. G., M. Akhavan, et al. (2001). "Isolation of multipotent adult stem cells from the dermis of mammalian skin." Nature cell biology **3**(9): 778-784.

Tona, A., G. Perides, et al. (1993). "Extracellular matrix in regenerating rat sciatic nerve: a comparative study on the localization of laminin, hyaluronic acid, and chondroitin sulfate proteoglycans, including versican." The journal of histochemistry and cytochemistry : official journal of the Histochemistry Society **41**(4): 593-599.

Topilko, P., P. Murphy, et al. (1996). "Embryonic Development of Schwann Cells: Multiple Roles for Neuregulins along the Pathway." Molecular and cellular neurosciences **8**(2/3): 71-75.

Topilko, P., G. Levi, et al. (1997). "Differential regulation of the zinc finger genes Krox-20 and Krox-24 (Egr-1) suggests antagonistic roles in Schwann cells." Journal of neuroscience research **50**(5): 702-712.

Treisman, J., E. Harris, et al. (1991). "The paired box encodes a second DNA-binding domain in the paired homeo domain protein." Genes & development **5**(4): 594-604.

Tremblay, P., S. Dietrich, et al. (1998). "A crucial role for Pax3 in the development of the hypaxial musculature and the long-range migration of muscle precursors." Developmental biology **203**(1): 49-61.

Tsukamoto, K., Y. Nakamura, et al. (1994). "Isolation of two isoforms of the PAX3 gene transcripts and their tissue-specific alternative expression in human adult tissues." Human genetics **93**(3): 270-274.

Underhill, D. A., K. J. Vogan, et al. (1995). "Analysis of the mouse Splotch-delayed mutation indicates that the Pax-3 paired domain can influence homeodomain

DNA-binding activity." Proceedings of the National Academy of Sciences of the United States of America **92**(9): 3692-3696.
Underhill, D. A. and P. Gros (1997). "The paired-domain regulates DNA binding by the homeodomain within the intact Pax-3 protein." The Journal of biological chemistry **272**(22): 14175-14182.
Venters, S. J., R. E. Argent, et al. (2004). "Precocious terminal differentiation of premigratory limb muscle precursor cells requires positive signalling." Developmental dynamics : an official publication of the American Association of Anatomists **229**(3): 591-599.
Vogan, K. J., D. J. Epstein, et al. (1993). "The splotch-delayed (Spd) mouse mutant carries a point mutation within the paired box of the Pax-3 gene." Genomics **17**(2): 364-369.
Vogan, K. J., D. A. Underhill, et al. (1996). "An alternative splicing event in the Pax-3 paired domain identifies the linker region as a key determinant of paired domain DNA-binding activity." Molecular and cellular biology **16**(12): 6677-6686.
Vogan, K. J. and P. Gros (1997). "The C-terminal subdomain makes an important contribution to the DNA binding activity of the Pax-3 paired domain." The Journal of biological chemistry **272**(45): 28289-28295.
Wakamatsu, Y., Y. Endo, et al. (2004). "Multiple roles of Sox2, an HMG-box transcription factor in avian neural crest development." Developmental dynamics : an official publication of the American Association of Anatomists **229**(1): 74-86.
Wang, Q., S. Kumar, et al. (2006). "Functional analysis of alternative isoforms of the transcription factor PAX3 in melanocytes in vitro." Cancer research **66**(17): 8574-8580.
Watanabe, A., K. Takeda, et al. (1998). "Epistatic relationship between Waardenburg syndrome genes MITF and PAX3." Nature genetics **18**(3): 283-286.
Wegner, M. (2000). "Transcriptional control in myelinating glia: the basic recipe." Glia **29**(2): 118-123.
Wehrle-Haller, B. and J. A. Weston (1995). "Soluble and cell-bound forms of steel factor activity play distinct roles in melanocyte precursor dispersal and survival on the lateral neural crest migration pathway." Development **121**(3): 731-742.
Weinberg, H. J. and P. S. Spencer (1978). "The fate of Schwann cells isolated from axonal contact." Journal of neurocytology **7**(5): 555-569.
Williams, B. A. and C. P. Ordahl (1994). "Pax-3 expression in segmental mesoderm marks early stages in myogenic cell specification." Development **120**(4): 785-796.
Wilson, C., G. Cotsarelis, et al. (1994). "Cells within the bulge region of mouse hair follicle transiently proliferate during early anagen: heterogeneity and functional differences of various hair cycles." Differentiation; research in biological diversity **55**(2): 127-136.
Xia, S. J. and F. G. Barr (2004). "Analysis of the transforming and growth suppressive activities of the PAX3-FKHR oncoprotein." Oncogene **23**(41): 6864-6871.
Xu, W., M. A. Rould, et al. (1995). "Crystal structure of a paired domain-DNA complex at 2.5 A resolution reveals structural basis for Pax developmental mutations." Cell **80**(4): 639-650.
Xu, H. E., M. A. Rould, et al. (1999). "Crystal structure of the human Pax6 paired domain-DNA complex reveals specific roles for the linker region and carboxy-terminal subdomain in DNA binding." Genes & development **13**(10): 1263-1275.
Yamauchi, J., J. R. Chan, et al. (2004). "Neurotrophins regulate Schwann cell migration by activating divergent signaling pathways dependent on Rho GTPases."

Proceedings of the National Academy of Sciences of the United States of America **101**(23): 8774-8779.

Yamauchi, J., J. R. Chan, et al. (2005). "The neurotrophin-3 receptor TrkC directly phosphorylates and activates the nucleotide exchange factor Dbs to enhance Schwann cell migration." Proceedings of the National Academy of Sciences of the United States of America **102**(14): 5198-5203.

Yu, H. S. (2002). "Melanocyte destruction and repigmentation in vitiligo: a model for nerve cell damage and regrowth." Journal of biomedical science **9**(6 Pt 2): 564-573.

Yu, W. M., M. L. Feltri, et al. (2005). "Schwann cell-specific ablation of laminin gamma1 causes apoptosis and prevents proliferation." The Journal of neuroscience : the official journal of the Society for Neuroscience **25**(18): 4463-4472.

Zammit, P. S., J. J. Carvajal, et al. (2004). "Myf5 expression in satellite cells and spindles in adult muscle is controlled by separate genetic elements." Developmental biology **273**(2): 454-465.

Zheng, H., L. Chang, et al. (2008). "Induction of abnormal proliferation by nonmyelinating schwann cells triggers neurofibroma formation." Cancer cell **13**(2): 117-128.

Zhu, Y., P. Ghosh, et al. (2002). "Neurofibromas in NF1: Schwann cell origin and role of tumor environment." Science **296**(5569): 920-922.

Zlotogora, J., I. Lerer, et al. (1995). "Homozygosity for Waardenburg syndrome." American journal of human genetics **56**(5): 1173-1178.

Zorick, T. S. and G. Lemke (1996). "Schwann cell differentiation." Current opinion in cell biology **8**(6): 870-876.

Zorick, T. S., D. E. Syroid, et al. (1999). "Krox-20 controls SCIP expression, cell cycle exit and susceptibility to apoptosis in developing myelinating Schwann cells." Development **126**(7): 1397-1406.

Table 3. **Assessment of fixation and permeabilisation procedures.**

	Permeabilisation method	**None**	**Methanol**			**0.5% Tw20 in PBS**			**0.2% TX100 in PBS**			**10% DMSO in PBS**		
	Permeabilisation time (min)		**5**	**10**	**20**	**5**	**10**	**20**	**5**	**10**	**20**	**5**	**10**	**20**
Fixation method														
4% PFA perfusion		++	+++	+	+	++	+	+	++	++	++	++	++	++
4% PFA perfusion & post-fix (2 hrs)		++	++	+	+	++	++	++	++	++	++	++	++	++
4% PFA post-fix (2 hrs)		++	+	+	+	+++	++	++	++	++	+++	++	++	++
Methanol, acetic acid, DDH_20, acetone		++	+	+	+	++	++	++	++	++	++	++	++	++
Acetone		++++	N/A	N/A	N/A	N/A	N/A	N/A	N/A	N/A	N/A	N/A	N/A	N/A

Table 4. **Assessment Criteria Used To Assess Immunohistochemical Methods.**

Score	Assessment criteria
+	Loss of tissue/cellular integrity
++	Good morphology, minimal non-specific background fluorescence
+++	Nuclei specific label, minimal non-specific background fluorescence
++++	Good morphology, nuclei specific label, minimal non-specific background fluorescence